UNCLASSIFIED

AD NUMBER
ADB012971
LIMITATION CHANGES
TO: **Approved for public release; distribution is unlimited.**
FROM: **Distribution authorized to U.S. Gov't. agencies only; Test and Evaluation; APR 1976. Other requests shall be referred to Air Force Flight Dynamics Laboratory, attn: FXS, Wright-Patterson AFB, OH45433. This document contains export-controlled technical data.**
AUTHORITY
AFWAL ltr, 12 Dec 1986

THIS PAGE IS UNCLASSIFIED

AD B0 12971

AUTHORITY:
AFWAL etc,
12 Dec 86

AFFTC-TR-76-10

COMPARISON OF FLIGHT TEST AND WIND TUNNEL PERFORMANCE CHARACTERISTICS OF THE X-24B RESEARCH AIRCRAFT

APRIL 1976

FINAL REPORT

Controlling Office: AFFDL/FXS
Wright-Patterson AFB, Ohio 45433

AIR FORCE FLIGHT TEST CENTER
EDWARDS AIR FORCE BASE, CALIFORNIA
AIR FORCE SYSTEMS COMMAND
UNITED STATES AIR FORCE

This technical report was submitted under Job Order Number 1366A0 by the Deputy Commander for Operations of the Air Force Flight Test Center, Edwards AFB, California 93523.

Foreign announcement and dissemination by the Defense Documentation Center are not authorized because of technology restrictions of the U.S. Export Control Acts as implemented by AFR 400-10.

Prepared by:

David F. Richardson
DAVID F. RICHARDSON
Aerospace Engineer

This report has been reviewed and is approved for publication:

Joseph A. Guthrie, Jr.
JOSEPH A. GUTHRIE, Jr.
Colonel, USAF
Deputy Commander for Operations

Thomas P. Stafford
THOMAS P. STAFFORD
Major General, USAF
Commander

Qualified requesters may obtain copies of this report from the Defense Documentation Center, Cameron Station, Alexandria, Virgina 22314. Department of Defense contractors must be established for DDC services, or have "need to know" certified by cognizant military agency of their project or contract.

DDC release to NTIS is not authorized

When U.S. Government drawings, specifications, or other data are used for any purpose other than a definitely related government procurement operation, the government thereby incurs no responsibility nor any obligation whatsoever; and the fact that the government may have formulated, furnished, or in any way supplied the said drawings, specifications, or any other data is not to be regarded by implication or otherwise, as in any manner licensing the holder or any other person or corporation or conveying any rights or permission to manufacture, use or sell any patented invention that may in any way be related thereto.

Do not return this copy; retain or destroy.

UNCLASSIFIED

SECURITY CLASSIFICATION OF THIS PAGE (When Data Entered)

REPORT DOCUMENTATION PAGE

READ INSTRUCTIONS BEFORE COMPLETING FORM

1. REPORT NUMBER: AFFTC-TR-76-10
2. GOVT ACCESSION NO.:
3. RECIPIENT'S CATALOG NUMBER:
4. TITLE (and Subtitle): Comparison of Flight Test and Wind Tunnel Performance Characteristics of the X-24B Research Aircraft.
5. TYPE OF REPORT & PERIOD COVERED: Final Report. 1 Aug 73 - 26 Nov 75
6. PERFORMING ORG. REPORT NUMBER:
7. AUTHOR(s): David F. Richardson
8. CONTRACT OR GRANT NUMBER(s):
9. PERFORMING ORGANIZATION NAME AND ADDRESS: Deputy Commander for Operations, Air Force Flight Test Center, Edwards AFB, CA 93523
10. PROGRAM ELEMENT, PROJECT, TASK AREA & WORK UNIT NUMBERS: JON: 1366AO
11. CONTROLLING OFFICE NAME AND ADDRESS: AFFDL/FXS, Wright-Patterson AFB, Ohio 45433
12. REPORT DATE: Apr[redacted]76
13. NUMBER OF PAGES: 124 p.
14. MONITORING AGENCY NAME & ADDRESS (if different from Controlling Office):
15. SECURITY CLASS. (of this report): UNCLASSIFIED
15a. DECLASSIFICATION/DOWNGRADING SCHEDULE:

16. DISTRIBUTION STATEMENT (of this Report)
Distribution limited to U.S. Government agencies only (Test and Evaluation), April 1976. Other requests for this document must be referred to AFFDL (FXS), Wright-Patterson AFB, OH 45433.

17. DISTRIBUTION STATEMENT (of the abstract entered in Block 20, if different from Report)

18. SUPPLEMENTARY NOTES

19. KEY WORDS (Continue on reverse side if necessary and identify by block number)

X-24B	aircraft performance	lift-to-drag ratio
research aircraft	wind tunnel	position error
rocket powered	flight test	
glide flight	lift coefficient	
lifting body	drag coefficient	

20. ABSTRACT (Continue on reverse side if necessary and identify by block number)

This report presents the flight-determined lift and drag characteristics of the X-24B research aircraft and compares them to wind tunnel predictions. Lift and drag data were computed from onboard measured accelerations and flight conditions while the aircraft was in gliding flight. Performance data were obtained up to a maximum Mach number of 1.72. Flight test and wind tunnel data were in general agreement, although the lift curve slope was less than → next page

DD FORM 1 JAN 73 1473 EDITION OF 1 NOV 65 IS OBSOLETE

UNCLASSIFIED

SECURITY CLASSIFICATION OF THIS PAGE (When Data Entered)

012 / 00

(block 20 continued)
predicted at most Mach numbers. The drag-due-to-lift was higher than predicted in all cases. Values of maximum lift-to-drag ratio were less than predicted for all flight conditions where comparisons could be made. The maximum subsonic lift-to-drag ratio was 4.5.

SUMMARY

This report discusses the flight-determined lift and drag characteristics of the X-24B research aircraft and compares them to wind tunnel predictions. Lift and drag data were computed from onboard measured accelerations and flight conditions while the aircraft was in gliding flight. Performance data were obtained up to a maximum Mach number of 1.72.

Flight test and wind tunnel data were in general agreement, although the lift curve slope was less than predicted at most Mach numbers. The drag-due-to-lift was higher than predicted in all cases. Values of maximum lift-to-drag ratio were less than predicted for all flight conditions where comparisons could be made. The maximum subsonic lift-to-drag ratio was 4.5.

PREFACE

This report is one of four technical reports prepared by the Air Force Flight Test Center (AFFTC) to provide final documentation of the X-24B flight test program. References 1, 2, 9 and 10 are related documents reporting on other aspects of the test program. To satisfy early reporting requirements, a preliminary report summarizing significant flight data was published after each of the 36 X-24B flights and distributed to all interested agencies. The X-24B program was a joint effort involving the Air Force Flight Dynamics Laboratory (AFFDL), the Air Force Flight Test Center and the National Aeronautics and Space Administration (NASA) Hugh L. Dryden Flight Research Center. Program participation was authorized by Project Directive 73-87 and was accomplished under Job Order Number 1366A0.

The author wishes to acknowledge the efforts of Mr. Christopher J. Nagy for writing the computer program used to calculate performance parameters from flight data and for developing the position error data in Appendix B.

table of contents

list of illustrations

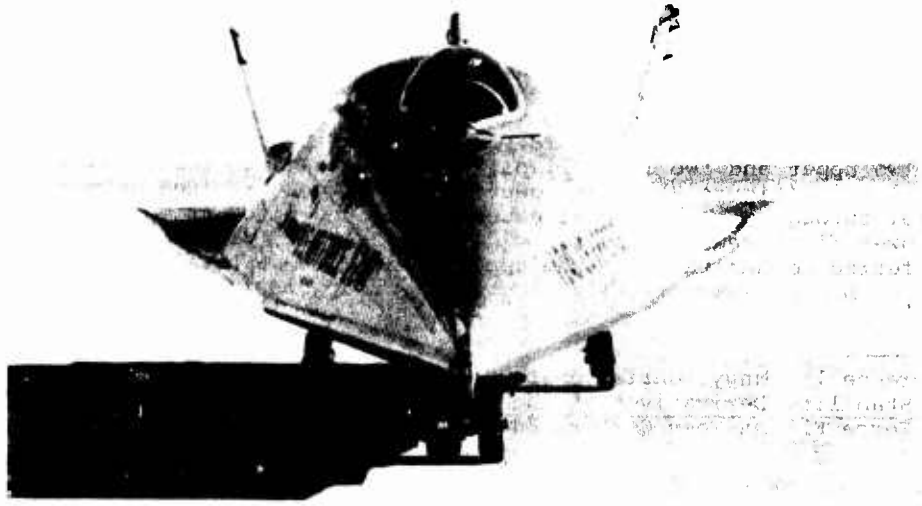

INTRODUCTION

This report contains the performance data obtained during the 36 X-24B flights. The basic research program consisted of 6 glide flights and 24 powered flights. After completion of these 30 flights, 6 additional glide flights were flown to check out three new test pilots. These 36 flights were conducted between August 1973 and November 1975. In addition to providing performance data, extensive flight data were obtained to define the handling qualities and stability and control characteristics of the X-24B configuration through the subsonic, transonic and supersonic Mach number regions up to a maximum Mach number of 1.76. The handling qualities and stability and control data are presented in reference 1.[1]

Predictions of the flight characteristics of the X-24B aircraft were based on wind tunnel data obtained from small scale models. Verification of these data was a major objective of the flight test program. To accomplish this objective, lift and drag data were obtained from maneuvers performed while the aircraft was in gliding flight and these data were compared to wind tunnel predictions. Flight test performance data were obtained in 7 upper flap bias configurations, 3 rudder bias configurations and 2 aileron bias configurations, covering a Mach number range of 0.26 to 1.72 and an angle of attack range of -0.5 to 20.7 degrees. Some data were also obtained in a configuration where the aileron bias was used to control angle of attack while the upper and lower flaps remained fixed. Effects of Mach number, wedge angle,[2] rudder bias, aileron bias and landing gear on flight performance parameters are analyzed and discussed.

Aircraft Description

The X-24B was a rocket-powered, piloted, research aircraft. The aircraft had a double delta planform with a flat bottom and flat sides. The upper surface was a curved airfoil with three vertical fins. The overall shape and dimensions are shown in figure 1. The X-24B aircraft was a high hypersonic lift-to-drag ratio shape (L/D_{max} = 2.5) as compared to previous lifting bodies which were in the class of low to medium hypersonic L/D (L/D_{max} = 1.2 to 1.4). This high hypersonic L/D could provide increased cross range maneuvering capability during orbital reentry. Although the X-24B shape was optimized for hypersonic flight, the X-24B aircraft was designed only to evaluate the flight characteristics of this shape below 2.0 Mach number.

Ten surfaces were available for aerodynamic control. They consisted of: two upper and two lower flaps, two upper and two lower rudders, and two ailerons (figure 2). The lower flap surfaces provided primary pitch control through a conventional center stick and pitch trim (δe_L). When the lower flaps reached the fully closed position, pitch inputs were transferred mechanically to the upper flaps. The upper flap surfaces could be biased symmetrically (δU_B). The flap bias feature was used as

[1] Reference 1: Nagy, Christopher J. and Kirsten, Paul W., Handling Qualities and Stability Derivatives of the X-24B Research Aircraft, AFFTC-TR-76-8, Air Force Flight Test Center, Edwards AFB, California, March 1976.

[2] Wedge angle was defined as the total angle between the upper and lower flaps ($\delta w = \delta e_L - \delta U_B$).

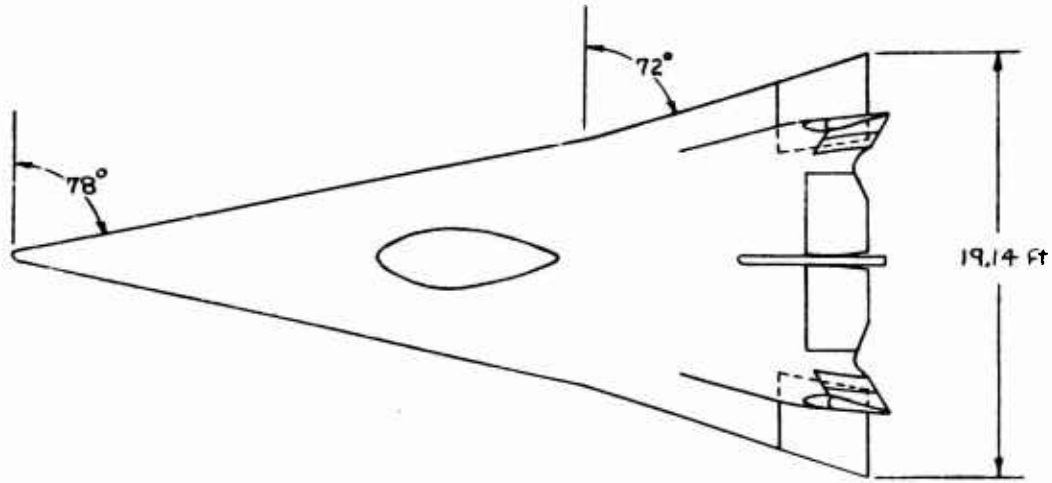

REFERENCE DIMENSIONS

AREA	S = 330.5 ft²
LENGTH	c̄ = 37.5 ft
SPAN	b = 19.0 ft
CG	= 66% c̄

TYPICAL MASS PROPERTIES

	LAUNCH	LANDING
WEIGHT	13800 lbs	8500 lbs
CG	66% c̄	64% c̄

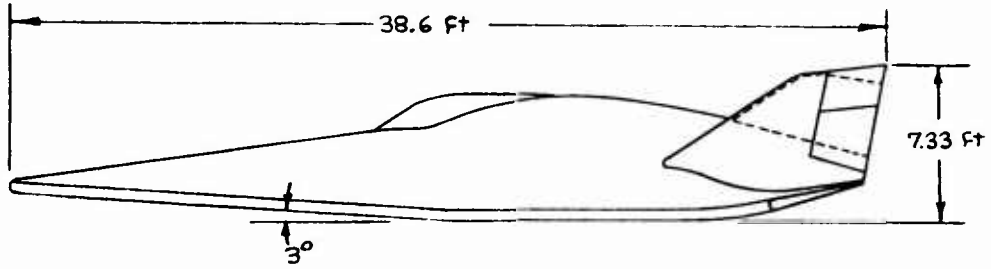

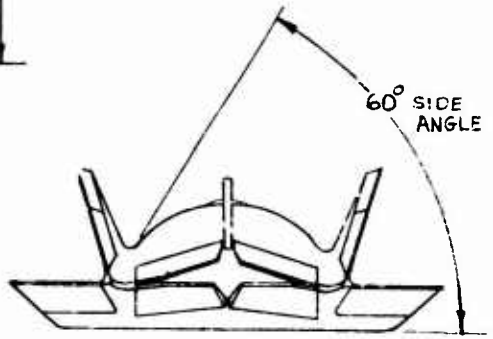

Figure 1. Three-View Drawing of the X-24B

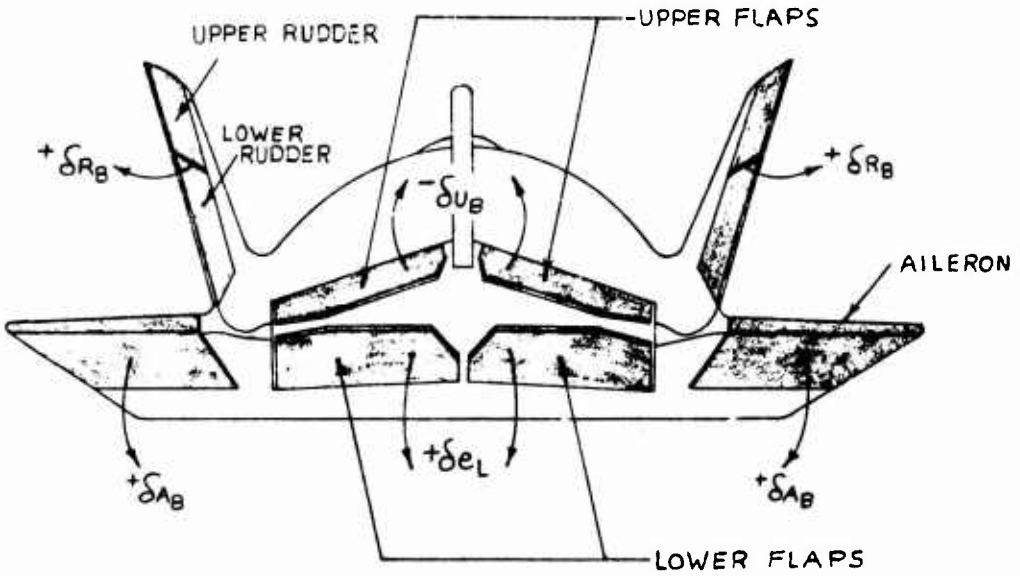

X-24B AFT END VIEW
ALL CONTROLS IN NEUTRAL
($\delta = 0$ deg) POSITION

Figure 2. X-24B Control Surface and Bias Designations

a speed brake. The outboard fins supported the four rudder surfaces, but the center fin did not contain any movable surfaces. The upper rudders provided directional trim through the rudder pedals and yaw trim. All four rudder surfaces could also be biased symmetrically (δR_B), independent of pilot control inputs. The rudder bias was programmed as a function of upper flap bias. The ailerons were deflected differentially for roll control through the stick and for roll trim or they could be biased symmetrically (δA_B) for additional pitch trim. The control surface bias designations are shown in figure 2. A triply redundant, rate feedback stability augmentation system provided artificial stability in all three axes. A complete description of the control system may be found in reference 1.

Aircraft Configurations

The aircraft was flown in two basic configurations with minor variations to each as required for additional data. The "subsonic" configuration was used below 0.6 Mach number to provide the high lift-to-drag ratios required for approach and landing. The control surface bias settings for this configuration were: upper flap bias at -20°, rudder bias at -10°, and aileron bias at 7°. The "transonic" configuration was used above 0.6 Mach number to provide adequate stability at transonic and supersonic speeds. The control surface bias settings for this configuration were: upper flap bias at -40°, rudder bias at 0°, and aileron bias at 7°. These two configurations are shown in figure 3. Although the transonic configuration provided satisfactory stability above 0.6 Mach number, it did not provide adequate performance for landing. The subsonic configuration did not have adequate stability for flight at Mach numbers much above 0.7.

Some perturbations of these configurations were flown during the test program to assess their effect on performance and flying qualities. These included flying with the upper flap bias at -13°, -23°, -28°, -30° and -34°, moving the rudder bias to 5° with -40° upper flap bias, and flying with 11° aileron bias.

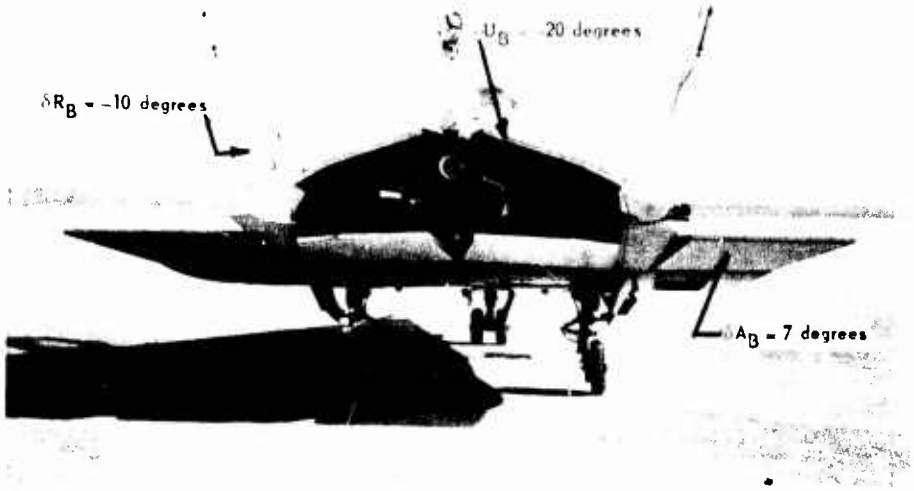

Subsonic Configuration

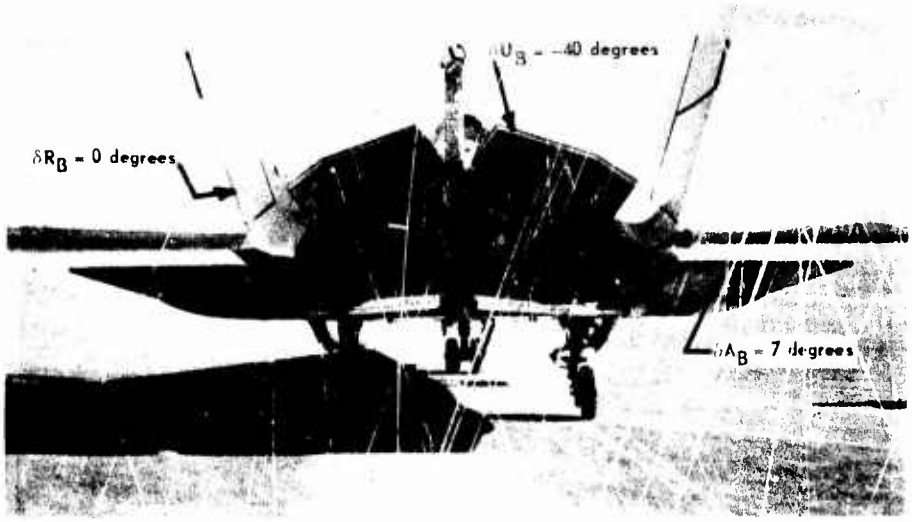

Transonic Configuration

Figure 3. X-24B Configurations

TEST AND ANALYSIS TECHNIQUE

The basic flight research program was primarily an incremental Mach number and angle of attack envelope expansion program. On powered flights, after launch from the NB-52B mothership, the X-24B was accelerated to a predetermined Mach number and altitude where the rocket engine was shut down and the aircraft glided to an unpowered landing. Depending on the type of flight (glide or powered) the pilot had two to five minutes to perform data maneuvers after which his attention was devoted to the approach and landing task. A detailed description of the test program is contained in reference 2.[3]

Data Maneuvers

A pushover-pullup maneuver was used to obtain most of the performance data. A typical maneuver covered an angle of attack range of 2 to 16 degrees in the subsonic areas with a few pullups going as high as 20 degrees. The maximum angle of attack for the supersonic maneuvers was limited to 12 degrees or less to avoid areas of low directional stability. The pilot tried to perform this task slow enough to avoid large pitch rates, but fast enough to minimize the Mach number change. The tradeoff between these two parameters resulted in an average Mach number change of 0.045 during the subsonic maneuvers and 0.13 during the supersonic maneuvers. Except for a few pushover-pullups which were performed by sweeping the aileron bias, all performance data maneuvers were executed using the primary pitch control surface (lower flaps).

Besides the planned performance maneuvers, additional data were obtained from any substantial angle of attack change. In fact a large portion of the supersonic data, as well as all of the data with the landing gear extended, was obtained by this method. All performance data maneuvers were performed with the aircraft in gliding flight. No attempt was made to obtain lift and drag while the rocket engine was running or during propellant jettison due to the uncertainty of accurately determining thrust.

Instrumentation and Data Analysis

The X-24B data system was a pulse code modulation telemetry system. Accelerations were measured by sensitive linear accelerometers located near the aircraft's center of gravity. Angle of attack, static pressure and total pressure were measured by a standard NASA pitot static nose boom. All parameters were telemetered to a ground station and recorded on magnetic tape. The raw data were processed through a NASA computer program which calculated Mach number and dynamic pressure as well as

---

[3] Reference 2: Armstrong, Johnny G., Flight Planning and Conduct of the X-24B Research Aircraft Flight Test Program, AFFTC-TR-76-11, Air Force Flight Test Center, Edwards AFB, California, to be published.

applied a boom bending/pitch rate correction to angle of attack[4] and a position error correction to static pressure (Appendix B). The data were stored on an engineering units tape at 50 samples per second.

Selected parameters from the engineering units tape along with calculated gross weight and center of gravity (reference 2) were used as the input to an AFFTC CDC 6500 digital computer program. This program made additional corrections to the flight data and computed lift and drag. Corrections were made to the accelerometers for displacement from the test center of gravity (cg). Part of the data required for the cg correction to the accelerometers were the pitch, roll and yaw accelerations. These angular accelerations were computed by differentiating the rates using Taylor-series expansions. For each performance maneuver, data were selected at points where the pitch acceleration was approximately zero ($\dot{q} \leq \pm 0.5$ deg/sec^2). This was done to obtain more consistent data at trimmed flight conditions. Other corrections were made to the lift and drag data for pitch rate and for cg variation from a reference cg of 66 percent.

The body axis force coefficients were computed from the corrected accelerations which were smoothed by averaging over a 0.1 second time interval. The lift coefficient (C_L), drag coefficient (C_D) and L/D were computed by rotating the body axis coefficients to the stability axis using true angle of attack. A byproduct of the performance computer program was the longitudinal trim data as presented in reference 1. A complete description of the equations used in the performance program is contained in reference 3.[5]

Wind Tunnel Tests

Extensive force and moment data were obtained on small scale models of the X-24B in several wind tunnels. A summary of these tests is presented in table 1. A wide range of control surface configurations were tested over a Mach number and angle of attack range that encompassed the X-24B flight envelope. Most of the data for the subsonic and transonic configurations came from the Cornell 8-foot wind tunnel[6] with the exception of the data above 1.5 Mach number, which came from the Arnold Engineering Development Center (AEDC) VKF wind tunnel.[7] The data with variable

---

[4] An upwash correction was not applied to angle of attack. Wind tunnel tests on a small scale model of the X-24B with a nose boom, indicated that the upwash correction would be negligible. Since the X-24B never flew at stabilized flight conditions, the upwash could not be determined from flight data.

[5] Reference 3: Ash, Lawrence G., Captain USAF, Flight Test and Wind Tunnel Performance Characteristics of the X-24A Lifting Body, Vol 1, FTC-TD-71-8, Air Force Flight Test Center, Edwards AFB, California, June 1972.

[6] Reference 4: DeKuyper, R.E., Transonic Wind Tunnel Tests on a .08 Scale Model of the FDL-8 Lifting Body, Vol. 1-4, Report No. AA-4024-W-2, Cornell Aeronautical Laboratory, Inc., Buffalo, New York, January-March 1971.

[7] Reference 5: Lindsay, E. Earl, Aerodynamic Characteristics of the AFFDL X-24B Configuration at Mach Numbers from 1.5 to 5.0, AEDC-TR-74-87, Arnold Engineering Development Center, Arnold AFS, Tennesse, September 1974.

Table 1

SUMMARY OF X-24B WIND TUNNEL TESTS

Wind Tunnel Location	Wind Tunnel Size (ft x ft)	Date	Model Size	Mach Number Range	Primary Test Configurations	ReX10^{-6}
Cornell Aero Lab- 8-Foot	8 x 8	Jan-Mar 1971	8%	0.4-1.3	δU_B=-15°,-20°&-40° δe_L=0°,10°,20°,25° &30° δR_B=0°&-10° δA_B=7°	23.2-9.8
Air Force Institute of Technology 5-Foot	5 x 5	June-Sep 1972	8%	0.17	Gear Down δU_B=-20° δe_L=0°,10°&20° δR_B=-10° δA_B=0°,5°&17°	3.3
Arnold Engineering Development Center- 16T	16 x 16	Aug 1973	8%	0.6-1.3	δU_B=-30°&-40° δe_L=20° δR_B=0° δA_B=2°,7°&12°	12.0
Arnold Engineering Development Center- VKF Tunnel A	3.33 x 3.33	Feb 1974	5.5%	1.5-5.0	δU_B=-40° δe_L=20°&30° δR_B=0° δA_B=7°	8.2
Arnold Engineering Development Center- 4T	4 x 4	July 1974	5.5%	0.8-1.3	δU_B=-40° δe_L=20°,22°,24°,&28° δR_B=0° δA_B=7°	8.2

aileron bias settings came from the AEDC 16T wind tunnel.[8] The data with the landing gear extended was obtained in the Air Force Institute of Technology (AFIT) 5-foot wind tunnel.[9] Late in the program some additional wind tunnel data were obtained in the AEDC 4T tunnel[10] in an effort to determine why the static longitudinal stability of the full scale X-24B was less than predicted by the previous wind tunnel tests. For the AEDC 4T wind tunnel tests, a new 5.5-percent scale model was fabricated which included some minor configuration changes that were not in the previous models but were on the full scale aircraft. Comparison of the predicted data at similar Mach numbers and model control surface configurations revealed small differences in the data from the several wind tunnel sources. These differences in data cannot be traced exclusively to the slight discrepancies that existed between the 8- and 5.5-percent model configurations.

Since the performance data of the X-24B were a strong function of control surface configuration and Mach number, only wind tunnel data which corresponded to the configuration and Mach number of a particular flight test maneuver were used for comparisons in this report. There was an exception in the case of the gear-down wind tunnel data which were obtained at a Mach number of 0.17. All of the wind tunnel data presented in this report were corrected to trim conditions and a reference cg of 66 percent. The predicted drag data represent the total measured drag of the model and therefore do not contain any base drag corrections.

---

[8] Reference 6: White, Warren E., Documentation of Wind Tunnel Test Data From a 0.08 Scale Model of the X-24B at Mach Numbers from 0.6 to 1.3, AEDC-TR-73-18, Arnold Engineering Development Center, Arnold AFS, Tennessee, October 1973.

[9] Reference 7: Norris, Richard B., et al., Parametric Study of an 8% Scale Model of the X-24B in the Landing Configuration, AFFDL-TM-73-21-FXS, Air Force Flight Dynamics Laboratory, Wright-Patterson AFB, Ohio, April 1973.

[10] Reference 8: Whoric, J.M., Aerodynamic Characteristics of a 5.5 Percent Scale Model of the AFFDL X-24B Flight Test Vehicle, AEDC-TR-75-10, Arnold Engineering Development Center, Arnold AFS, Tennessee, February 1975.

COMPARISON OF FLIGHT AND WIND TUNNEL DATA

Performance flight test data are presented in figures A1 through A33, Appendix A. Plots of L/D and C_D versus C_L, and C_L and C_D versus angle of attack are shown. All of the flight data points were trim data corrected to a reference cg of 66 percent for comparison with the wind tunnel data. The plots are arranged in order of decreasing upper flap bias setting ending with the gear-down data and the aileron-bias-sweep data. For each upper flap bias configuration, a set of performance data is presented for each Mach number for which flight data were obtained and placed in order of increasing Mach number.

The flight data were compared to all available wind tunnel trim data points obtained at the same Mach number and configuration. Lines were faired through the Cornell and AEDC VKF wind tunnel data since these were the primary sources for comparison with the flight test data.

Some of the wind tunnel data were obtained at several different Reynolds numbers (Re) for the same Mach number. These data did not show any significant effect of Re on lift and drag over the range of Re's tested. On each figure in Appendix A, the Re is shown for both the wind tunnel and the flight test data.[11] There were no variations in the flight data that could be attributed to Re effects over the range of Re's tested. Since the flight values of Re were significantly larger than wind tunnel values at the same Mach number, no conclusions could be reached as to the influence of Re on the discrepancies observed between flight test and wind tunnel performance data.

Lift Coefficient

The lift coefficient data in figures A1 through A27 were in general agreement with wind tunnel predictions at intermediate angles of attack (α) but were above predictions at low α's and dropped below predictions at high α's. As a result, the α for zero lift was 2 degrees lower than predicted in all cases where the flight data were obtained at a condition of zero lift. Flight values of trimmed lift curve slope (C_{L_α}) averaged 11 percent below wind tunnel predictions for subsonic Mach numbers and 19 percent below predictions for supersonic Mach numbers. This is consistent with the reduction in C_{N_α} discussed in reference 1. The flight data at 0.5 Mach number were an exception in that the lift coefficient compared well with predictions at all α's (figures A1, A23 and A27).

Flight test data with the landing gear extended were obtained with three upper flap configurations (figures A28 through A30). The flight data with -20 degrees δU_B compared well with AFIT wind tunnel predictions.

The lift coefficient data in figures A31 through A33 came from flight maneuvers where the aileron bias was used to control angle of attack while the lower flap remained fixed. Here again the lift curve slope was less than predicted.

---

[11] All Re data were referenced to the reference length of the X-24B - 37.5 feet for the full scale aircraft, 3.0 ft for the 8-percent scale model and 2.062 ft for the 5.5-percent scale model.

Drag Coefficient

Drag coefficient data were plotted versus angle of attack and as drag polars (C_D vs C_L) in figures A1 through A33. The drag polar data for all configurations and Mach numbers show a higher drag-due-to-lift than predicted. This discrepancy has been common to all of the previous lifting body vehicles as well as the X-24B.

The C_D versus α flight data for the transonic configuration (δU_B = -40°) were slightly below Cornell wind tunnel predictions at low α's and slightly above predictions at higher α's for Mach numbers below 0.95. Compared to the AEDC 4T wind tunnel data at 0.8 and 0.9 Mach number, the flight data were slightly lower at all α's where a comparison could be made. The data at 0.95 Mach number compared well with the Cornell wind tunnel but were below the AEDC 4T data. The C_D versus α data at 1.0 Mach number were above both wind tunnel predictions. The supersonic data generally show good agreement with predictions.

As previously mentioned, the static longitudinal stability (C_{m_α}) of the X-24B aircraft was less than predicted by the wind tunnel tests (reference 1). At low α's the trim lower flap was less than predicted (lower trim lift and drag) and at high α's the trim lower flap was greater than predicted (higher trim lift and drag). This meant that Cornell wind tunnel values of trim drag coefficient versus α would show excellent agreement with the flight data when compared at flight trim α's. The trim lift curve slope would still be less than predicted. Also the comparison of drag polar data would remain essentially the same (drag-due-to-lift higher than predicted), which means that most of the change in drag-due-to-lift would be due to differences in the trim lift data.

The C_D versus α data for the subsonic configuration (δU_B = -20° or -13°) shows excellent agreement with wind tunnel predictions at 0.5 and 0.6 Mach number but were slightly higher than predicted at 0.64 Mach number (figures A23 through A27).

The drag with the landing gear extended was slightly greater than predicted at the higher angles of attack (figure A30).

Drag data obtained from the aileron-bias-sweep maneuver were less than predicted at all angles of attack (figure A31).

The minimum drag or zero lift drag (C_{D_0}) was approximated by plotting the near linear relationship of C_L^2 versus C_D and extrapolating the flight data to C_L = 0. Flight values of C_{D_0} for the transonic configuration averaged 5 percent lower than wind tunnel predictions for all Mach numbers except in the area of Mach 1.0 where it was 10 percent greater than predicted (figure 4). Flight values of C_{D_0} for the subsonic configuration were very close to predictions.

Lift-to-Drag-Ratio

Lift-to-drag ratios were plotted versus lift coefficient in figures A1 to A33. At the lower lift coefficients, flight data were generally in good agreement or slightly above wind tunnel predictions for all configurations and Mach numbers except for 1.0 Mach number. At this Mach number the L/D was lower than predicted at all lift coefficients. Due to stability boundaries, many of the flight maneuvers in the transonic configuration and at supersonic Mach numbers were not taken to an angle of attack high enough to reach maximum L/D. In all cases where flight maneuvers were

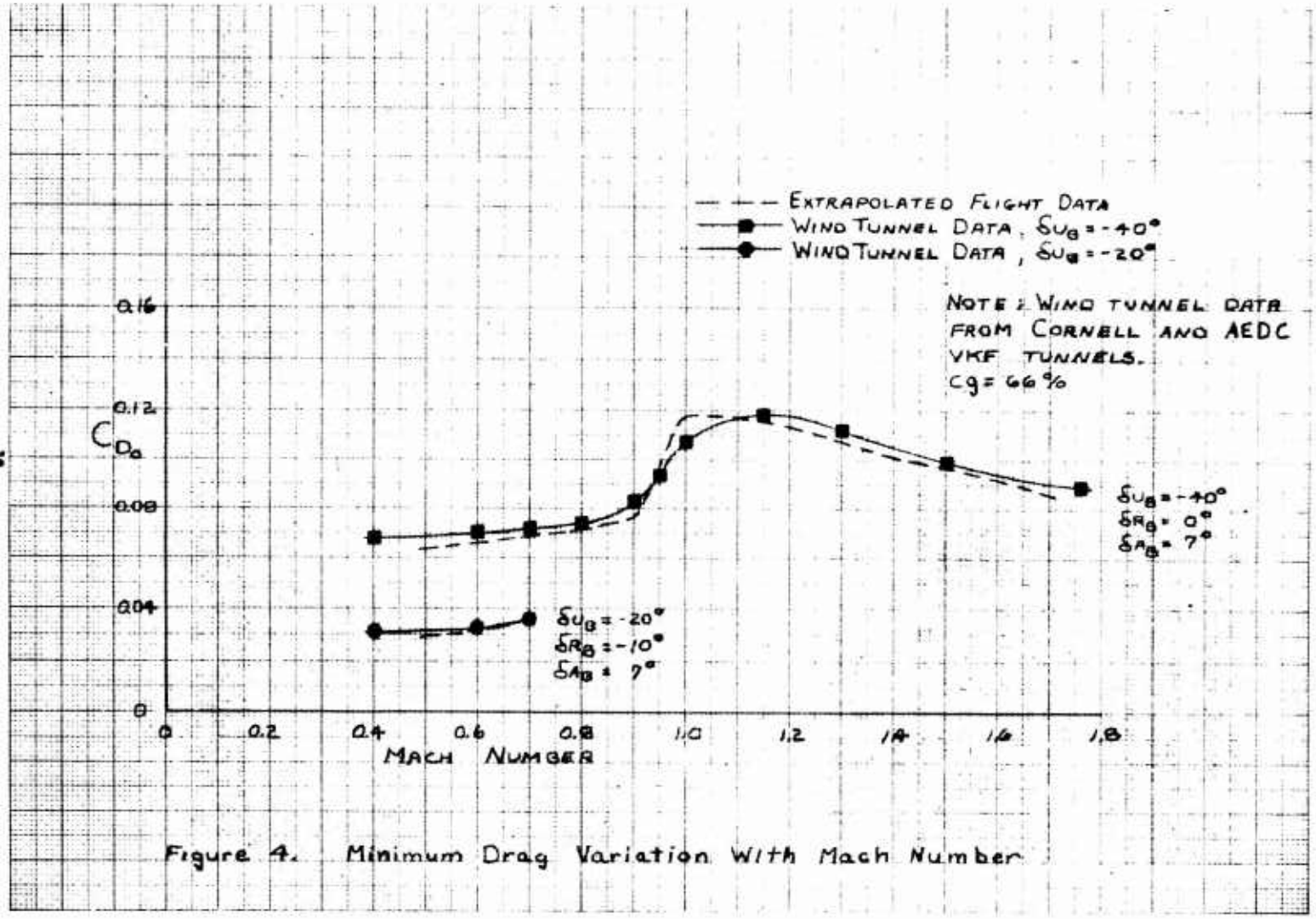

Figure 4. Minimum Drag Variation With Mach Number

taken to the α for maximum L/D, including the subsonic configuration, the values of maximum L/D and the corresponding lift coefficient were below wind tunnel predictions. Maximum L/D data are shown as a function of Mach number in figure 5. Compared to the wind tunnel data, flight values for maximum L/D averaged 7 percent lower than predicted for Mach numbers less than 1.0 and was 14 percent below predictions at 1.0 Mach number.

The reason that flight values of maximum L/D were less than predicted was probably that the flow separation on the aft portion of the aircraft, particularly on the outboard fins, occurred at a lower angle of attack and was more intense than on the small scale wind tunnel models. The fact that this flow separation was occurring on the inside of the outboard fins of the aircraft was substantiated by observations of static pressure data from orifices and motion pictures of tufts on the outboard fins (reference 9) [12], in conjunction with analysis of the rudder hinge moment data.

A summary of all the flight test data comparisons with wind tunnel predictions is presented in table 2.

[12] Reference 9: Selegan, David R. and Norris, Richard B., Comparison of X-24B Flight and Wind Tunnel Pressure Distributions, Air Force Flight Dynamics Laboratory, Wright-Patterson AFB, Ohio, to be published.

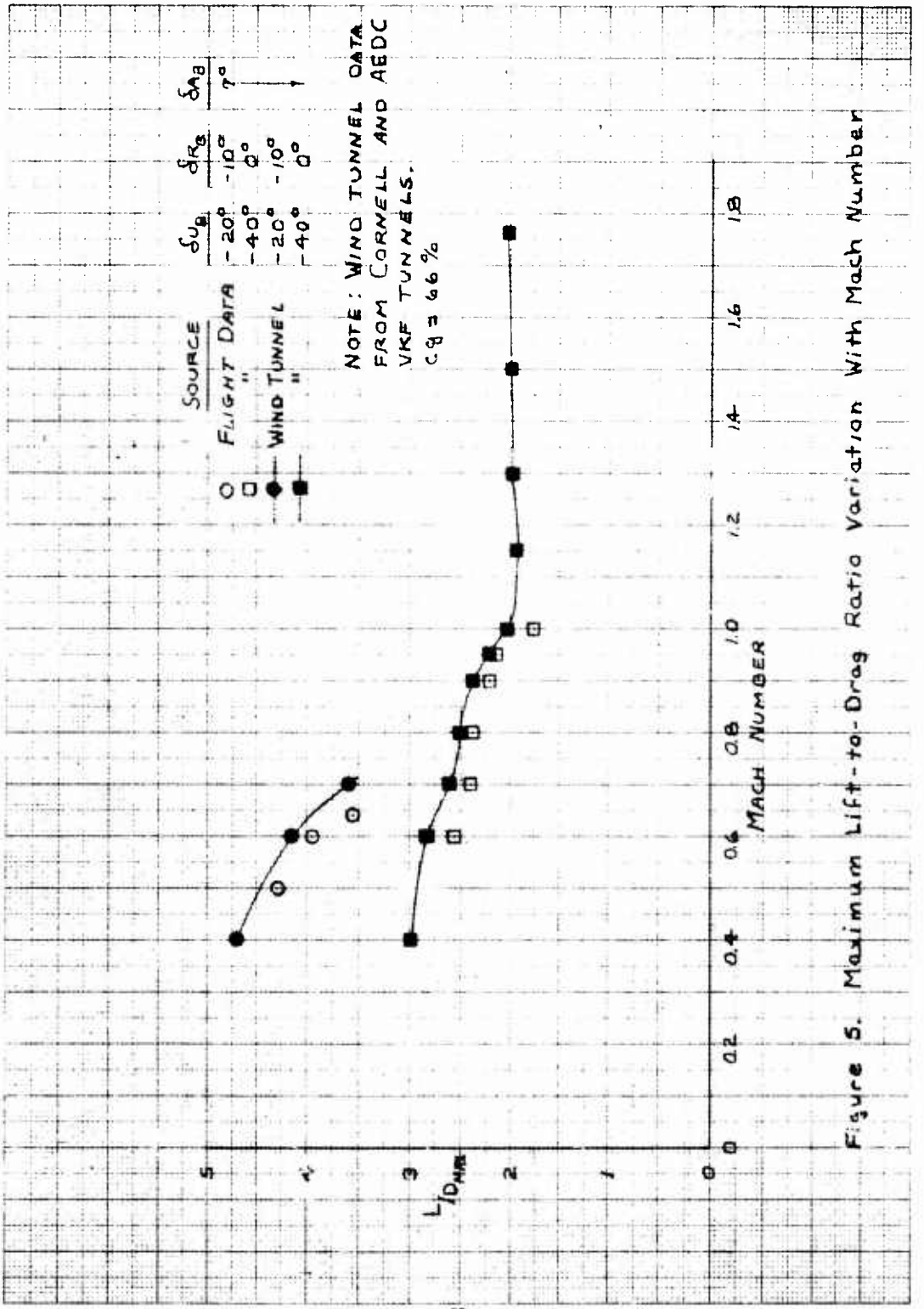

Figure 5. Maximum Lift-to-Drag Ratio Variation With Mach Number

Table 2

FLIGHT TEST DATA COMPARISON WITH WIND TUNNEL DATA

Performance Parameter	Gear Up Subsonic Configuration	Gear Up Transonic Configuration	Gear Down Subsonic Configuration
C_L	Good agreement at M = .5 Above predictions @ low α's Below predictions @ high α's } M>.5	Good agreement at M = .5 Above predictions @ low α's Below predictions @ high α's } M>.5	Good agreement
C_{L_α}	Good agreement at M=.5 11% below predictions for M>.5	Good agreement at M=.5 11% below predictions for .5<M≤1.0 19% below predictions for M>1.0	Good agreement
α at C_L=0	2° below predictions	2° below predictions	No data
C_D	Good agreement for M≤.6 Above predictions @ M=.64	Below predictions @ low α's Above predictions @ high α's } M<.95 Above predictions @ all α's for M=1.0 Good agreement for M=.95 & M>1.0	Above predictions @ high α's
drag-due-to-lift	Higher than predicted	Higher than predicted	Higher than predicted
C_{D_0}	Good agreement	10%above predictions at M=1.0 5% below predictions at other M's	No data
L/D	Good agreement or slightly above predictions at low C_L's	Good agreement or slightly above predictions at low C_L's for 1.0<M<1.0 Below predictions for M=1.0	Good agreement at low C_L's
L/D_{max}	7% below predictions	7% below predictions for M<1.0 14% below predictions for M=1.0 No L/D_{max} data for M>1.0	7% below predictions

FAIRED FLIGHT DATA COMPARISONS

Faired flight data are presented in terms of L/D and C_D versus C_L, and C_D and C_L versus α. Comparisons are made to show Mach number, wedge angle, rudder bias and aileron bias effects on performance characteristics. In addition, the effects of landing gear deployment are analyzed.

Mach Number Effects

Faired flight data curves are compared over the entire Mach number range in which data were obtained for both the transonic and subsonic configurations (figures 6, 7 and 8).

Mach Number Effects on Lift Coefficient

Flight data were obtained in the transonic configuration over the entire Mach number range of the X-24B program from 0.5 to 1.7 Mach number (figures 6 and 7). Data in the subsonic configuration covered the Mach number range below 0.64 (figure 8). In the subsonic/transonic Mach region from M = 0.5 to 0.95 there was very little change in the C_L versus α curves as a function of Mach number. Between 0.95 and 1.0 Mach number the magnitude of C_L at a particular angle of attack decreased a small amount. Above Mach 1.0 the lift data changed very little at α's below 8 degrees; however, above 8 degrees α it decreased slightly as Mach number increased.

The lift curve slope remained essentially constant at a value of 0.02 per degree for Mach numbers up to 1.0 (figures 6 and 8). Above 1.0 Mach number the lift curve slope decreased to a value of 0.016 per degree (figure 7).

Mach Number Effects on Drag Coefficient

Faired drag coefficient versus angle of attack data and drag polars are presented for both aircraft configurations in figures 6, 7 and 8. These figures in conjunction with figure 4 show that the drag increased slightly with Mach number up to 0.9 Mach number where the drag rapidly increased to a peak value at 1.0 Mach number. Above 1.0 Mach number the drag decreased as the Mach number continued to increase.

For the transonic configuration, the drag-due-to-lift increased slightly as the Mach number increased to 0.9. At 0.95 Mach number the drag-due-to-lift decreased and then increased again at 1.0 Mach number where it remained relatively constant at supersonic speeds. For the subsonic configuration, the drag-due-to-lift increased more rapidly in the 0.6 Mach number region than it did for the transonic configuration. This was because the flow separation on the inside of the outboard fins was more intense with -20 degrees upper flap than with -40 degrees upper flap in the area of 0.6 Mach number. [13]

[13] This conclusion was substantiated during the X-24B program when it was observed that the intensity of the rudder hinge moment buffet at 0.6 Mach number was greatest at the lower upper-flap settings.

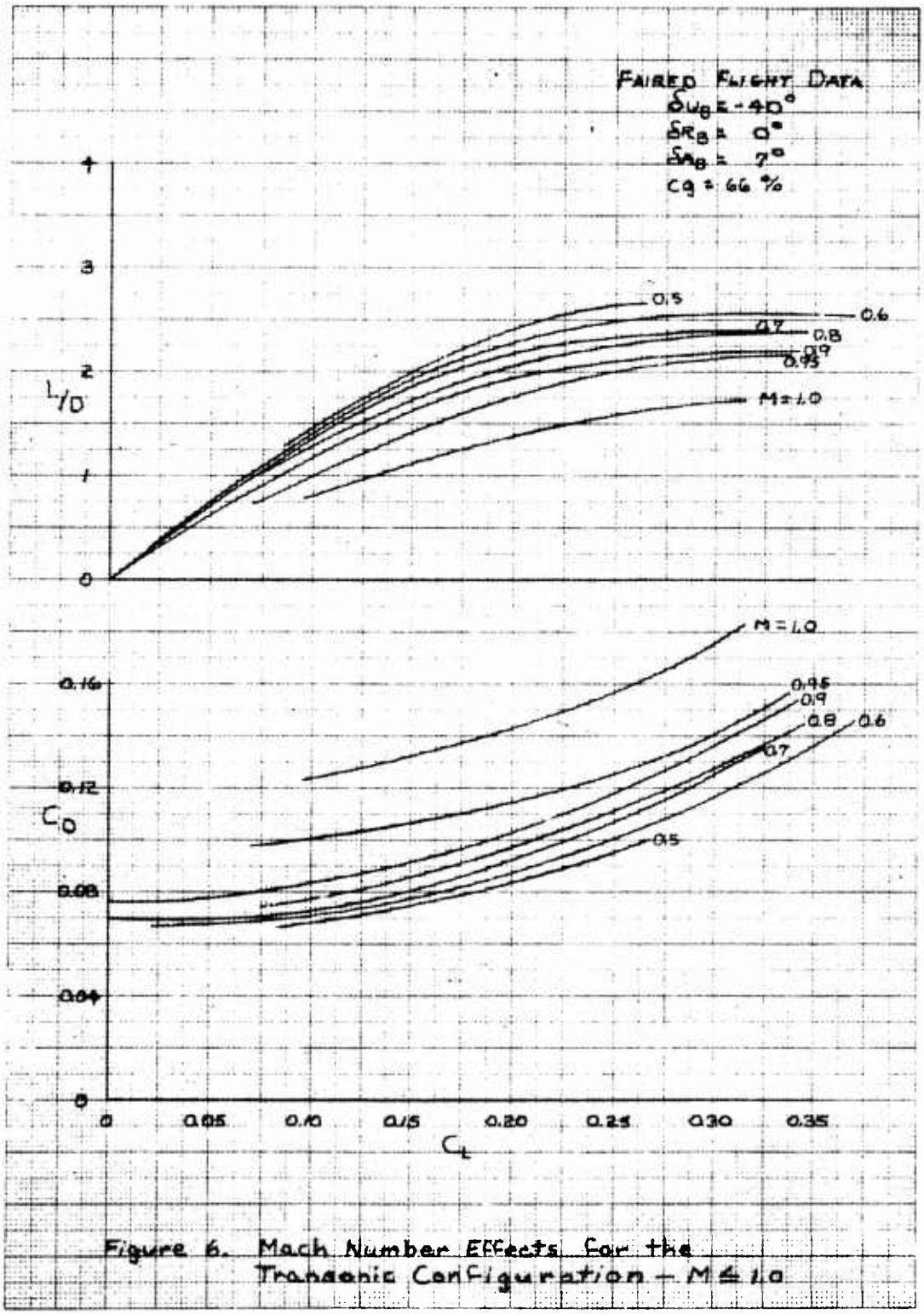

Figure 6. Mach Number Effects for the Transonic Configuration – $M \leq 1.0$

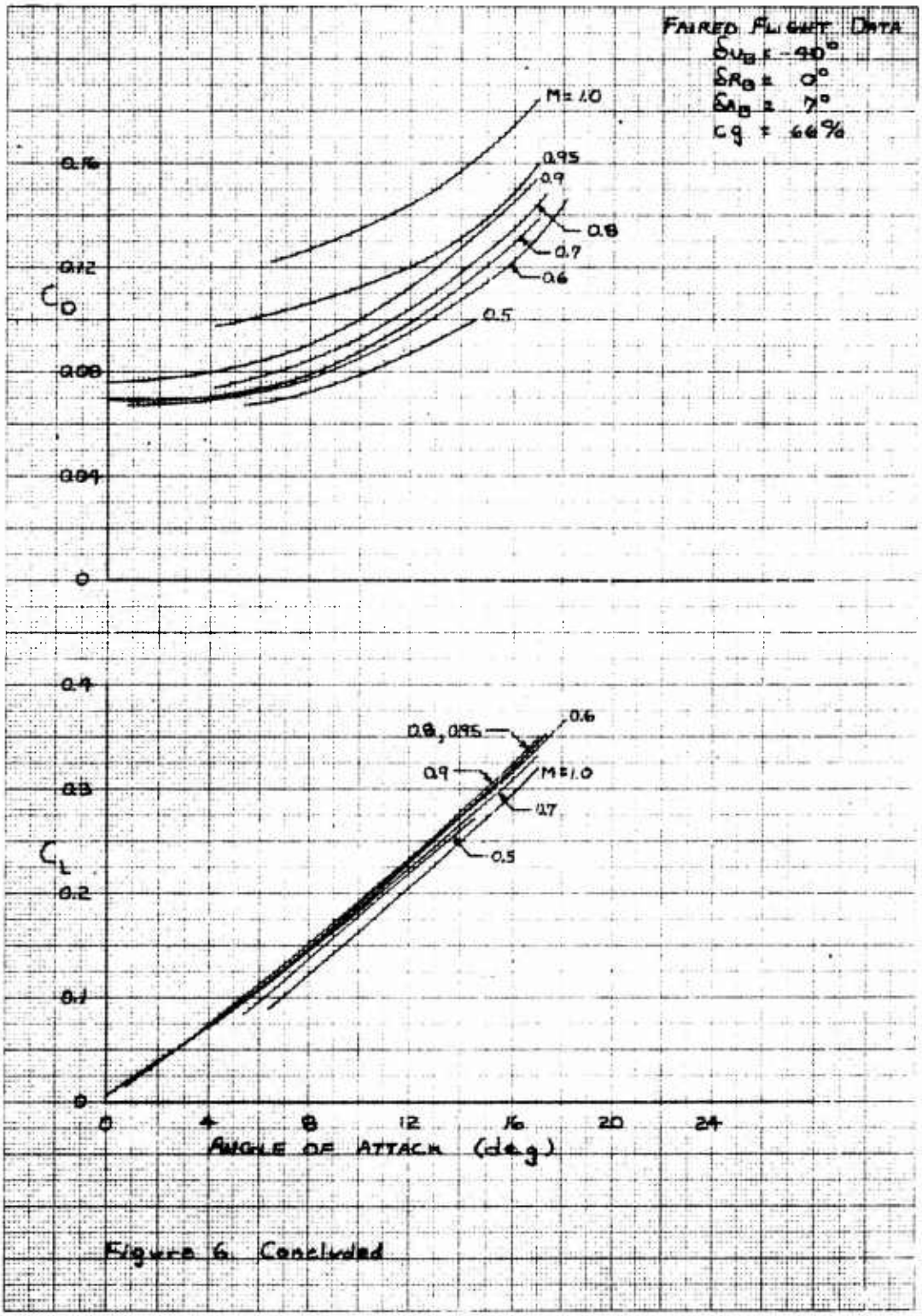

Figure 6. Concluded

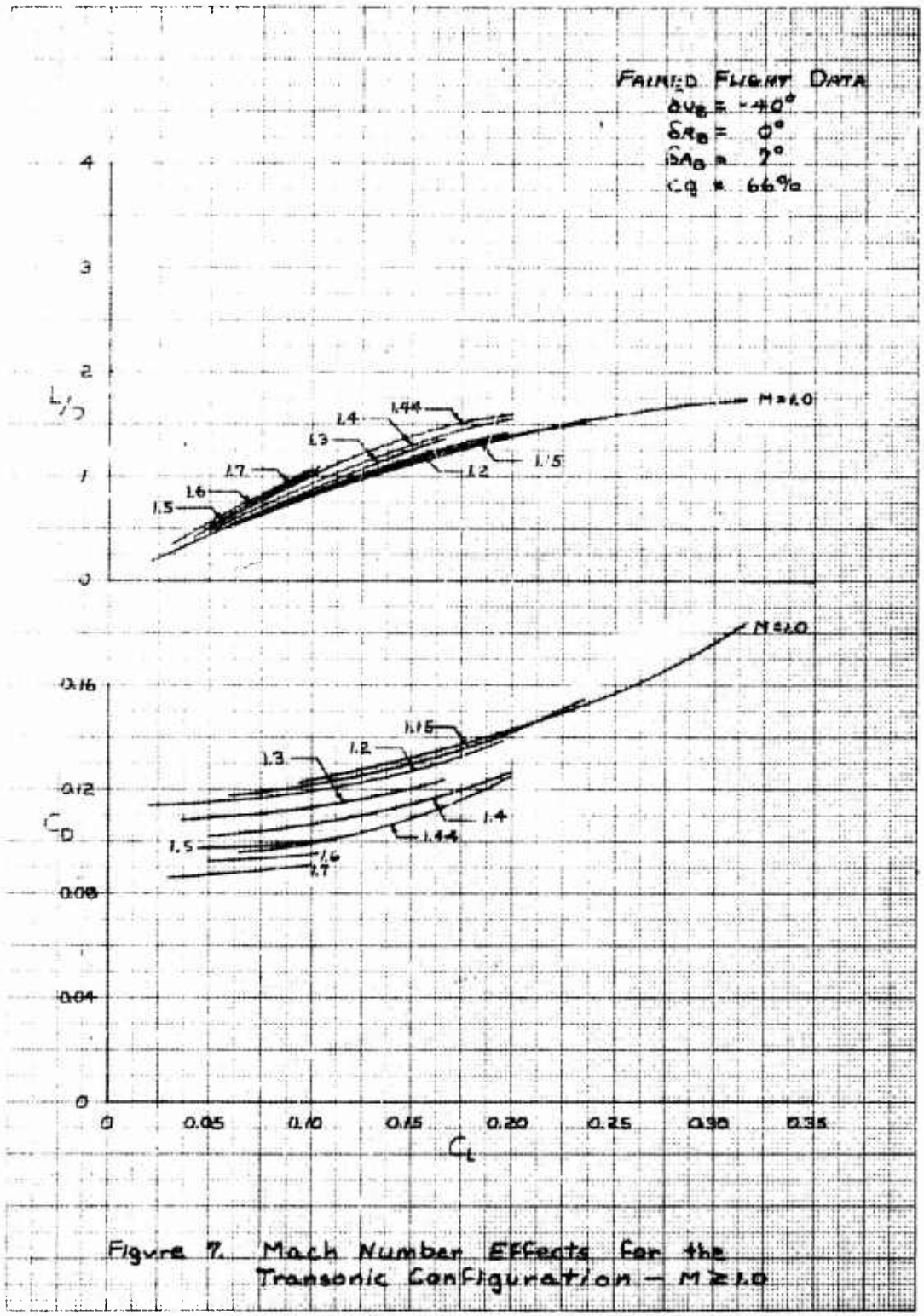

Figure 7. Mach Number Effects for the Transonic Configuration — M ≥ 1.0

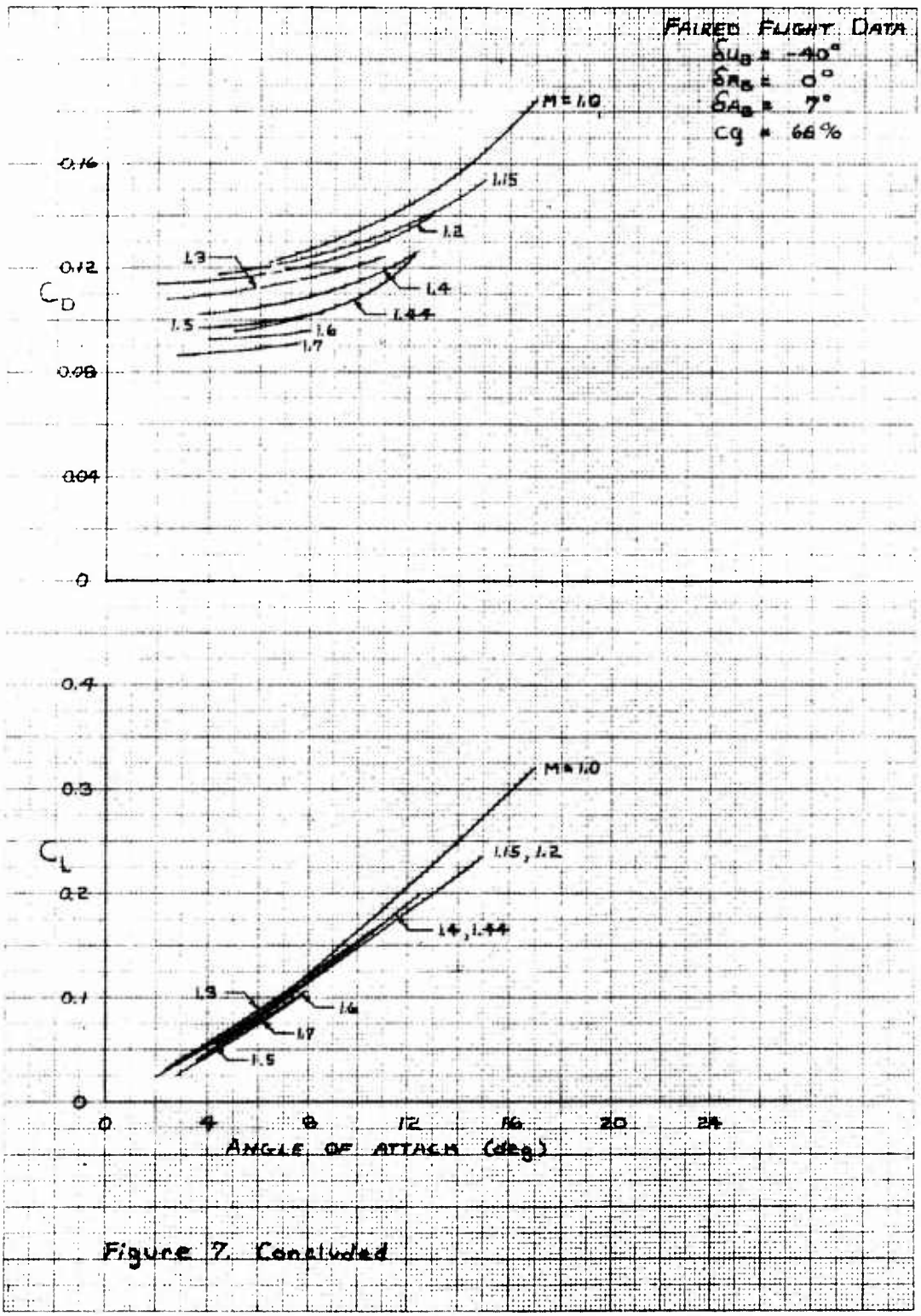

Figure 7. Concluded

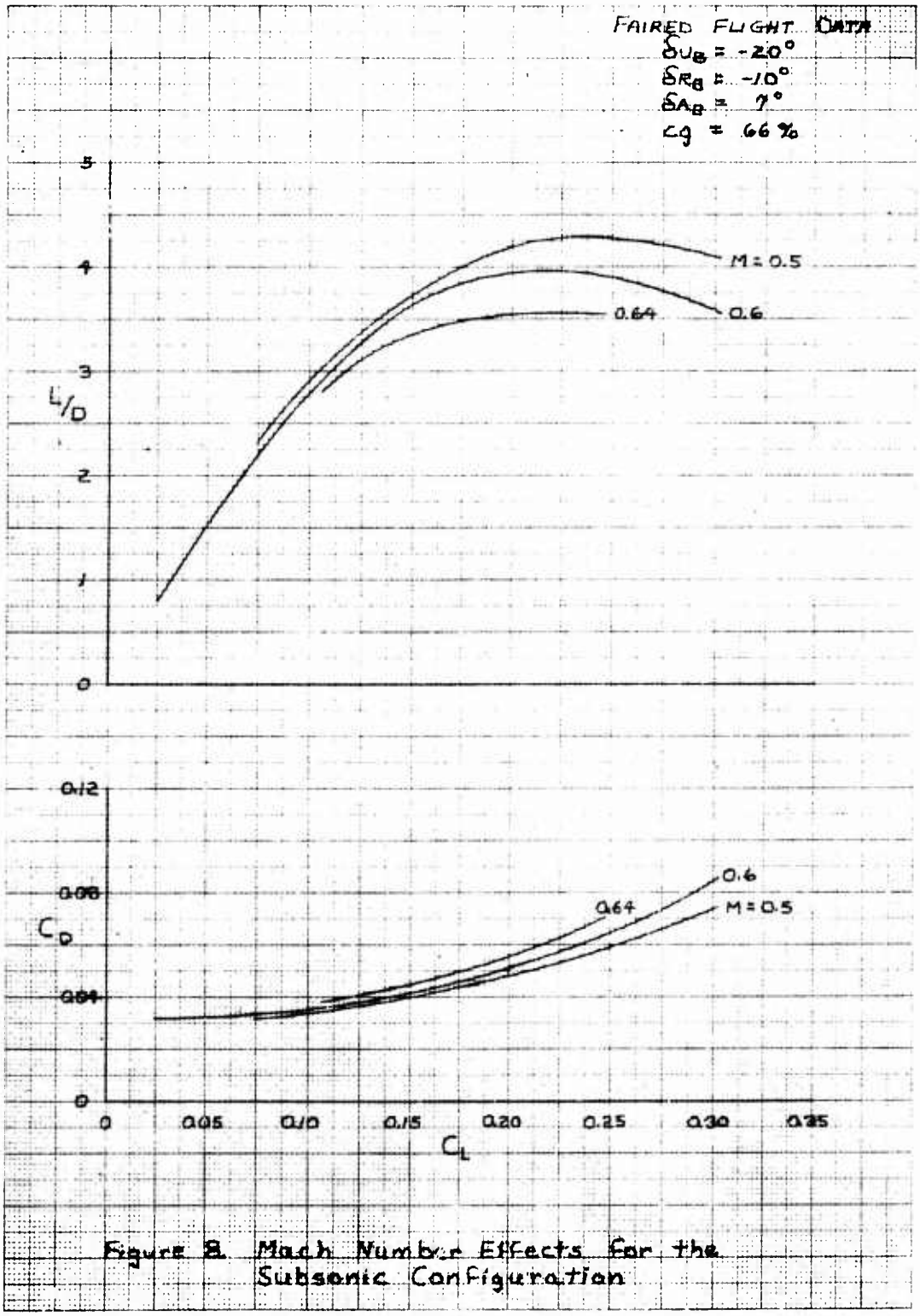

Figure 8. Mach Number Effects for the Subsonic Configuration

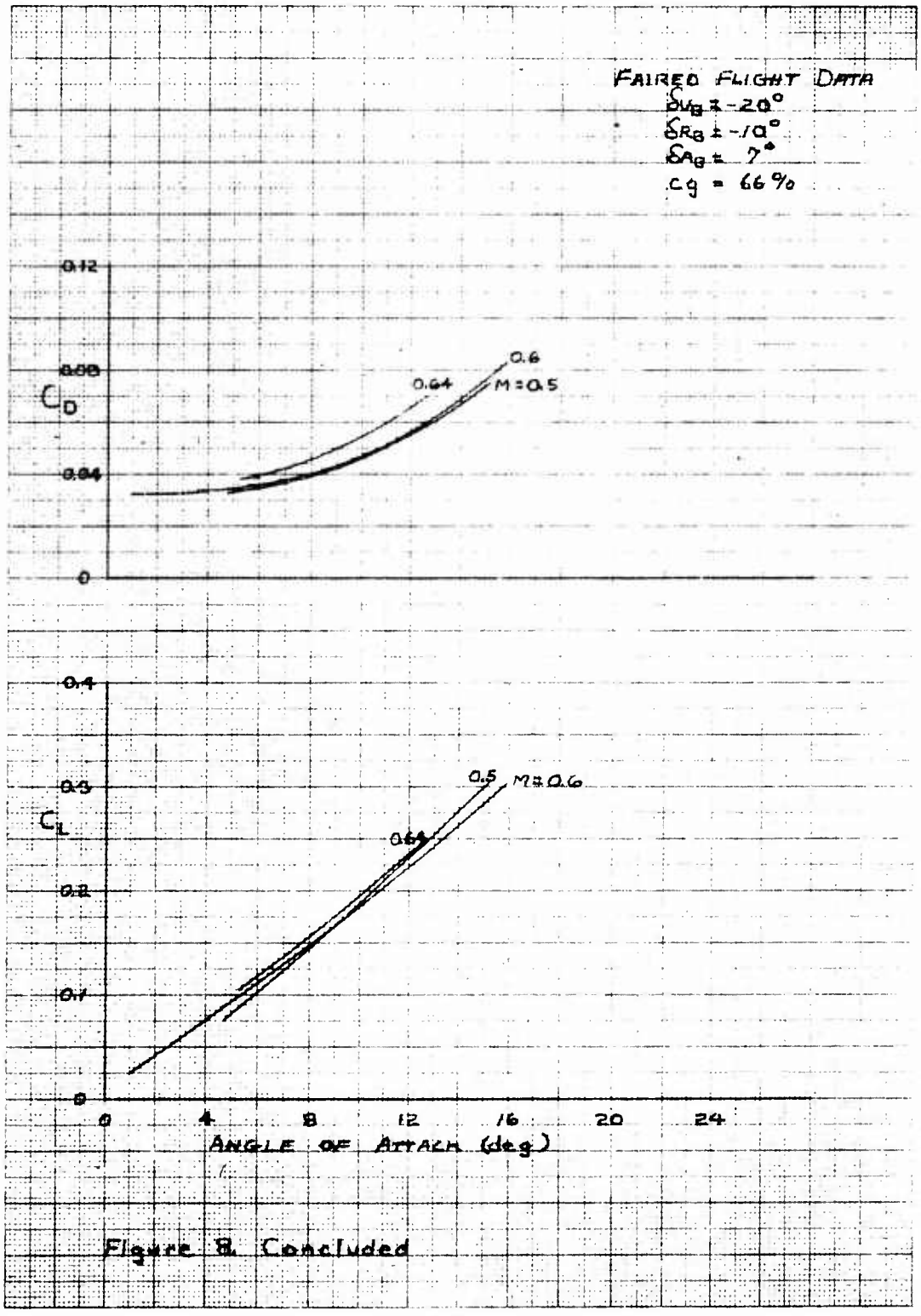

Figure 8. Concluded

Mach Number Effects on Lift-to-Drag Ratio

Flight values of maximum L/D were plotted in figure 5 for the flight maneuvers which were taken to maximum L/D. The maximum L/D for the subsonic configuration (-20 δ_B) in the landing approach phase was 4.3. These data show that in the subsonic Mach region the decrease in maximum L/D with increasing Mach number was greater for the subsonic configuration than for the transonic configuration. Again this was attributed to the intensity of the flow separation on the outboard fins in this configuration.

Faired L/D curves are plotted as a function of C_L in figures 6, 7 and 8. These data show that the L/D at the same C_L decreased as the Mach number increased to 1.0 and then it increased slightly at supersonic speeds.

Effect of Aircraft Configuration on Lift Coefficient

Since the centers of pressure of the upper flaps, lower flaps, rudders and ailerons were essentially the same distance from the center of gravity it follows that for trimmed flight, the lift-due-to-tail required for trim at a certain α would be the same regardless of which control surface was used to trim the aircraft. This also means that the trimmed lift coefficient would be independent of the flap, rudder bias or aileron bias configuration. This effect was apparent in the analysis of the wind tunnel data and was confirmed by the flight data shown in figures 9 and 10. Within the scatter of the flight test data, the trimmed lift curve was unaffected by changes in the upper flap bias, rudder bias or aileron bias settings. The movement of these control surfaces did affect the trim drag and this effect will be discussed in the ensuing sections of this report.

Data from a maneuver of special interest are shown in figure A20, Appendix A. The maximum α experienced during the X-24B program was obtained during this pullup-pushover maneuver (maximum α was 20.7 degrees). These data show a linear lift curve slope up to the maximum α at 0.5 Mach number. As expected for a delta wing shape, there was no indication of impending stall at this angle of attack.

Wedge Angle and Rudder Bias Effects

The flexibility of the X-24B flight control system provided the capability to collect performance data over a wide range of upper flap bias, lower flap, rudder bias and aileron bias positions. (The effects of aileron bias will be discussed in a later section.) Figures 11, 12 and 13 are plots of faired flight data at Mach numbers of 0.5, 0.56, and 0.64 respectively. At these Mach numbers, flight data were obtained for a wide range of aircraft configurations; however, because of predicted poor stability levels at high Mach numbers with low upper flap settings, the upper flap bias was limited to -40 degrees for all flight conditions above 0.7 Mach number. These variable control surface settings were very effective in altering the performance (trim drag) of the X-24B, particularly at 0.5 Mach number where the maximum L/D increased from approximately 2.7 to a value of 4.5 as the configuration was changed from -40 degrees to -13 degrees upper flap bias. The variable upper

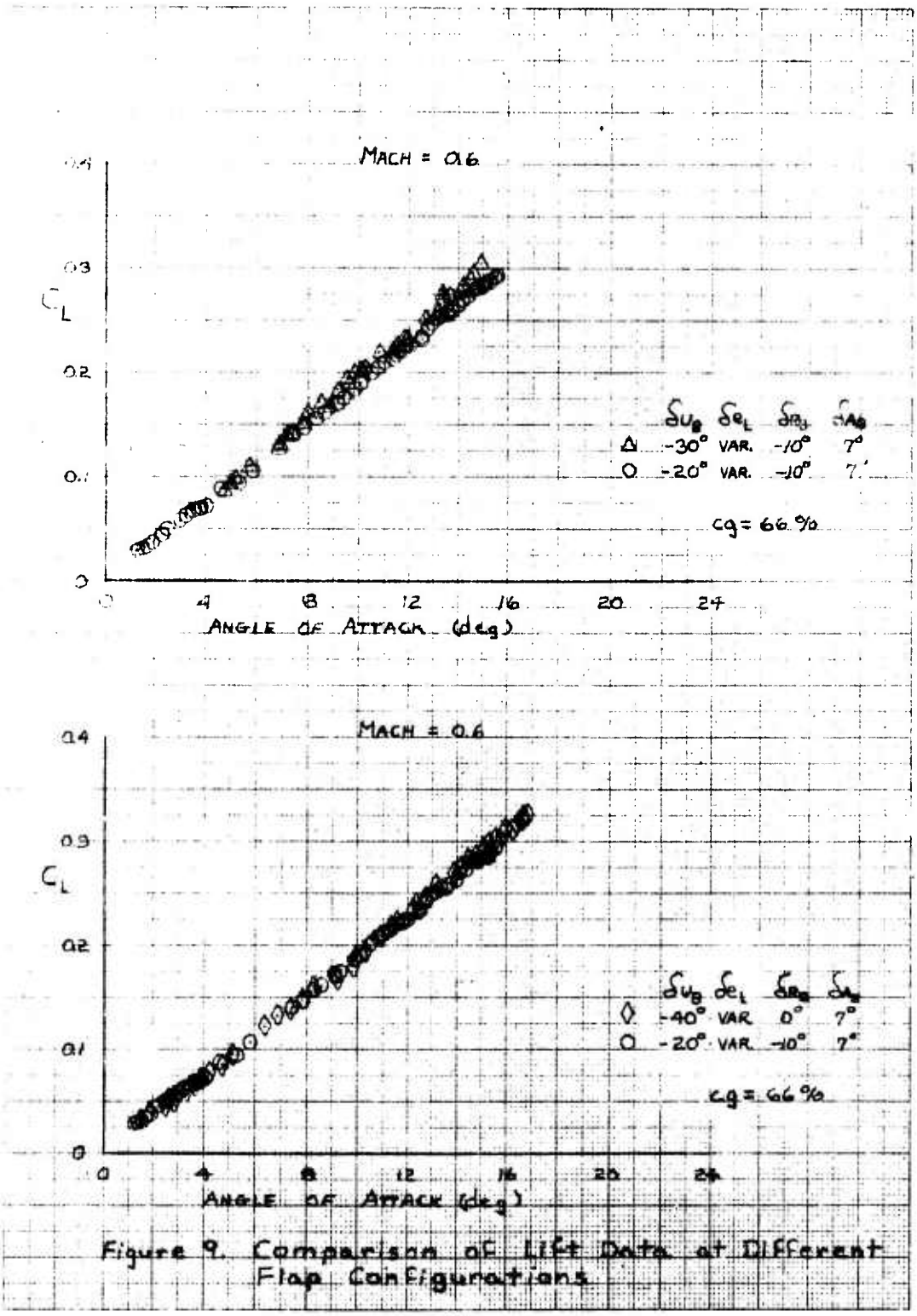

Figure 9. Comparison of Lift Data at Different Flap Configurations.

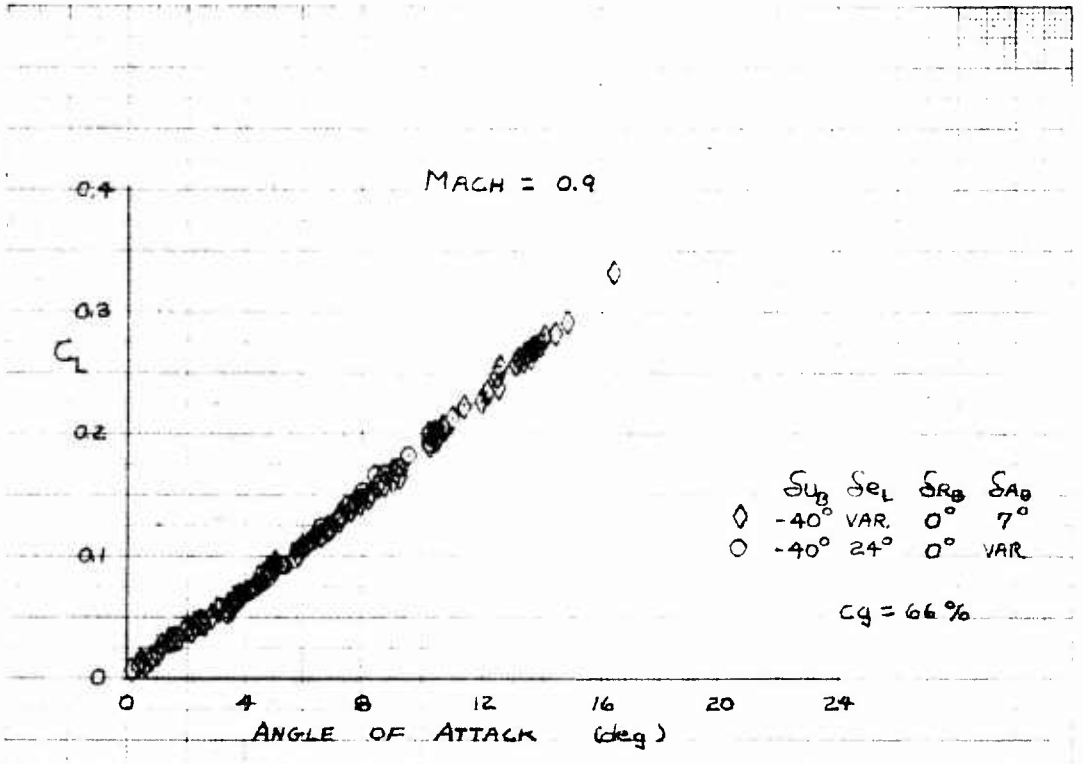

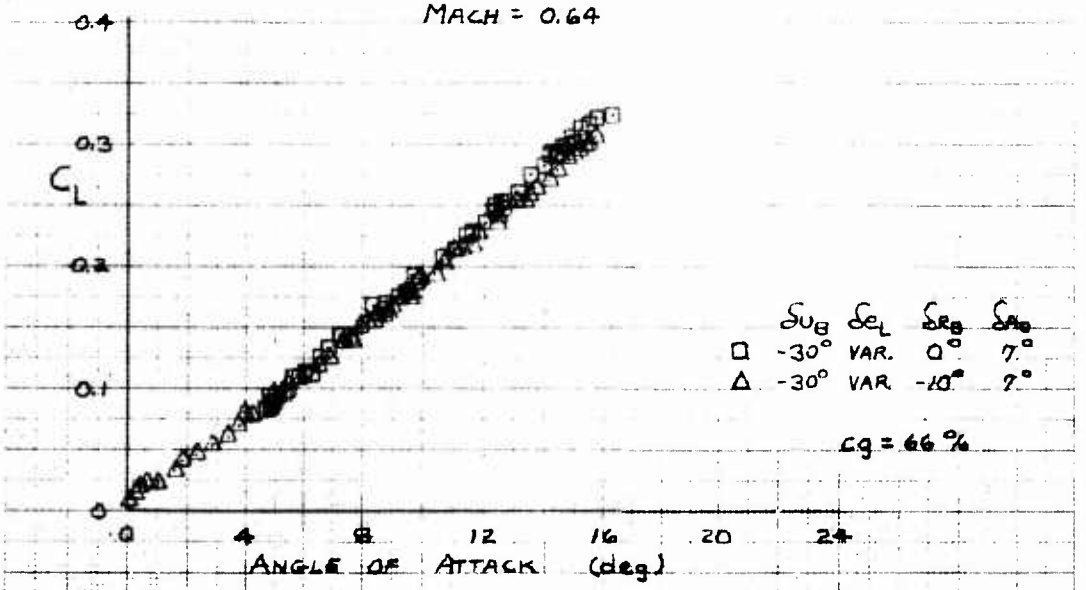

Figure 10. Comparison of Lift Data at Different Rudder and Aileron Bias Configurations

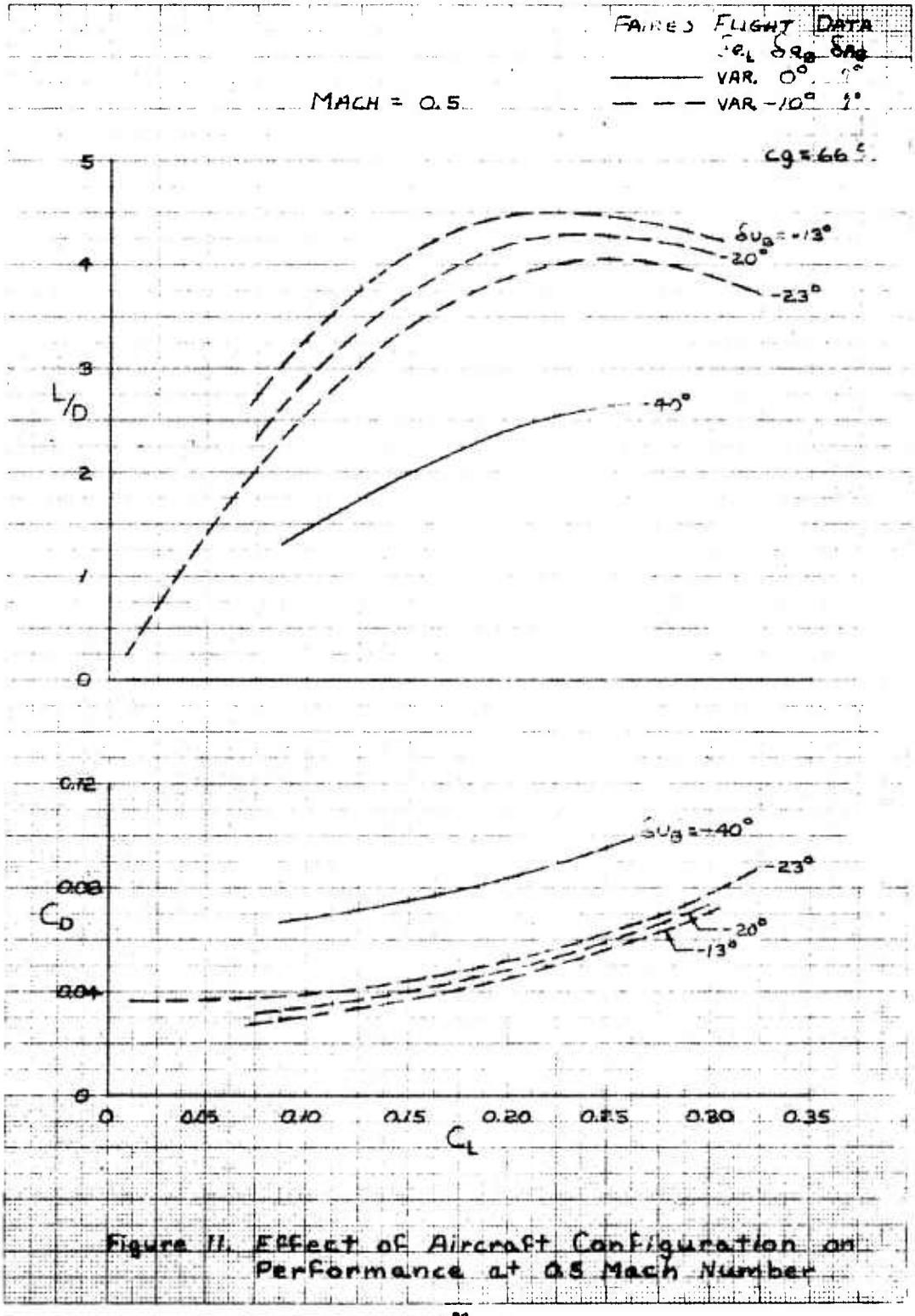

Figure 11. Effect of Aircraft Configuration on Performance at 0.5 Mach Number

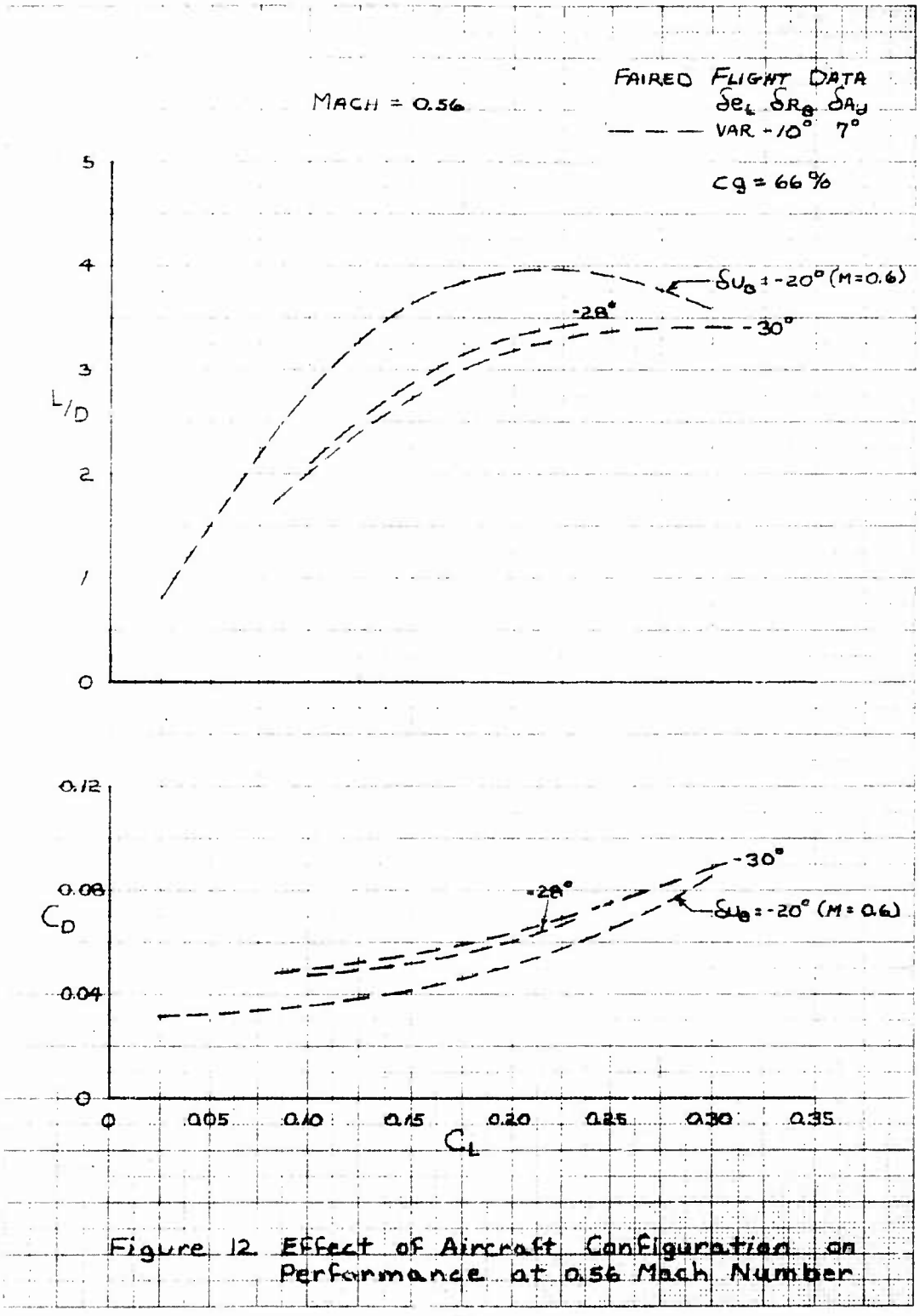

Figure 12. Effect of Aircraft Configuration on Performance at 0.56 Mach Number

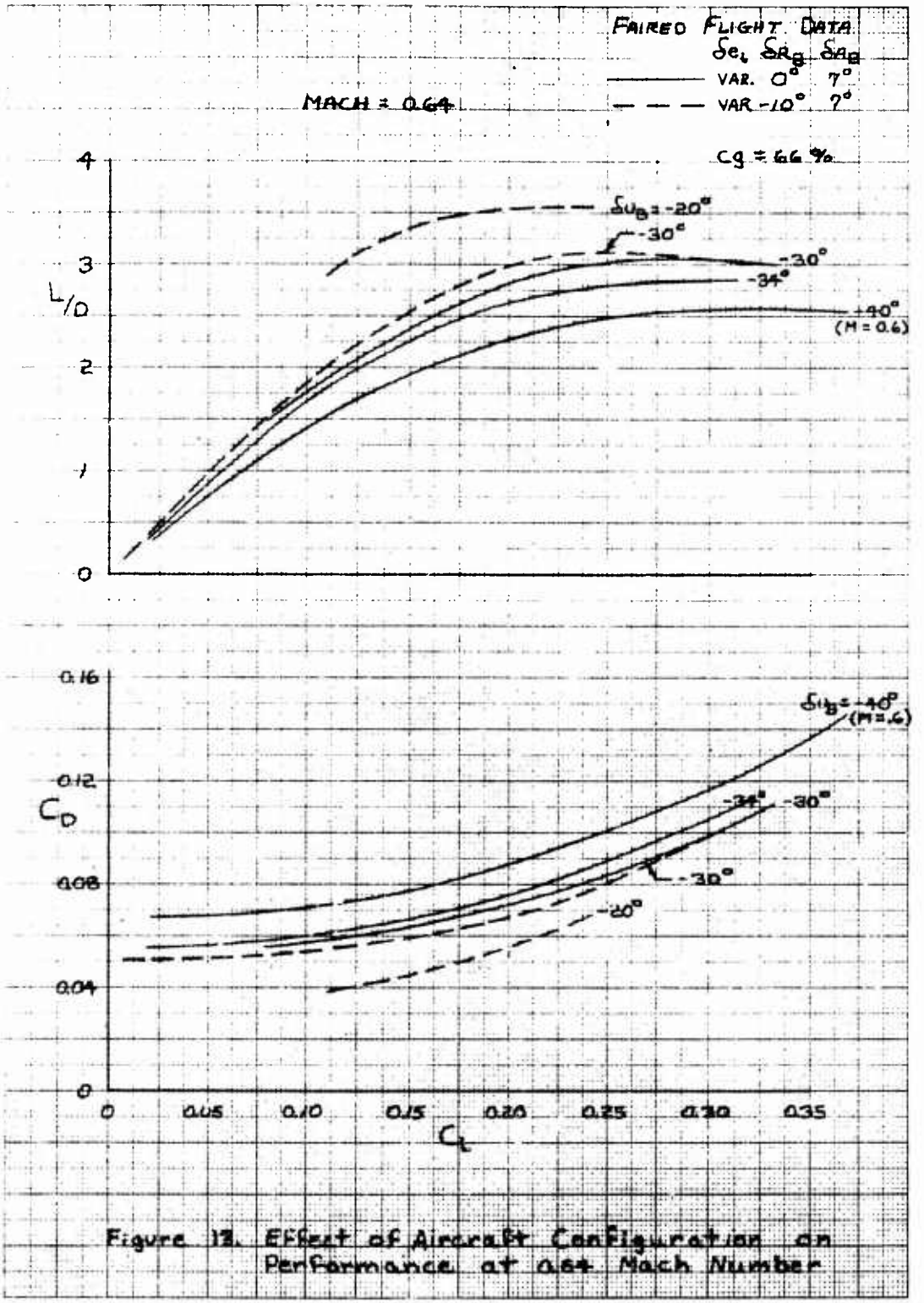

Figure 12. Effect of Aircraft Configuration on Performance at 0.64 Mach Number

flap bias feature was used as a speed brake for energy management during the landing approach pattern as discussed in reference 10.[14] As a speed brake, the upper flap bias could be modulated between the settings of -20 degrees and -40 degrees (figure 11) which provided a variation in maximum L/D from 4.3 to 2.7.

The primary effect of varying the upper flaps and lower flaps was to alter the base area and therefore the base drag of the aircraft. When the upper flaps were extended, a pitchup moment was produced which was counteracted by extending the lower flaps the correct amount to remain in trimmed flight. When the upper flaps were retracted the lower flaps were also retracted to remain in trim. The change in base area, and therefore base drag, associated with the changes in upper and lower flaps was additive and related to the change in the total angle between the upper and lower flaps or wedge angle.

Movement of the rudder bias had a direct as well as an indirect effect on trim drag. The direct effect was a strong influence on the surface pressures over the aft area of the aircraft resulting in both a change in drag and pitching moment. The indirect effect was a result of the change in pitching moment. When the rudders were biased inboard a pitchup moment was produced which was counteracted by either extending the lower flaps or by retracting the upper flaps, thereby changing the base area and thus the base drag.

Wedge Angle and Rudder Bias Effects on Drag Coefficient

Analysis of wind tunnel data indicated that the drag coefficient for a particular rudder bias, aileron bias, Mach number and trim lift coefficient could be related directly to wedge angle, regardless of the individual positions of upper and lower flaps. This was also assumed to be true of the flight data, thus allowing a comparison between flight and wind tunnel results. This meant that from the flight test data, the direct effect of the rudder bias could be separated from the indirect or wedge angle effect.

The faired lines in figures 11 and 12 were cross plotted as C_D versus δw for a constant trimmed C_L of 0.15 in figures 14 for 0.5 to 0.6 Mach number.[15] These data show that the slope $\Delta C_D/\Delta \delta w$ increased with wedge angle as was predicted by the wind tunnel data. There was good agreement between flight and predicted data at the low values of wedge angle; however, the flight data was 14 percent less than predicted at the larger wedge angles (table 3).

---

[14] Reference 10: Stuart, John L., Captain USAF, Analysis of the Approach, Flare, and Landing Characteristics of the X-24B Research Aircraft, AFFTC-TR-76-9, Air Force Flight Test Center, Edwards AFB, California, to be published.

---

[15] The data had to be plotted at constant values of lift coefficient to keep the effects of drag-due-to-lift constant for the different wedge angles. The C_L value of 0.15 was picked because it represents an average flight condition of 8 to 9 degrees α.

FAIRED FLIGHT DATA FROM FIGURES 11 & 12

	δ_{U_B}	δ_{e_L}	δ_{R_B}	δ_{A_B}	MACH
◇	-13°	1°	-10°	7°	0.5
◇	-20°	10.6°			
◁	-23°	14.7°			
○	-20°	10.8°			0.6
□	-28°	20.3°			0.56
△	-30°	22.0			

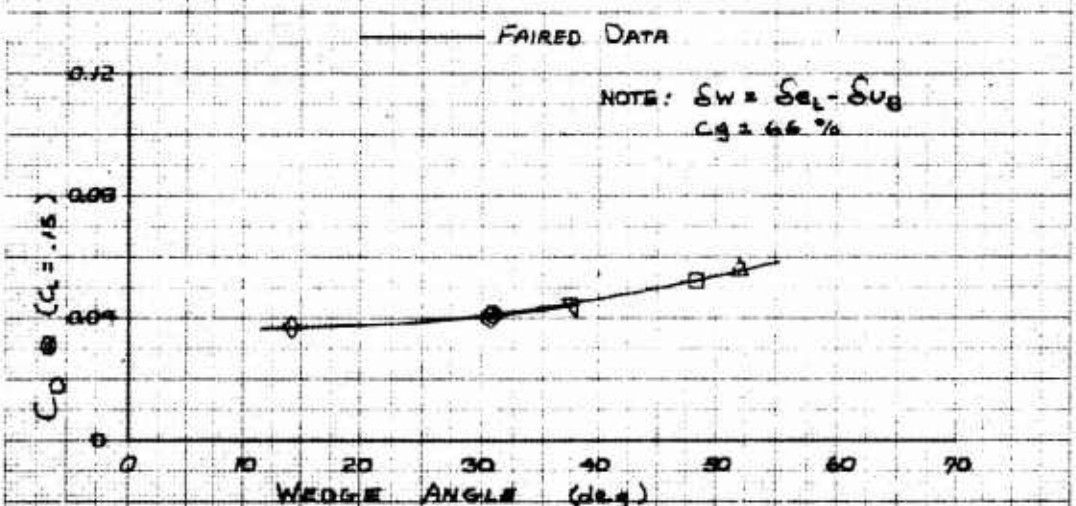

Figure 14. Drag Coefficient versus Wedge Angle

Table 3

EFFECT OF WEDGE ANGLE AND RUDDER BIAS ON DRAG

M =.5 to 0.6		
Wedge Angle (deg)	Predicted $\Delta C_D/\Delta\delta w$ (per deg)	Flight $\Delta C_D/\Delta\delta w$ (per deg)
17.5	0.00020	0.00020
25	0.00035	0.00030
35	0.00070	0.00060
50	0.00095	0.00082
65	0.00110	No Data
Predicted $\Delta C_D/\Delta\delta R_B$ = 0.00088/deg Flight $\Delta C_D/\Delta\delta R_B$ = 0.00080/deg	at M = .64	

The rudder bias effects were separated from the wedge angle effects by cross plotting the faired lines from figure 13 as C_D versus δw for a constant C_L of 0.15 in figure 15 for 0.64 Mach number. The vertical separation of the 0- and -10-degree δR_B lines in this figure shows a reduction in drag as the rudders were biased inboard at a constant wedge angle (direct effect of rudder bias). A comparison of the two -30-degree δR_B points shows that this decrease in drag was partially counteracted by the increase in wedge angle and drag associated with extension of the lower flap to return to trim (indirect effect of rudder bias). The net result was a decrease in drag as the rudders were biased inboard. The comparison between flight and predicted data for the direct effect of rudder bias was good at 0.64 Mach number (table 3).

A limited amount of data were obtained at 1.3 Mach number with the rudders biased outboard to 5 degrees (figure A10, Appendix A). These data show a small increase in drag as was predicted in the wind tunnel.

Rudder Bias Effects on Lift-to-Drag Ratio

The combined effects of rudder bias and wedge angle are shown in figure 15 for 0.64 Mach number. The vertical separation of the lines in this figure shows that the direct effect of biasing the rudders inboard was an increase in performance by an increment of 0.3 L/D. This increase in L/D was partially counteracted by the increase in wedge angle associated with the extension of the lower flap to return the aircraft to trim conditions. The net increase in L/D as the rudders were biased inboard was 0.16 L/D at a Mach number of 0.64 and a C_L of 0.15.

Aileron Bias Effects

Performance flight data with different aileron bias settings were obtained using two procedures. The first method was to fix the aileron bias at various settings and perform a pushover-pullup maneuver in the usual manner. The second method was to fix the upper and lower flap settings and then sweep the aileron bias to vary angle of attack. Figure 16 contains faired flight data obtained from both methods at 0.6 Mach number. Comparison of the performance data shows a net decrease in drag (increase in L/D) as the ailerons were biased downward from 7 degrees.

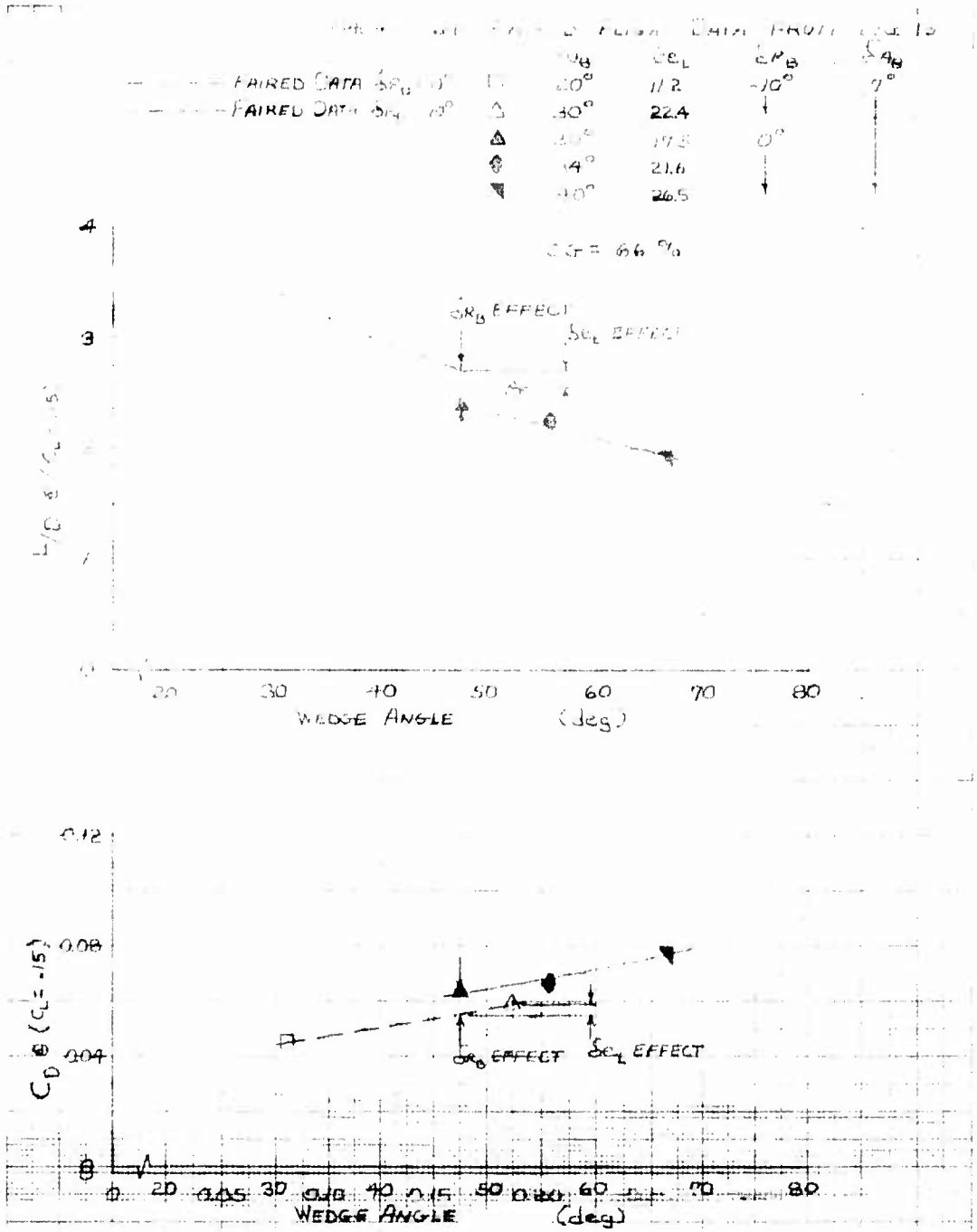

Figure 15. Effect of Wedge Angle and Rudder Bias on Performance

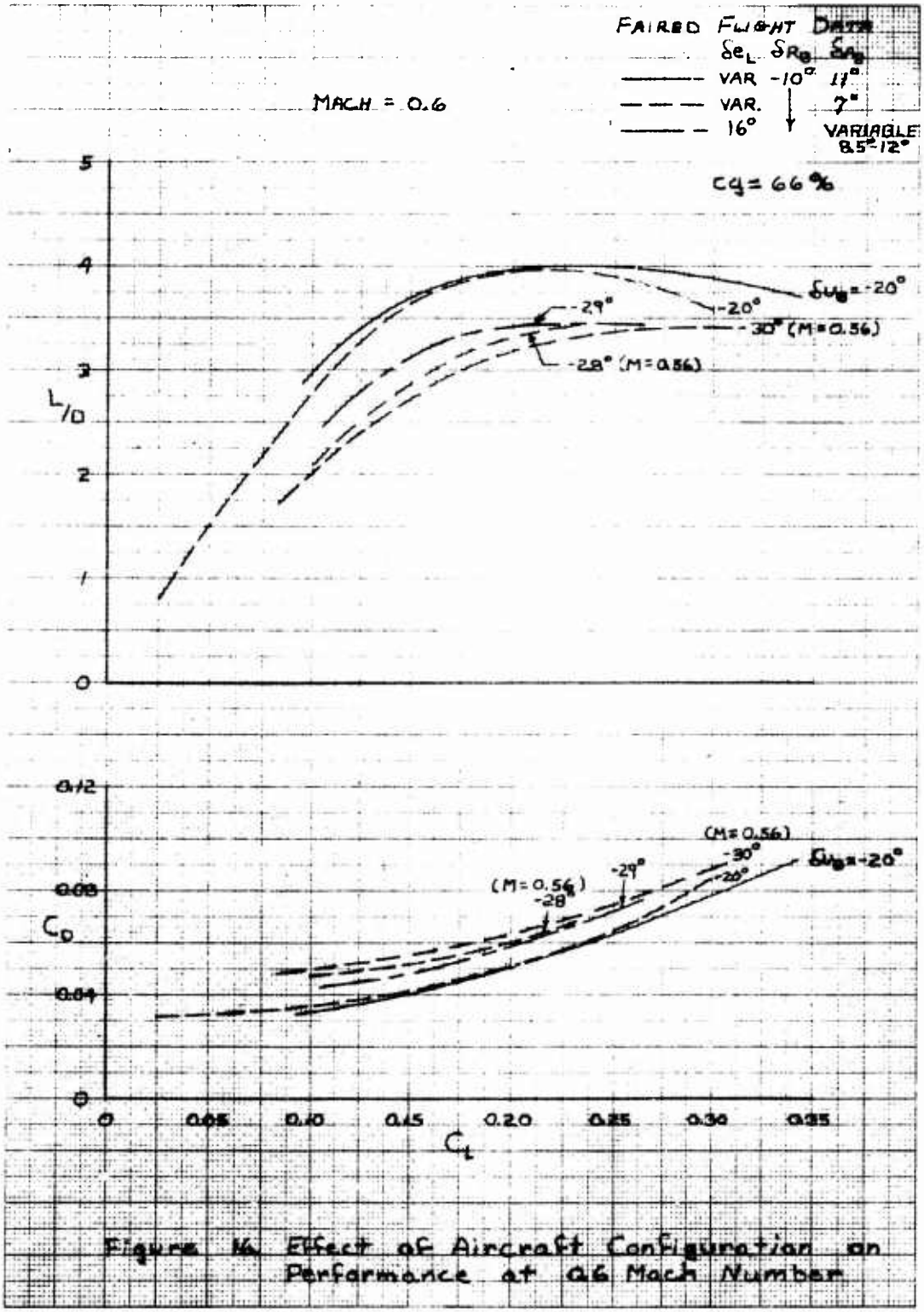

Figure 14 Effect of Aircraft Configuration on Performance at .6 Mach Number

Movement of the aileron bias had a direct, as well as an indirect effect, on trim drag in the same manner as rudder bias movements. The direct effect of aileron bias was separated from the wedge angle effect by cross plotting the data from figure 16 as plots of L/D and C_D versus δw for a constant C_L of 0.15 in figure 17. The vertical separation between the 7-degree δA_B line and the 11-degree δA_B data points in this figure shows a small increase in drag for one case and a decrease in drag in the other case as the ailerons were biased downward at a constant wedge angle (direct effect of aileron bias). The wind tunnel data predicted a small decrease in drag at 0.6 Mach number as the ailerons were biased from 7 to 11 degrees. In any event, the flight data was consistent with the predicted data in that the direct effect of moving δA_B was small. A comparison of the two -20-degree δU_B points, and the -38- to -30-degree δU_B points shows that the major portion of the net decrease in drag was due to the decrease in wedge angle associated with the retraction of the lower flaps to return the aircraft to trim (indirect effect of aileron bias).

Figure 18 contains flight data at 0.9 and 1.25 Mach number obtained from aileron-bias-sweep maneuvers. At these Mach numbers, the data showed a net increase in L/D as the ailerons were biased downward from 7 degrees. However, in these cases the direct effect of aileron bias could not be separated from the wedge angle effect because the flight data could be obtained at only one upper flap bias setting due to stability considerations at these Mach numbers.

Landing Gear Effects

Figures 19 and 20 compare landing gear-up and gear-down faired flight test data for the two upper flap bias configurations of -20 and -23 degrees. Most of the gear-down data was obtained in the -20-degree δU_B configuration (33 of the 36 X-24B landings were in this configuration). Gear-down data show an increase in lift curve slope at higher angles of attack, increased drag and a significant decrease in L/D (figure 22) when compared to the corresponding gear-up data. Deployment of the landing gear produced a very slight nose down trim change which required a small decrease in lower flap (less than two degrees) to return the aircraft to the same trim angle of attack. This decrease in lower flap had a negligible effect on drag at the low values of wedge angle associated with the landings (20 to 30 degrees δw; $\Delta C_D < 0.0006$). Therefore, the differences between gear-up and gear-down data were due almost entirely to the landing gear alone.

At angles of attack greater than 10 degrees, the gear-down lift curve slope was steeper than the gear-up slope by 30 to 40 percent (figures 19 and 20). The increase in lift curve slope was probably due to ground effect since the gear-down data were obtained during actual X-24B landings where the landing gear was extended at approximately 100 feet above the runway. The data at the higher angles of attack were obtained closer to the ground as the aircraft approached the touchdown point and were therefore more strongly influenced by ground effect.

The incremental change in drag due to the landing gear is summarized in figure 21. The average value of the drag increment was 0.015 and the comparison was excellent with the wind tunnel predictions.

The gear-up and gear-down L/D for the -20-degree δU_B configuration are shown in figure 22. The maximum L/D was reduced by 17 percent when the landing gear was deployed (L/D reduced from 4.3 to 3.55 in ground effect).

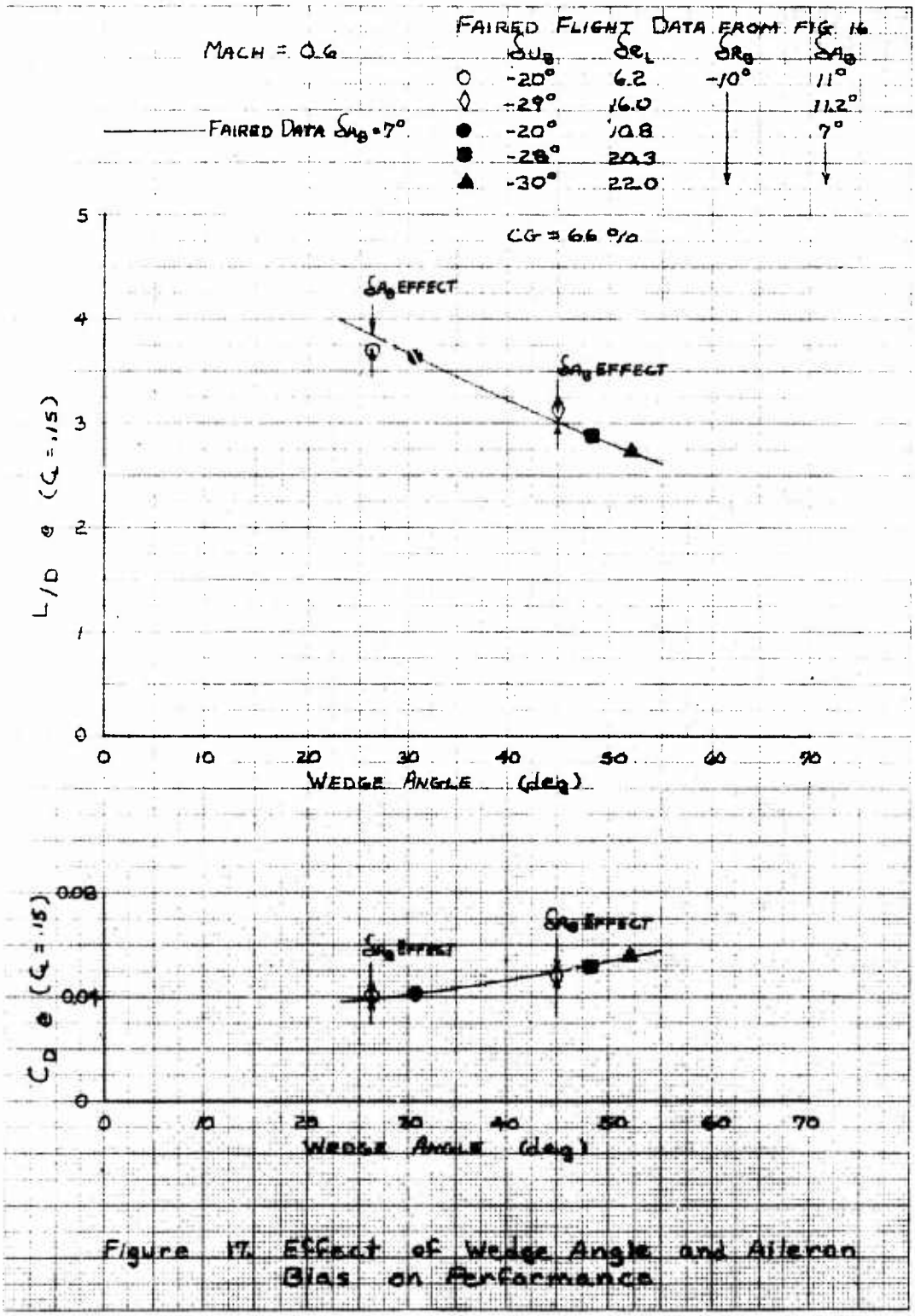

Figure 17. Effect of Wedge Angle and Aileron Bias on Performance

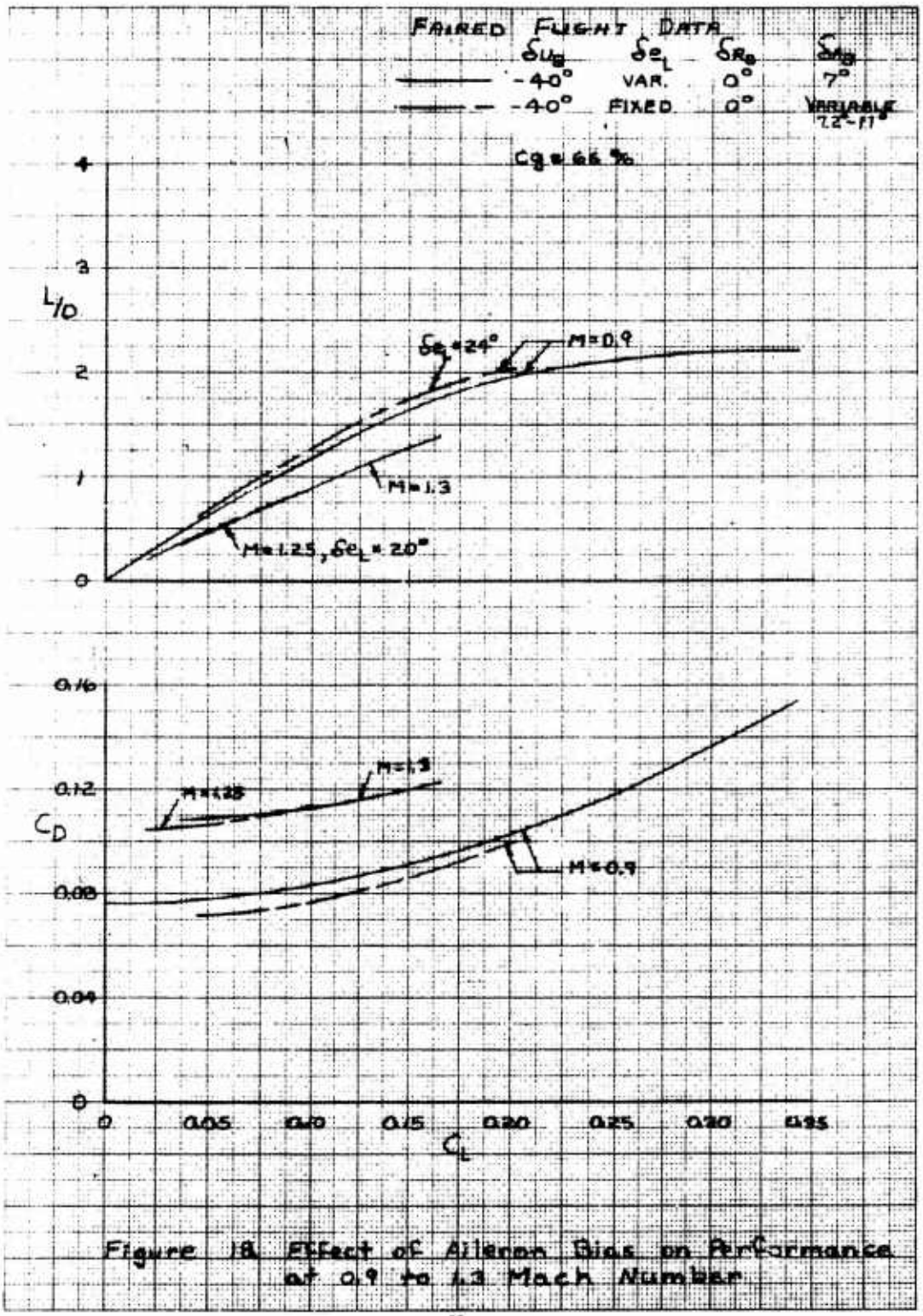

Figure 18. Effect of Aileron Bias on Performance at 0.9 to 1.3 Mach Number

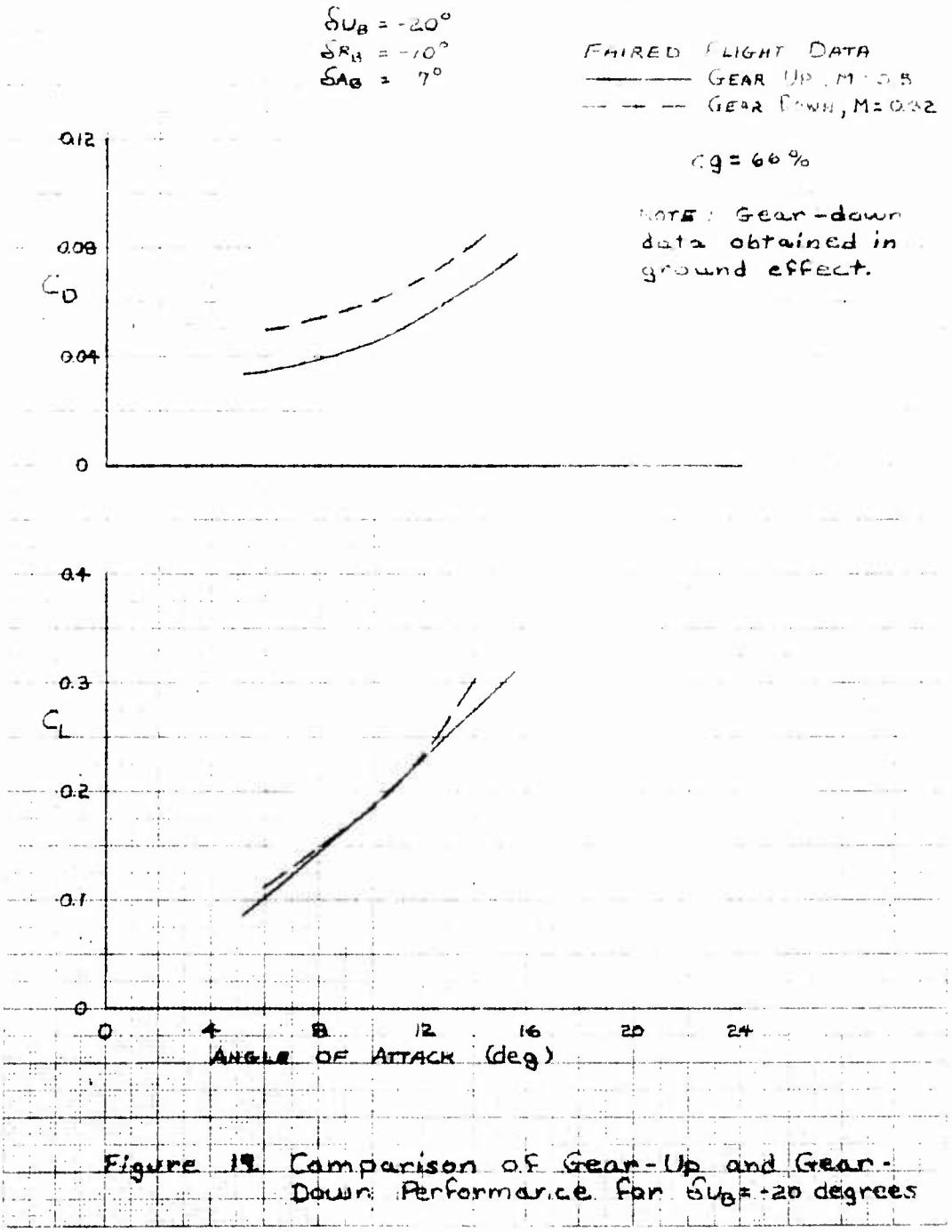

Figure 19. Comparison of Gear-Up and Gear-Down Performance for $\delta U_B = -20$ degrees

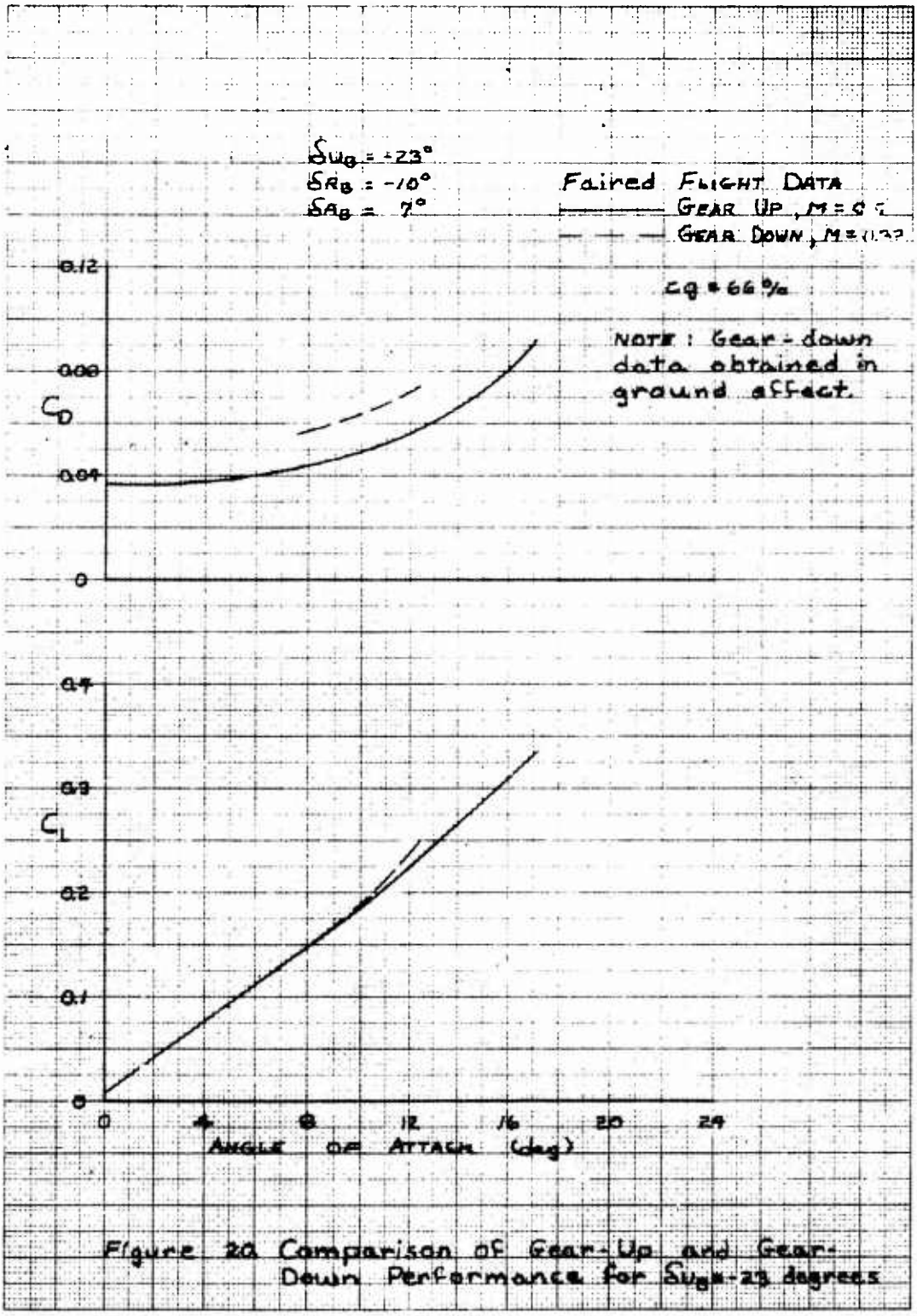

Figure 20 Comparison of Gear-Up and Gear-Down Performance for $\delta_{LE} = 23$ degrees

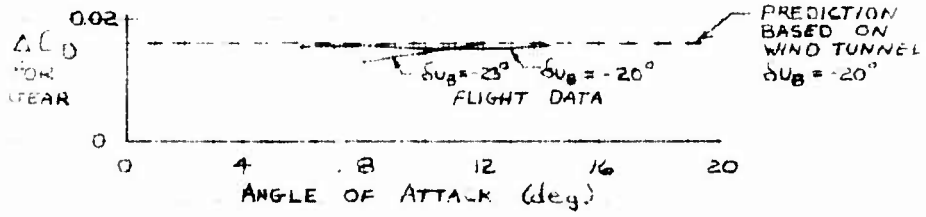

Figure 21. Drag Increment due to the Landing Gear

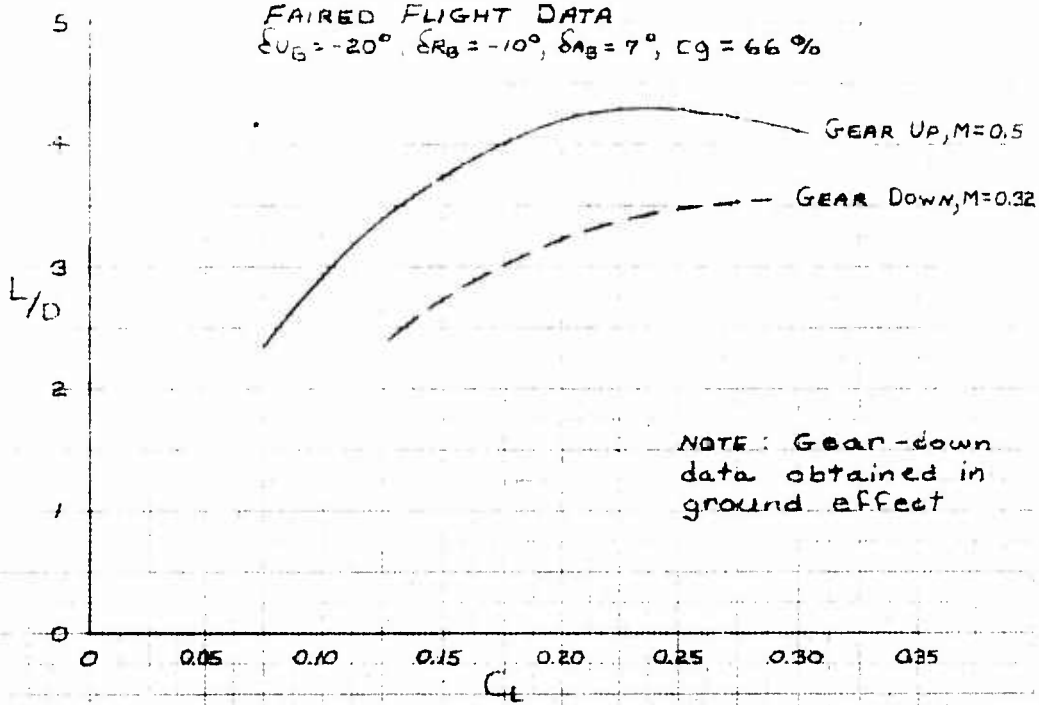

Figure 22. Comparison of Gear-Up and Gear-Down Lift-to-Drag Ratio for $\delta_{U_B} = -20$ degrees

CONCLUSIONS

The trim performance characteristics of the X-24B were determined for several configurations, including landing gear extended, and covered the Mach number range of 0.26 to 1.72. Although stabilized Mach number conditions were difficult to achieve and the flight time was limited, sufficient data were obtained to provide a comprehensive picture of the aircraft's lift and drag characteristics.

The magnitudes of lift and drag predicted by the wind tunnel tests were generally in good agreement with the flight data for most conditions. The angle of attack for zero lift was two degrees lower than predicted. The lift curve slope was less than predicted at all Mach numbers except 0.5. The drag-due-to-lift was greater than predicted in all cases primarily due to the differences in trim lift data. The reduction in static longitudinal stability, which resulted in a change in trim lower flap and trim drag, accounted for the differences between flight and predicted values of trim drag as function of α. The maximum L/D was less than predicted by 7 percent at subsonic Mach numbers and 14 percent at 1.0 Mach number. The maximum L/D at supersonic Mach numbers could not be obtained during the flight test program since the angle of attack for maximum L/D would have placed the aircraft in an area of low directional stability. The maximum subsonic flight value of L/D was 4.5.

Significant Mach number effects were apparent in the flight data. In the subsonic Mach number region, the magnitude of lift coefficient at a particular angle of attack did not change appreciably. However, above 0.95 Mach number the lift coefficient decreased somewhat with increasing Mach number, particularly at angles of attack above 8 degrees. The drag coefficient data showed a significant drag rise between the Mach numbers of 0.9 and 1.0, as expected. The reduction in L/D with increasing Mach number which occurred at Mach numbers less than 0.64 was attributed to the intensity of the flow separation on the outboard fins in the subsonic configuration.

There was no effect of aircraft configuration on trim lift coefficient. The effect of flap configuration on drag coefficient was a total wedge angle effect. A change in wedge angle produced a corresponding change in base area which affected the base drag. The variable upper flap bias feature was used as a speed brake which provided a variation in maximum L/D of 4.2 to 2.7. Use of the aileron bias as a pitch control surface increased the trim L/D a small amount.

The effect of deploying the landing gear was a 17-percent reduction in maximum L/D from 4.3 to 3.55 in ground effect. The drag increment of the landing gear was 0.015.

REFERENCES

1. Nagy, Christopher J. and Kirsten, Paul W., Handling Qualities and Stability Derivatives of the X-24B Research Aircraft, AFFTC-TR-76-8, Air Force Flight Test Center, Edwards AFB, California, March 1976.

2. Armstrong, Johnny G., Flight Planning and Conduct of the X-24B Research Aircraft Flight Test Program, AFFTC-TR-76-11, Air Force Flight Test Center, Edwards AFB, California, to be published.

3. Ash, Lawrence G., Captain USAF, Flight Test and Wind Tunnel Performance Characteristics of the X-24A Lifting Body, Vol 1, FTC-TD-71-8, Air Force Flight Test Center, Edwards AFB, California, June 1972.

4. DeKuyper, R. E., Transonic Wind Tunnel Tests on a .08 Scale Model of the FDL-8 Lifting Body, Vol 1-4, Report No. AA-4024-W-2, Cornell Aeronautical Laboratory, Inc., Buffalo, New York, January - March 1971

5. Lindsay, E. Earl, Aerodynamic Characteristics of the AFFDL X-24B Configuration at Mach Numbers from 1.5 to 5.0, AEDC-TR-74-87, Arnold Engineering Development Center, Arnold AFS, Tennessee, September 1974.

6. White, Warren E., Documentation of Wind Tunnel Test Data From a 0.08 Scale Model of the X-24B at Mach Numbers from 0.6 to 1.3, AEDC-TR-73-18, Arnold Engineering Development Center, Arnold AFS, Tennessee, October 1973.

7. Norris, Richard B., et al., Parametric Study of an 8% Scale Model of the X-24B in the Landing Configuration, AFFDL-TM-73-21-FXS, Air Force Flight Dynamics Laboratory, Wright-Patterson AFB, Ohio, April 1973.

8. Whoric, J. M., Aerodynamic Characteristics of a 5.5 Percent Scale Model of the AFFDL X-24B Flight Test Vehicle, AEDC-TR-75-10, Arnold Engineering Development Center, Arnold AFS, Tennessee, February 1975.

9. Seiegan, David R. and Norris, Richard B., Comparison of X-24B Flight and Wind Tunnel Pressure Distributions, Air Force Flight Dynamics Laboratory, Wright-Patterson AFB, Ohio, to be published.

10. Stuart, John L., Captain USAF, Analysis of the Approach, Flare and Landing Characteristics of the X-24B Research Aircraft, AFFTC-TR-76-9, Air Force Flight Test Center, Edwards AFB, California, to be published.

APPENDIX A
FLIGHT TEST AND WIND TUNNEL TRIM PERFORMANCE DATA

NOTE: The shaded symbols on the figures in this appendix are wind tunnel trim data points for the actual control surface configurations for which data were obtained during the wind tunnel tests.

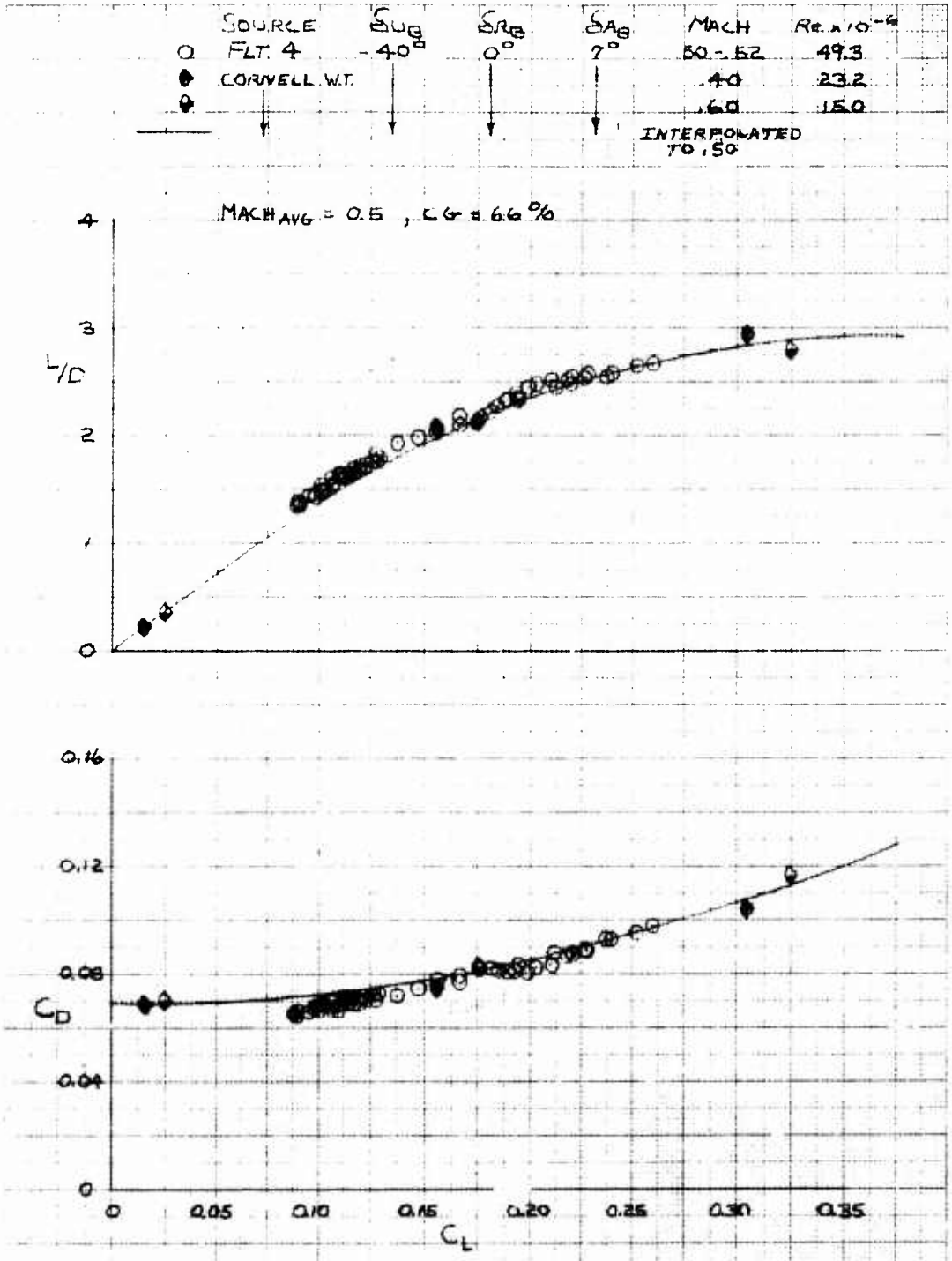

Figure A1. Trim Performance Data for δ_{u_B} = -40 degrees, δ_{R_B} = 0 degrees, δ_{A_B} = 7 degrees.

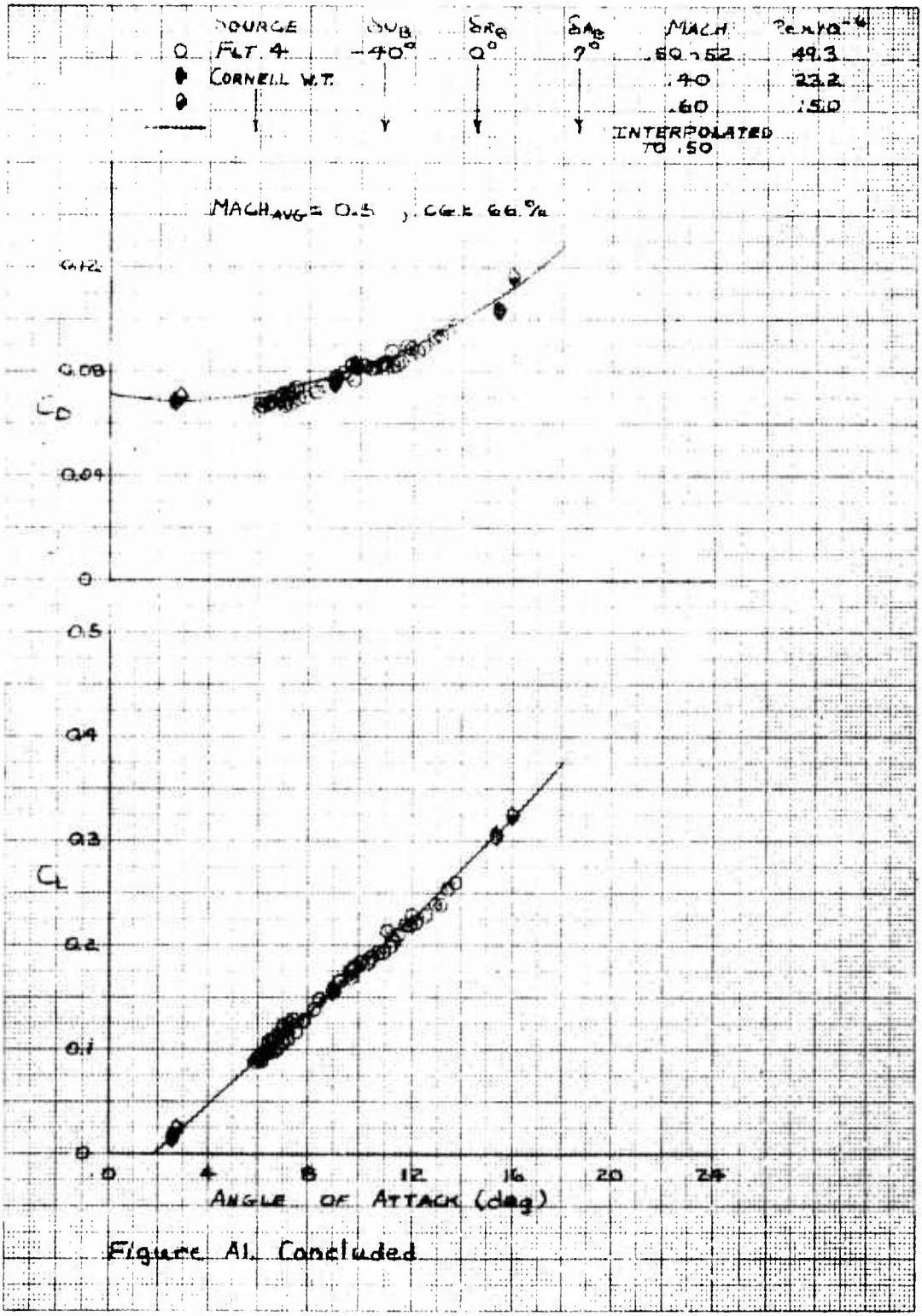

Figure A1. Concluded

	SOURCE	δ_{LE_B}	δ_{TE_B}	α	MACH	$Re \times 10^{-6}$
O	FLT 8131	-40	0	7	.59-.64	35.9 & 62.9
◆	CORNELL W.T.	↓	↓	↓	.60	15.0
▼	AEDC 16T	↓	↓	↓	.60	12.0

$MACH_{AVG} = 0.6$, $CG = 66\ \%$

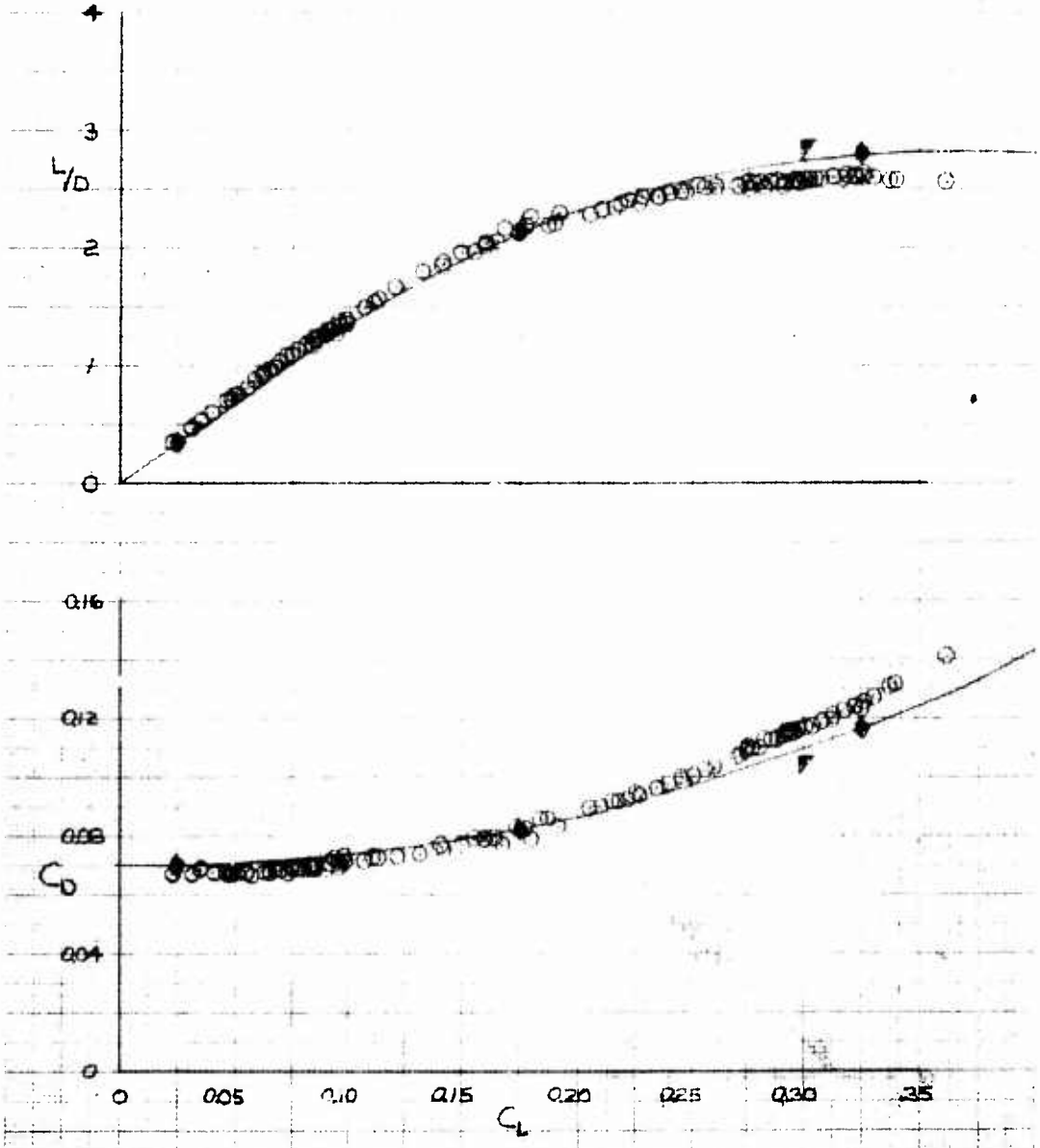

Figure A2. Trim Performance Data for $\delta_{LE_B} = -40$ degrees, $\delta_{TE_B} = 0$ degrees, $\delta_{TE_B} = 7$ degrees

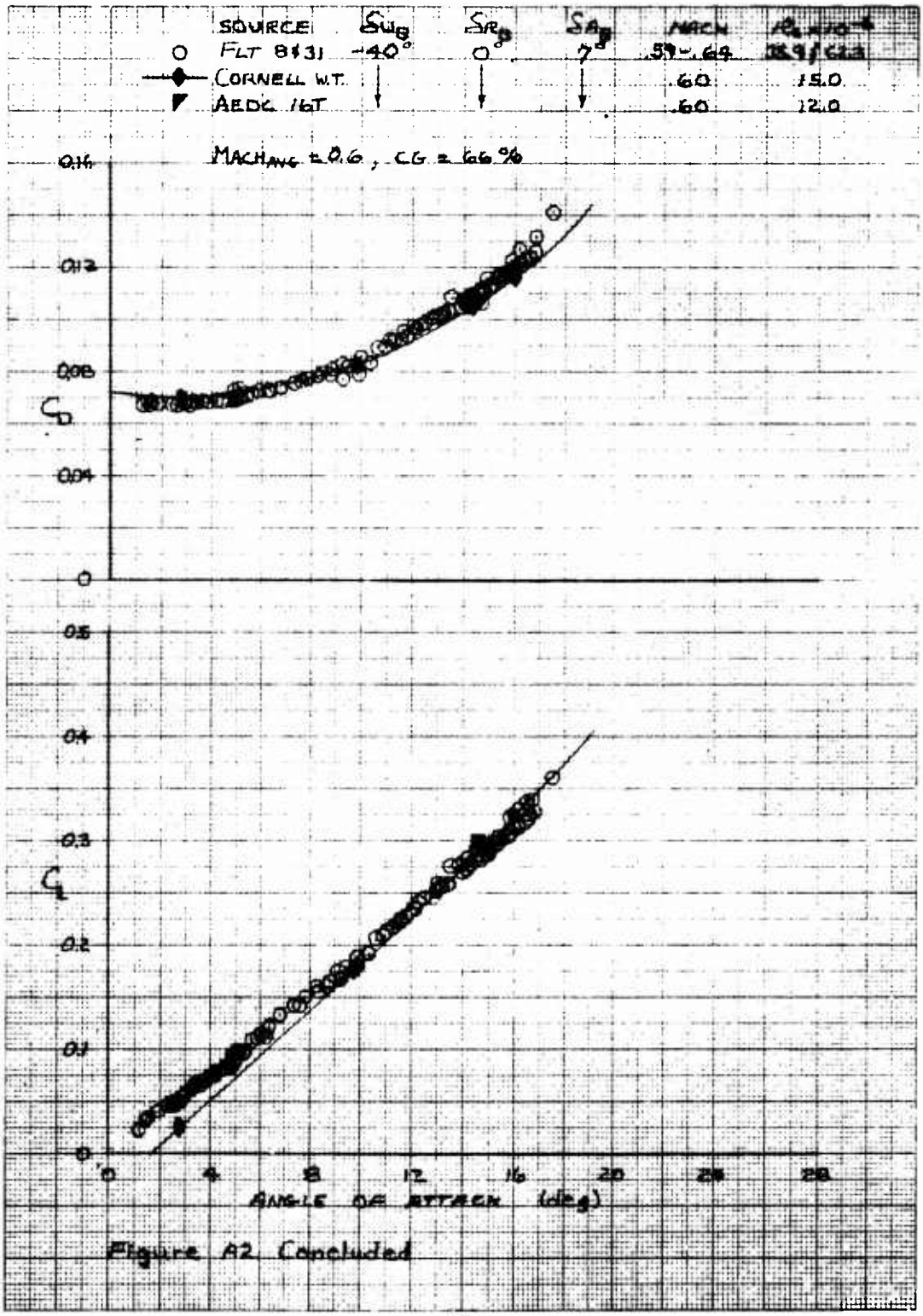

Figure A2 Concluded

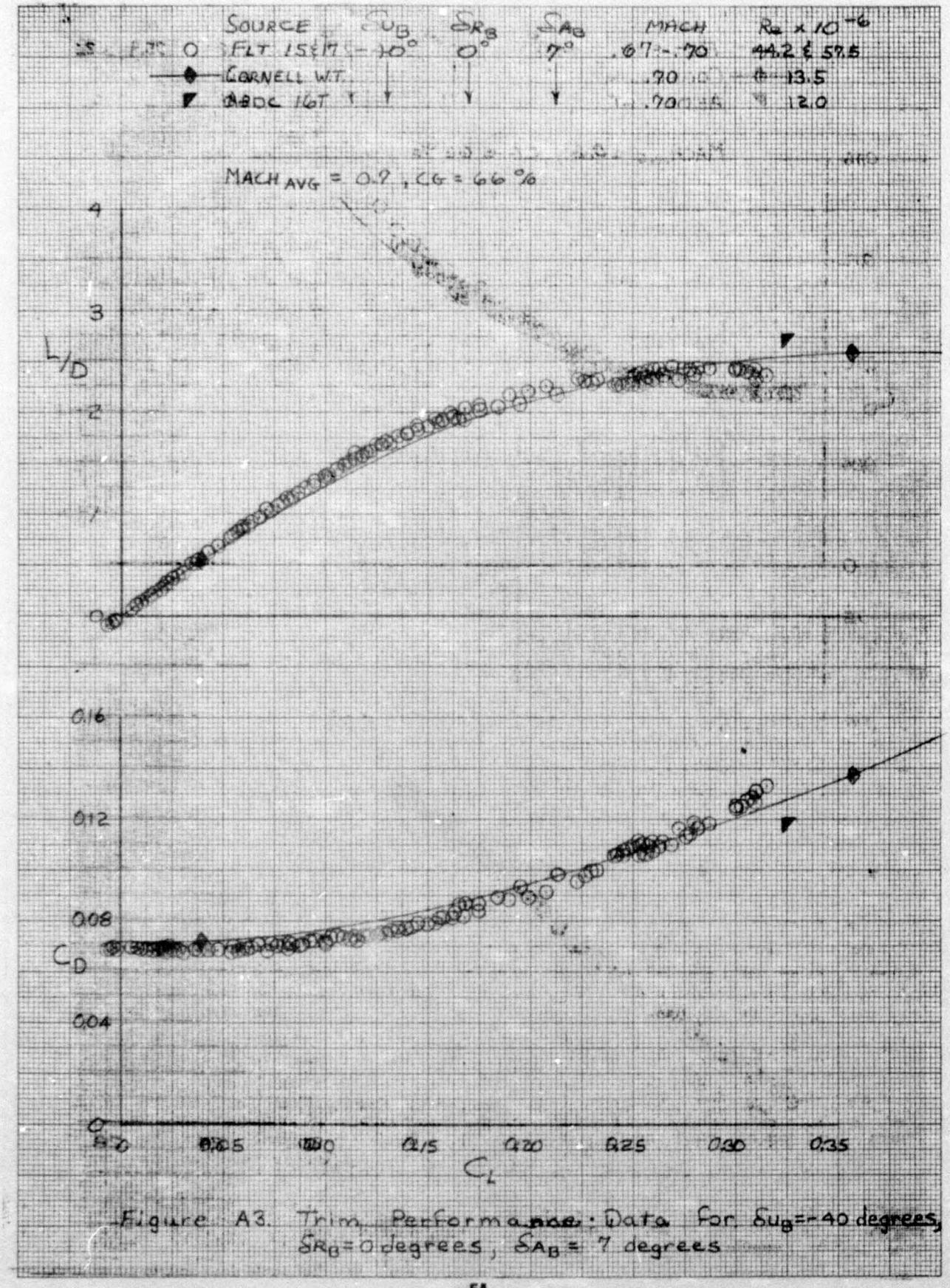

Figure A3. Trim Performance Data for δu_B = -40 degrees, δR_B = 0 degrees, δA_B = 7 degrees

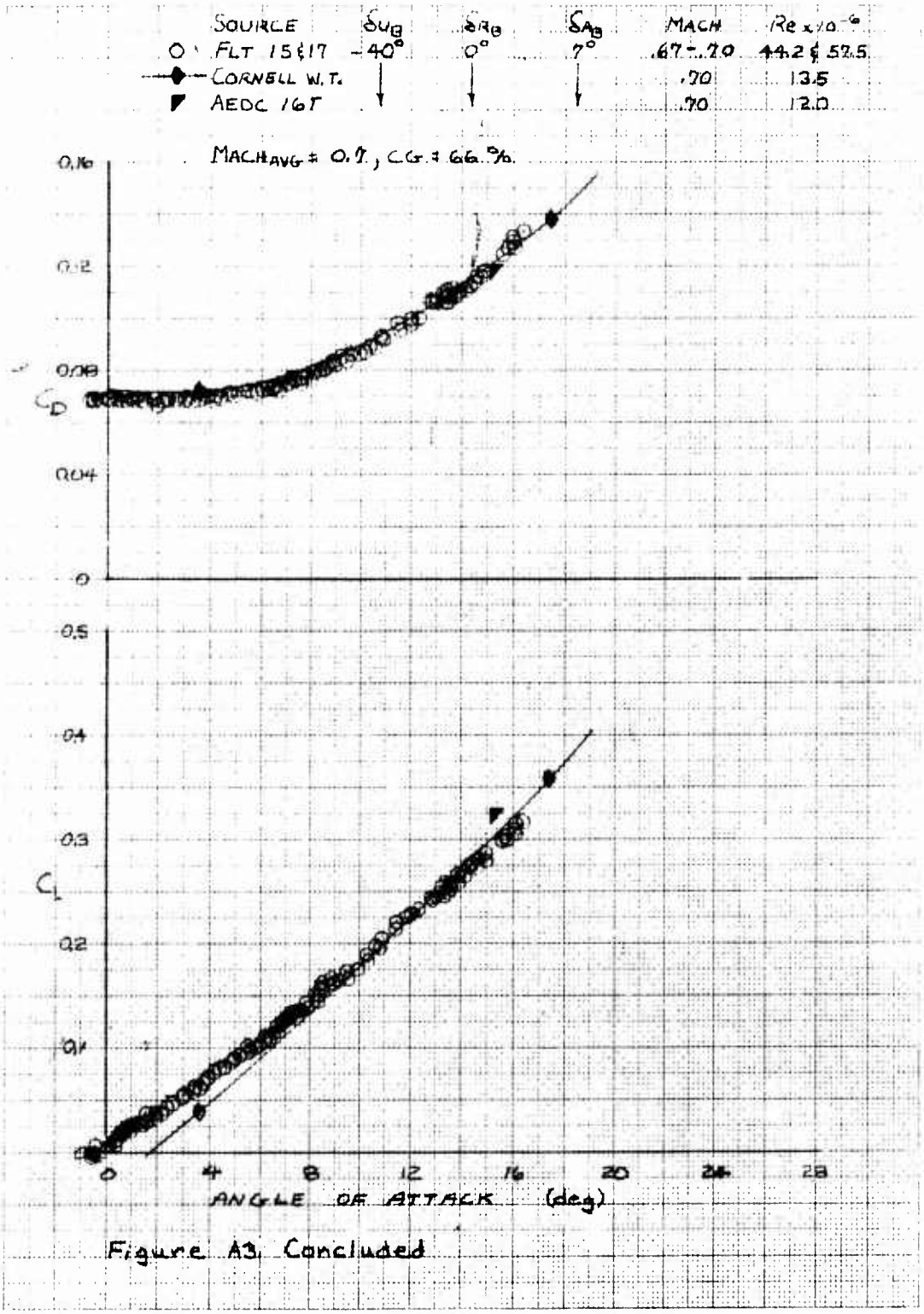

Figure A3. Concluded

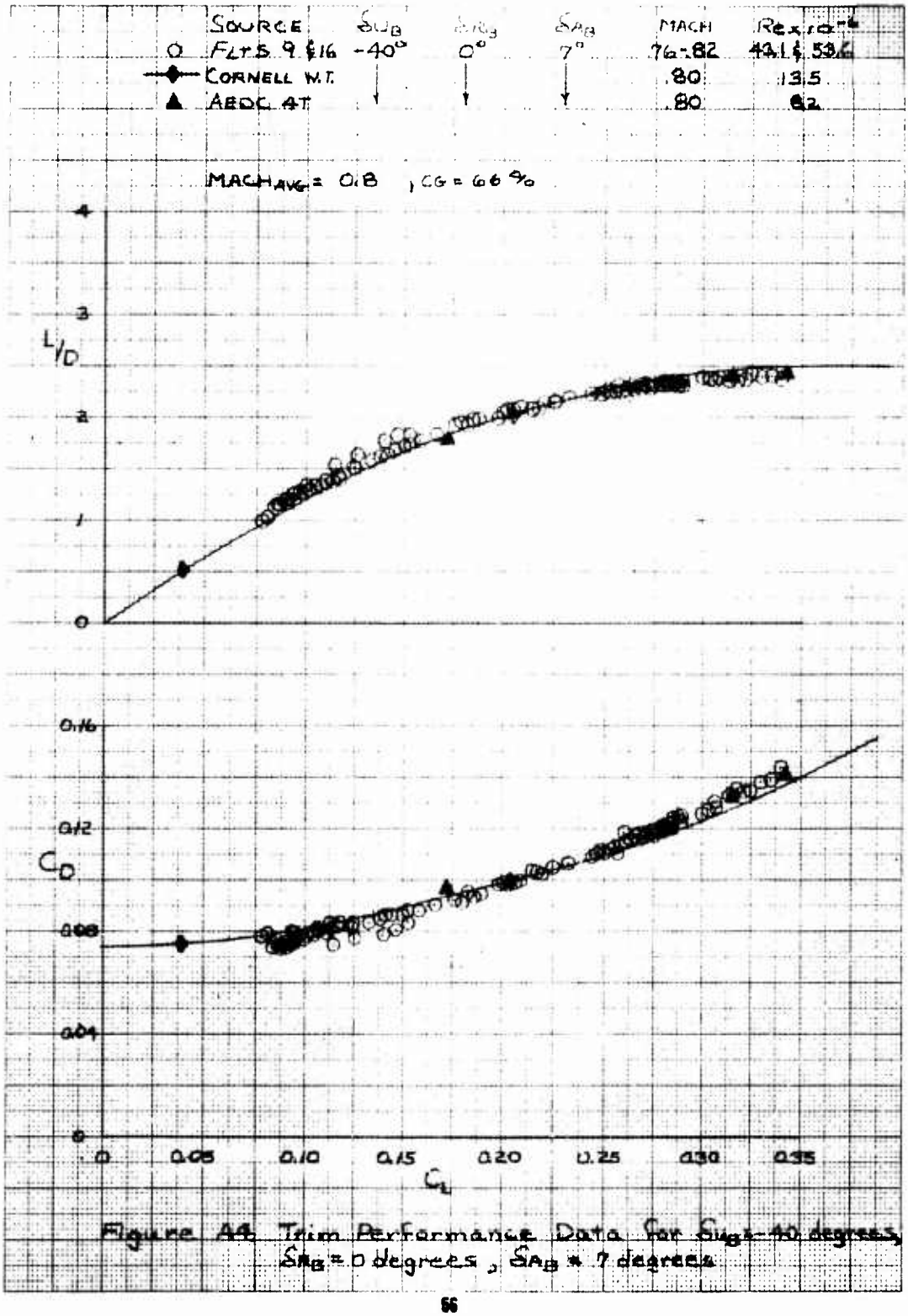

Figure A4. Trim Performance Data for δ_{UB} = -40 degrees, δ_{LEB} = 0 degrees, δ_{AB} = 7 degrees

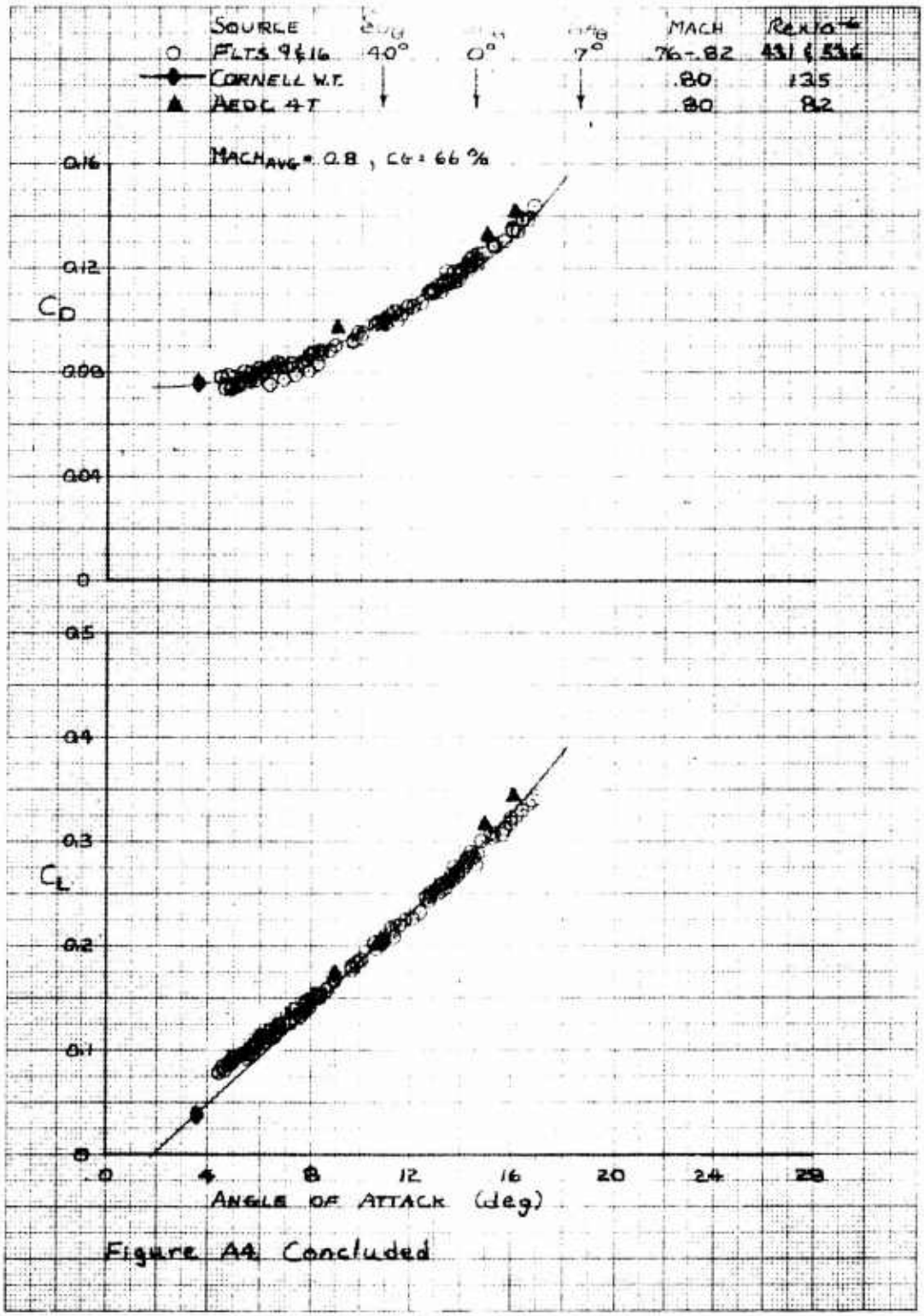

Figure A4 Concluded

	SOURCE	δ_{U_B}	δ_{R_B}	δ_{A_B}	MACH	$Re \times 10^{-6}$
O	FLTS 9 & 16	-40°	0°	7°	.87 - .92	34.3 & 48.7
◆	CORNELL W.T.				.90	12.0
▲	AEDC 4T				.90	8.2
▼	AEDC 16T				.90	12.0

$MACH_{AVG} = 0.9$, $CG = 66\%$

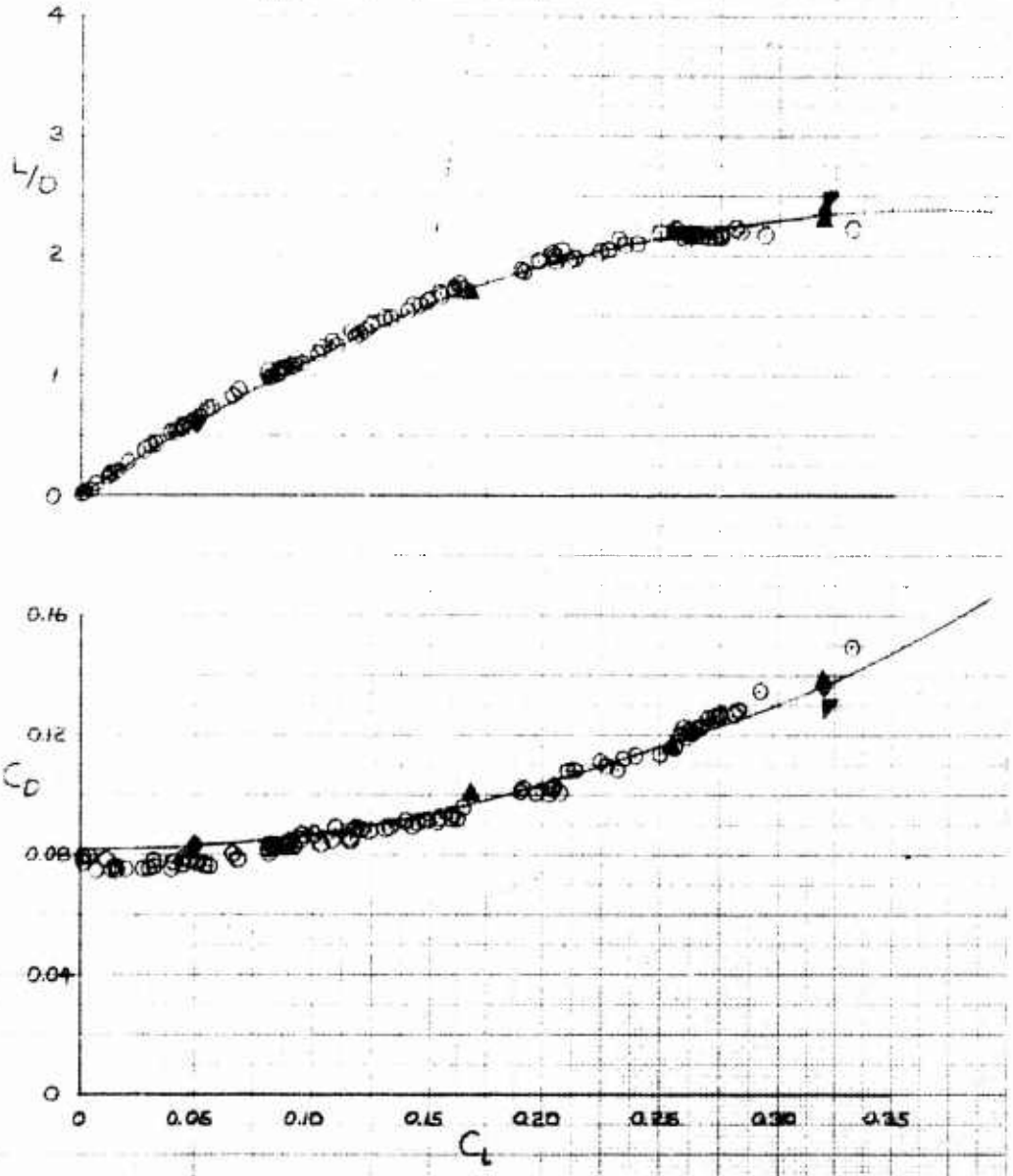

Figure A5. Trim Performance Data for δ_{U_B} = -40 degrees, δ_{R_B} = 0 degrees, δ_{A_B} = 7 degrees

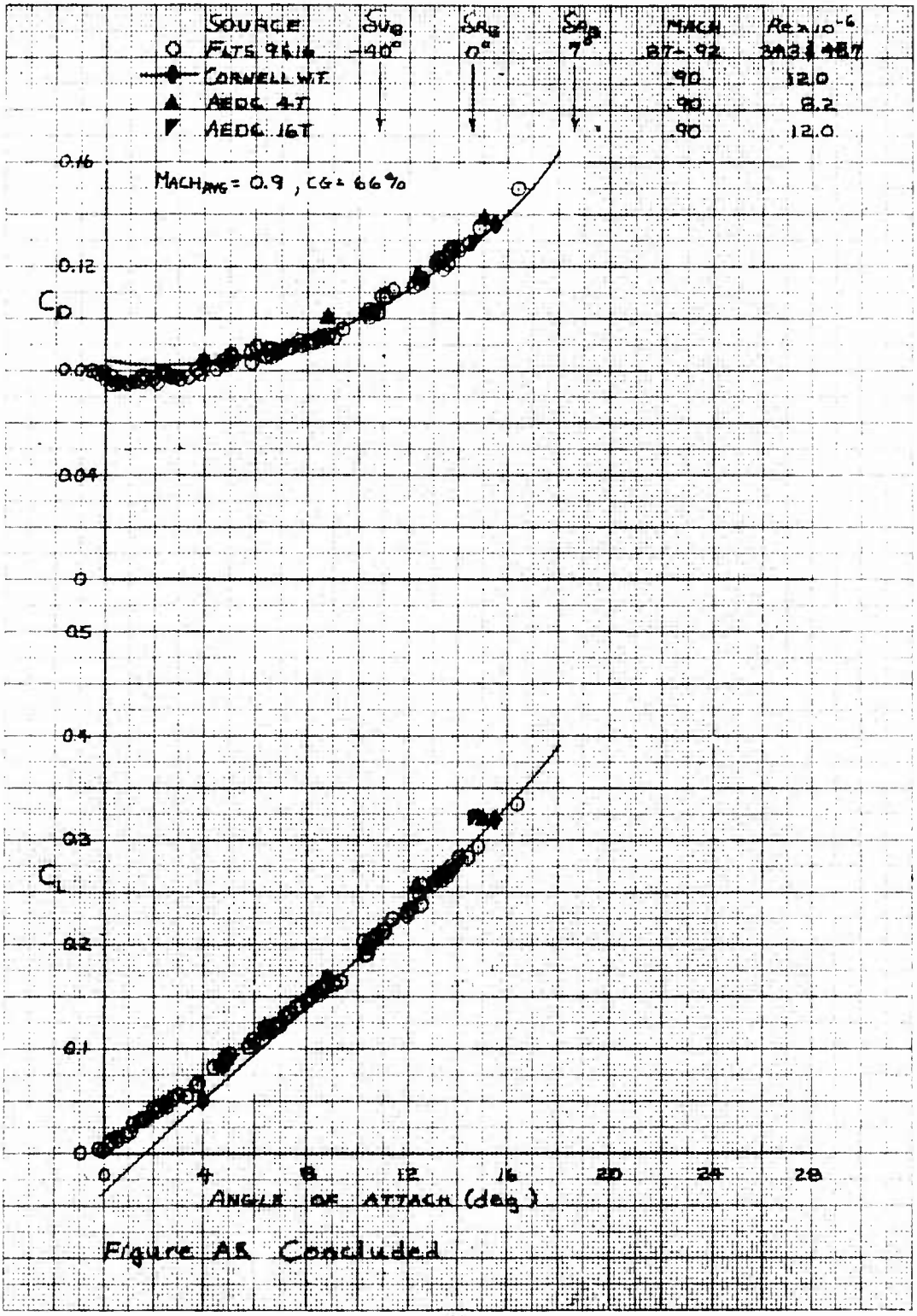

Figure A8. Concluded

SOURCE	δ_{LE_B}	δ_{SR_H}	δ_{TE_B}	MACH	R_e NO. $\times 10^{-6}$
○ FLTS. 9 & 11	-40°	0°	7°	.93-.97	32.7 & 42.4
◆ CORNELL W.T.	↓	↓	↓	.95	12.0
▲ AEDC 4T	↓	↓	↓	.95	8.2
▼ AEDC 16T	↓	↓	↓	.95	12.0

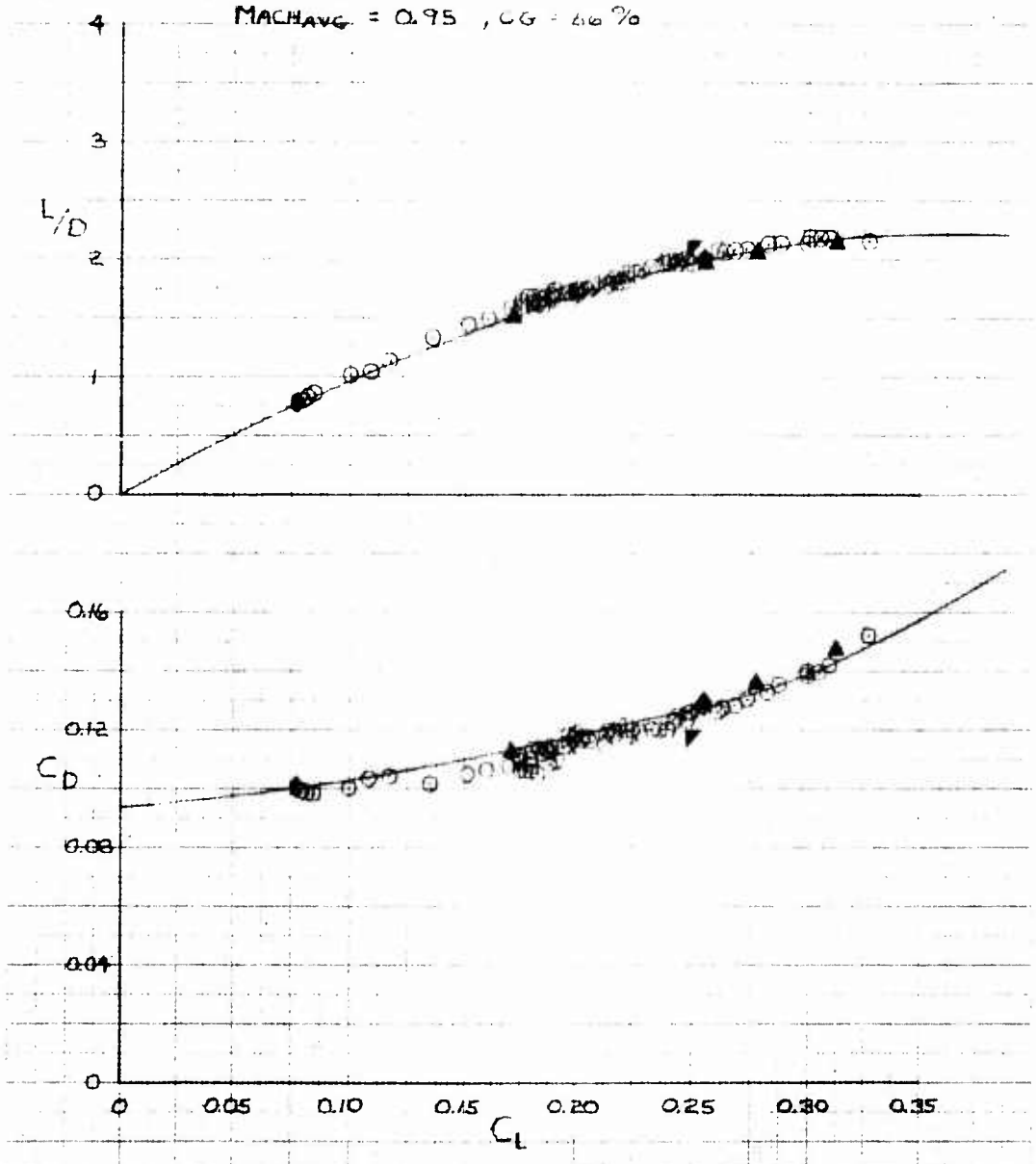

Figure A6. Trim Performance Data for δ_{LE_B} = -40 degrees, δ_{SR_B} = 0 degrees, δ_{TE_B} = 7 degrees

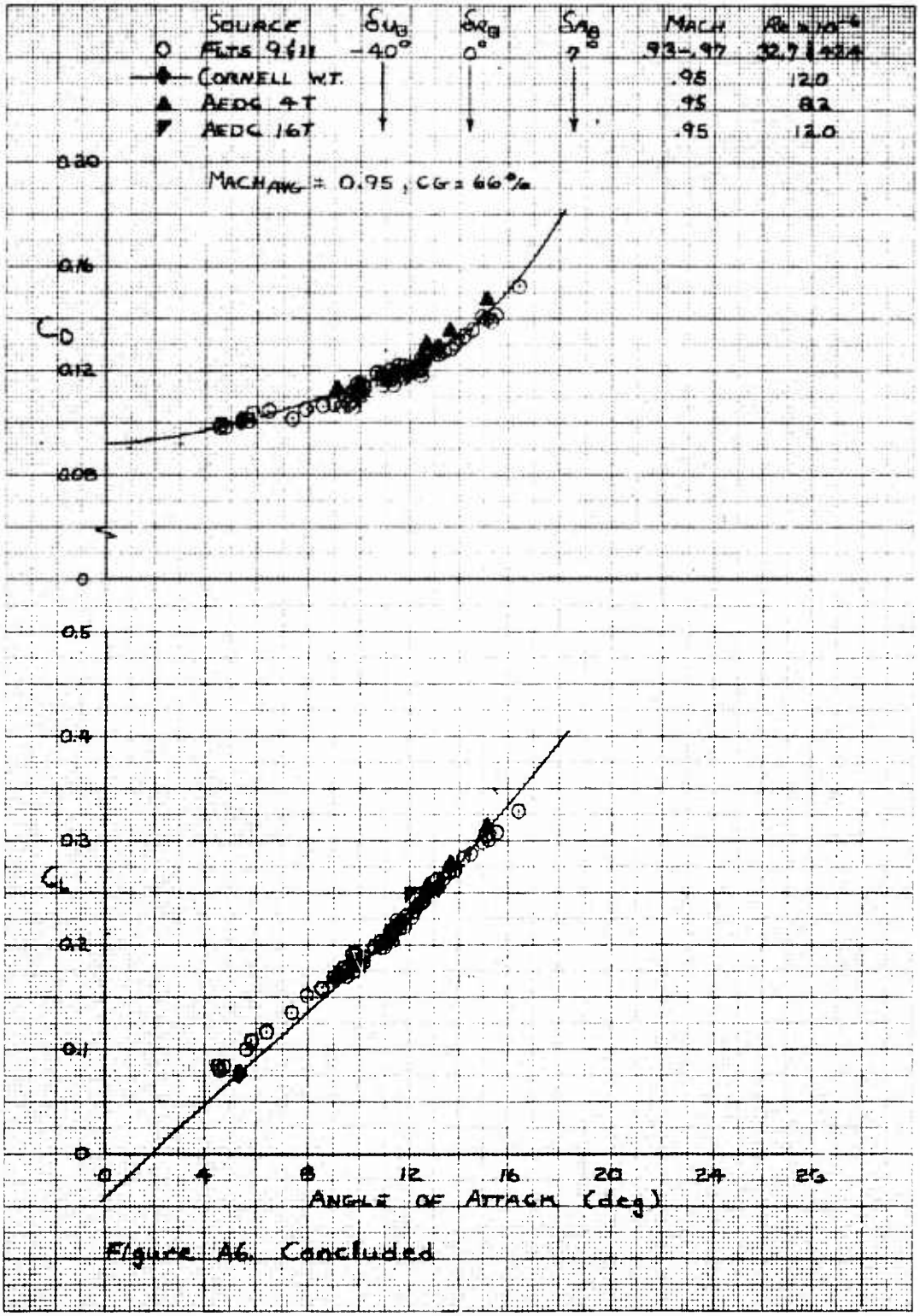

Figure A6. Concluded

SOURCE	δ_{U_B}	δ_{R_B}	δ_{A_B}	MACH	$Re \times 10^{-6}$
○ FLT 15	-40°	0°	7°	1.0 - 1.04	16.1
◆ CORNELL W.T.	↓	↓	↓	1.0	12.0
▲ AEDC 4T	↓	↓	↓	1.0	8.2

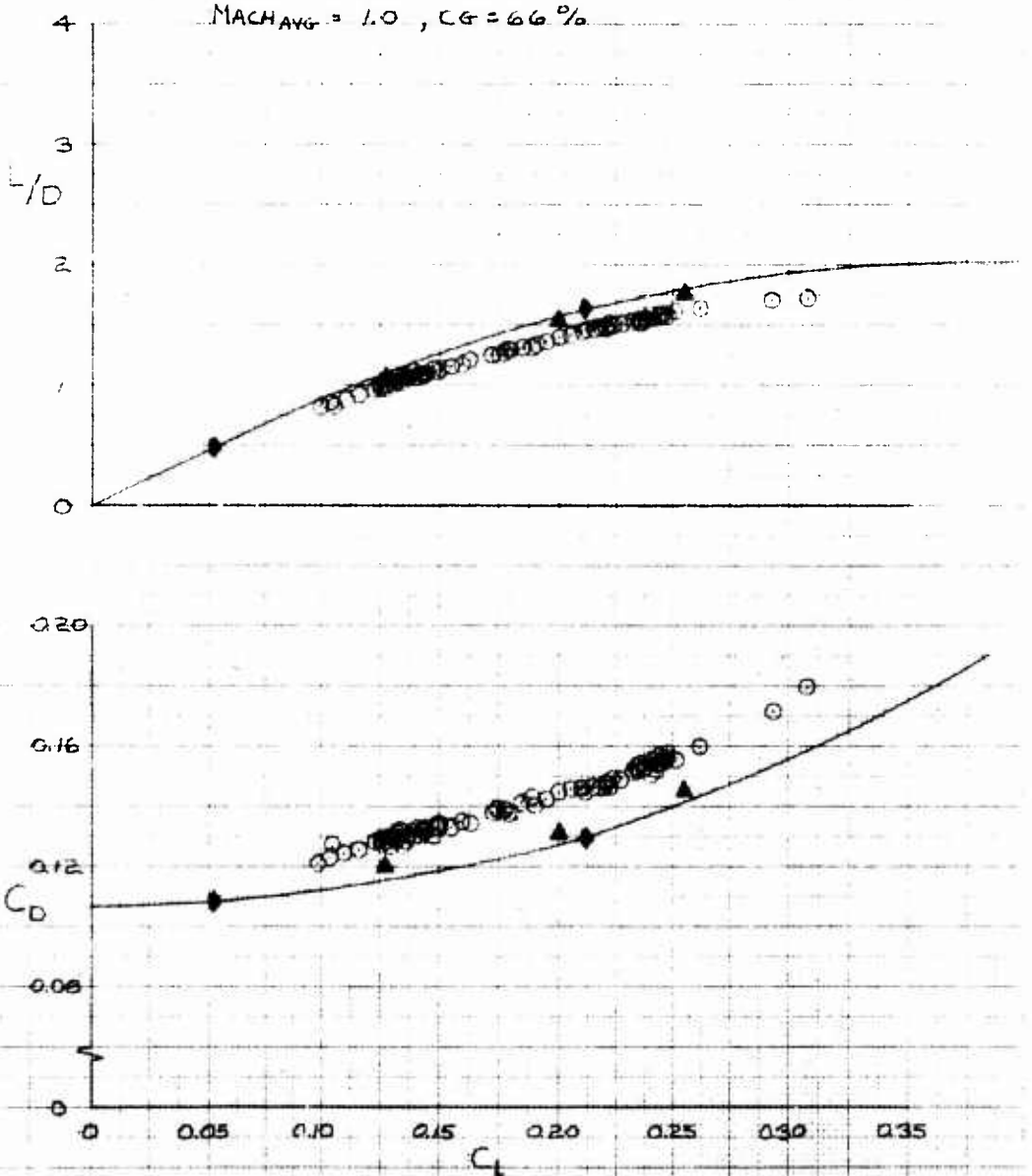

Figure A7. Trim Performance Data for δ_{U_B} = -40 degrees, δ_{R_B} = 0 degrees, δ_{A_B} = 7 degrees

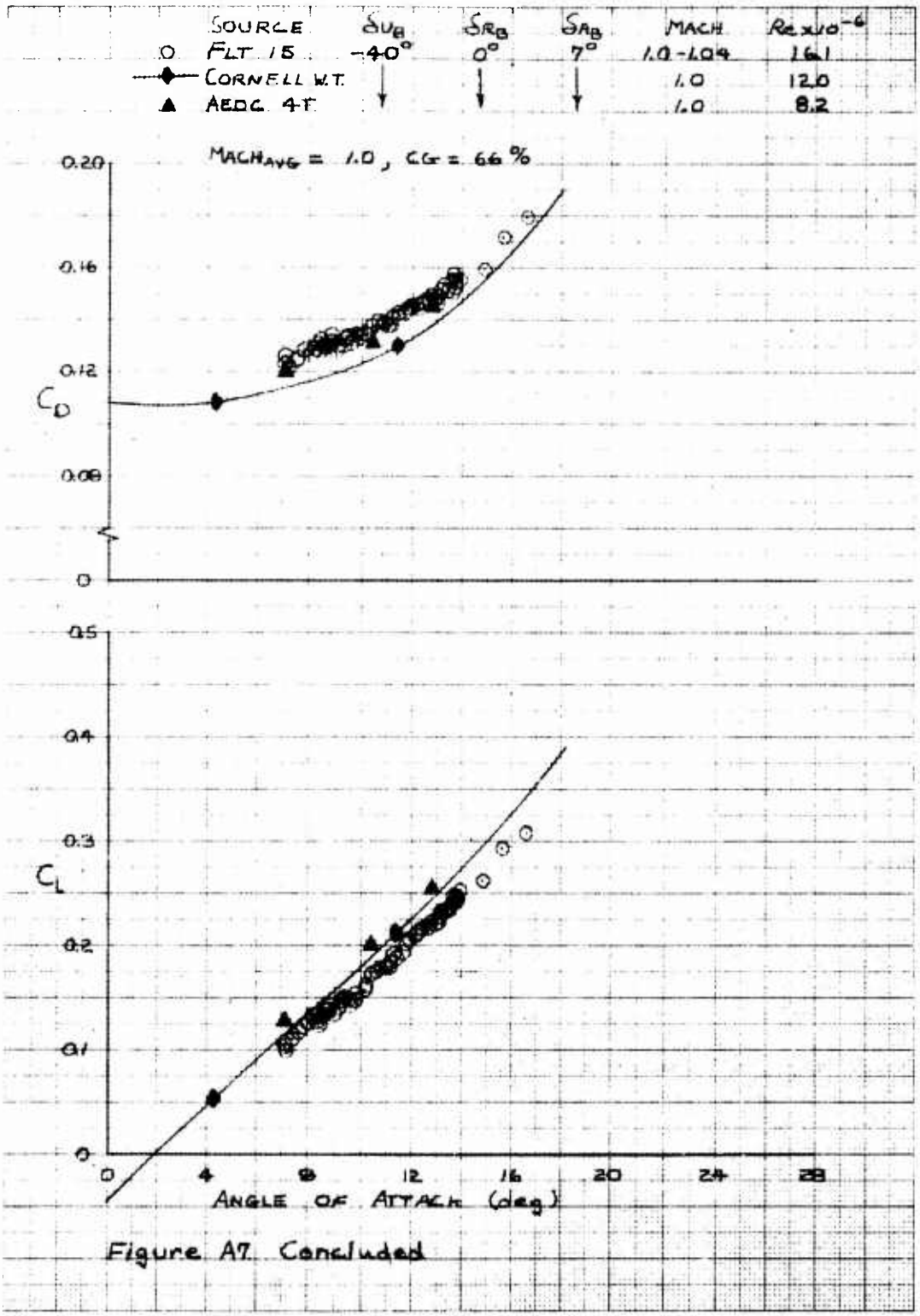

Figure A7. Concluded

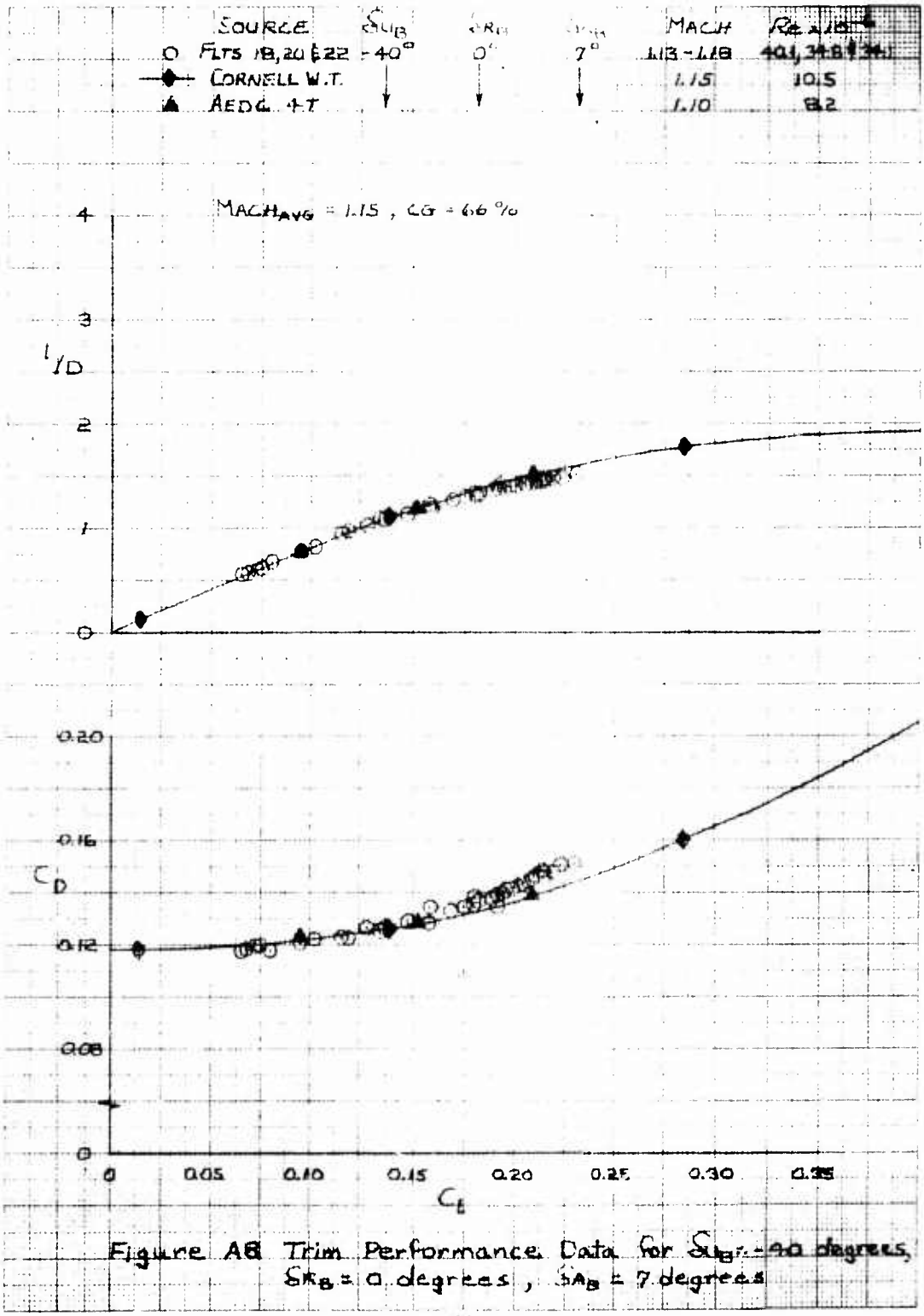

Figure A8 Trim Performance Data for δ_{LE_B} = -40 degrees, δ_{R_B} = 0 degrees, δ_{A_B} = 7 degrees

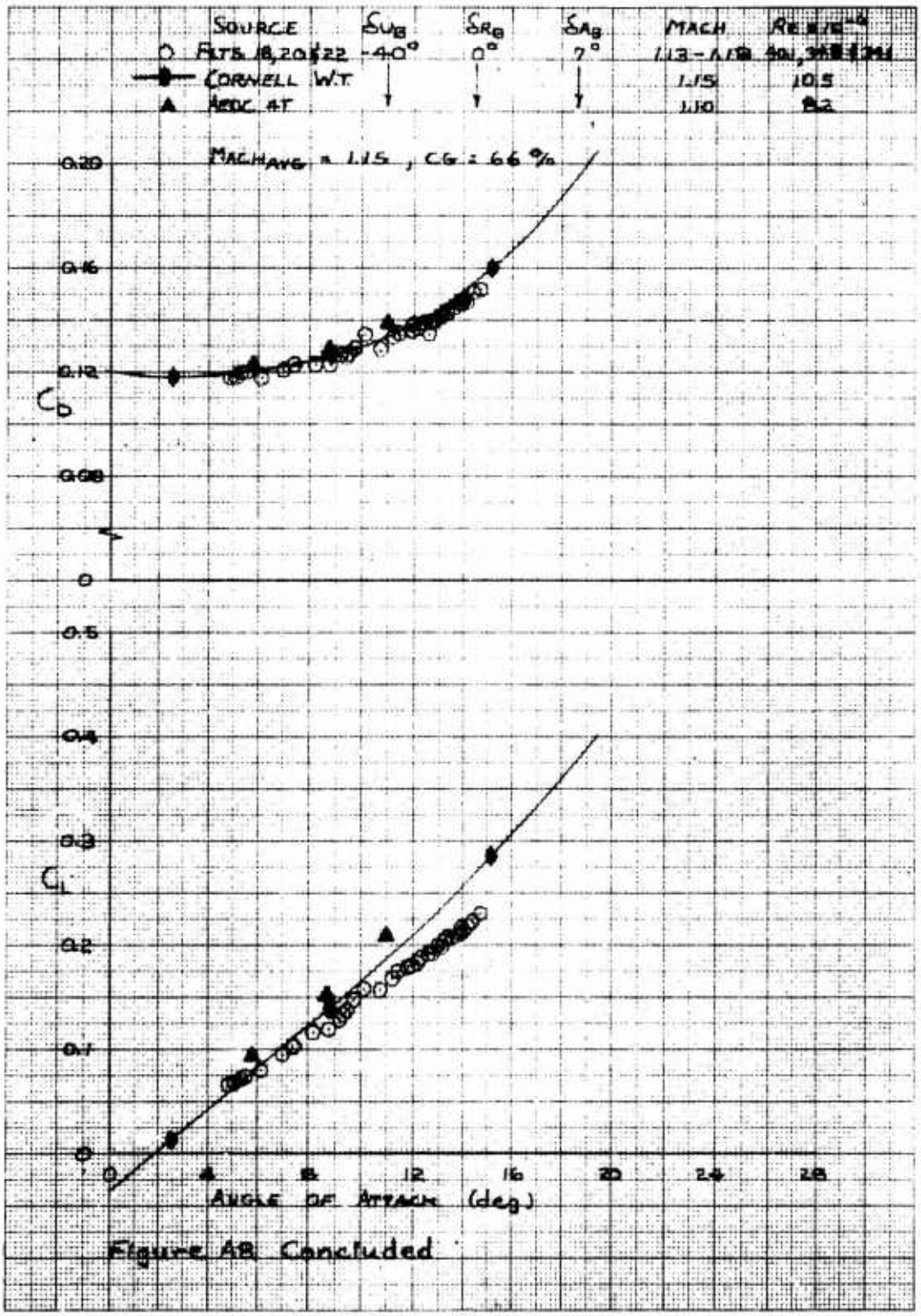

Figure AB Concluded

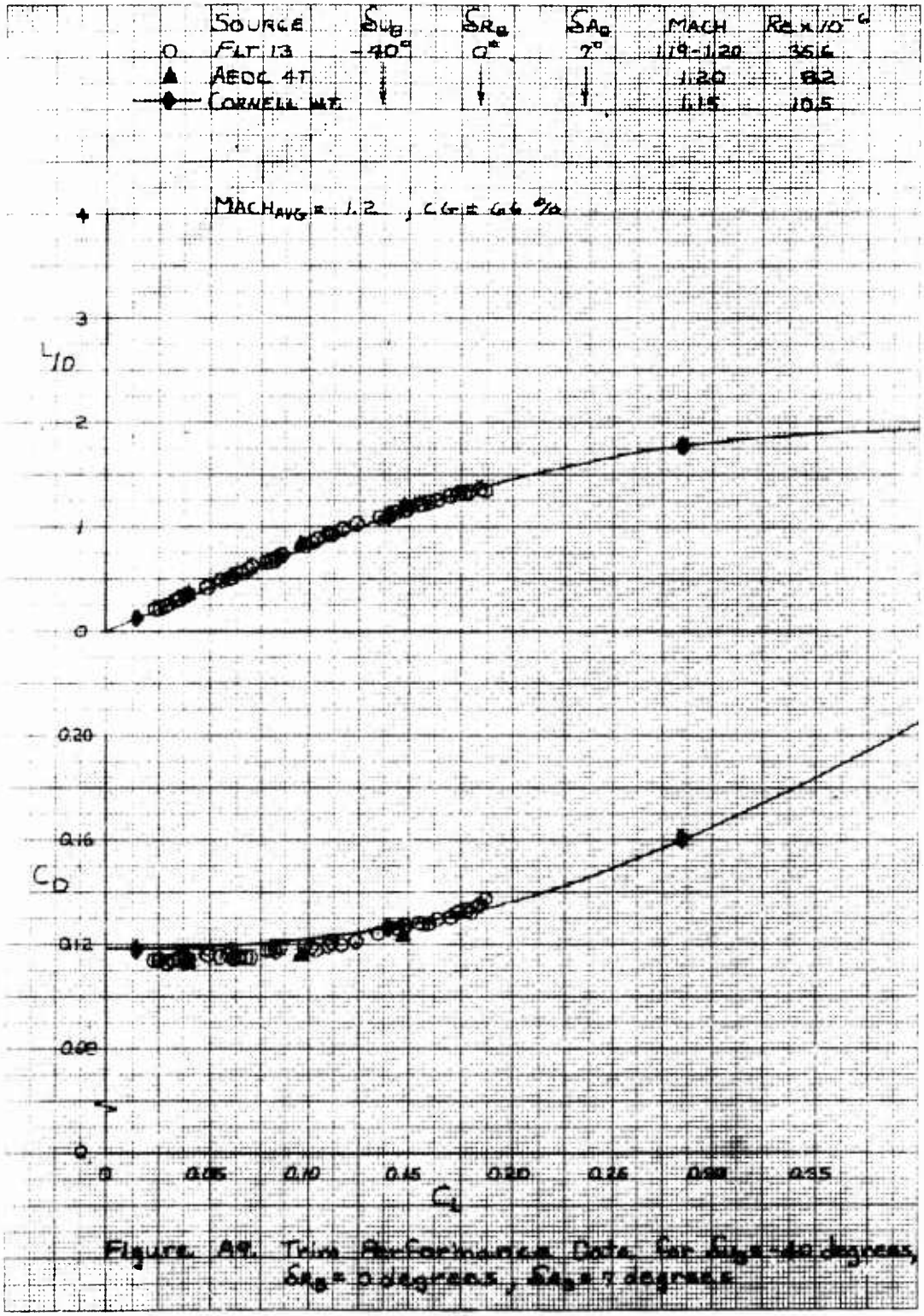

Figure A9. Trim Performance Data for δe_B = -40 degrees, δR_B = 0 degrees, δA_B = 7 degrees.

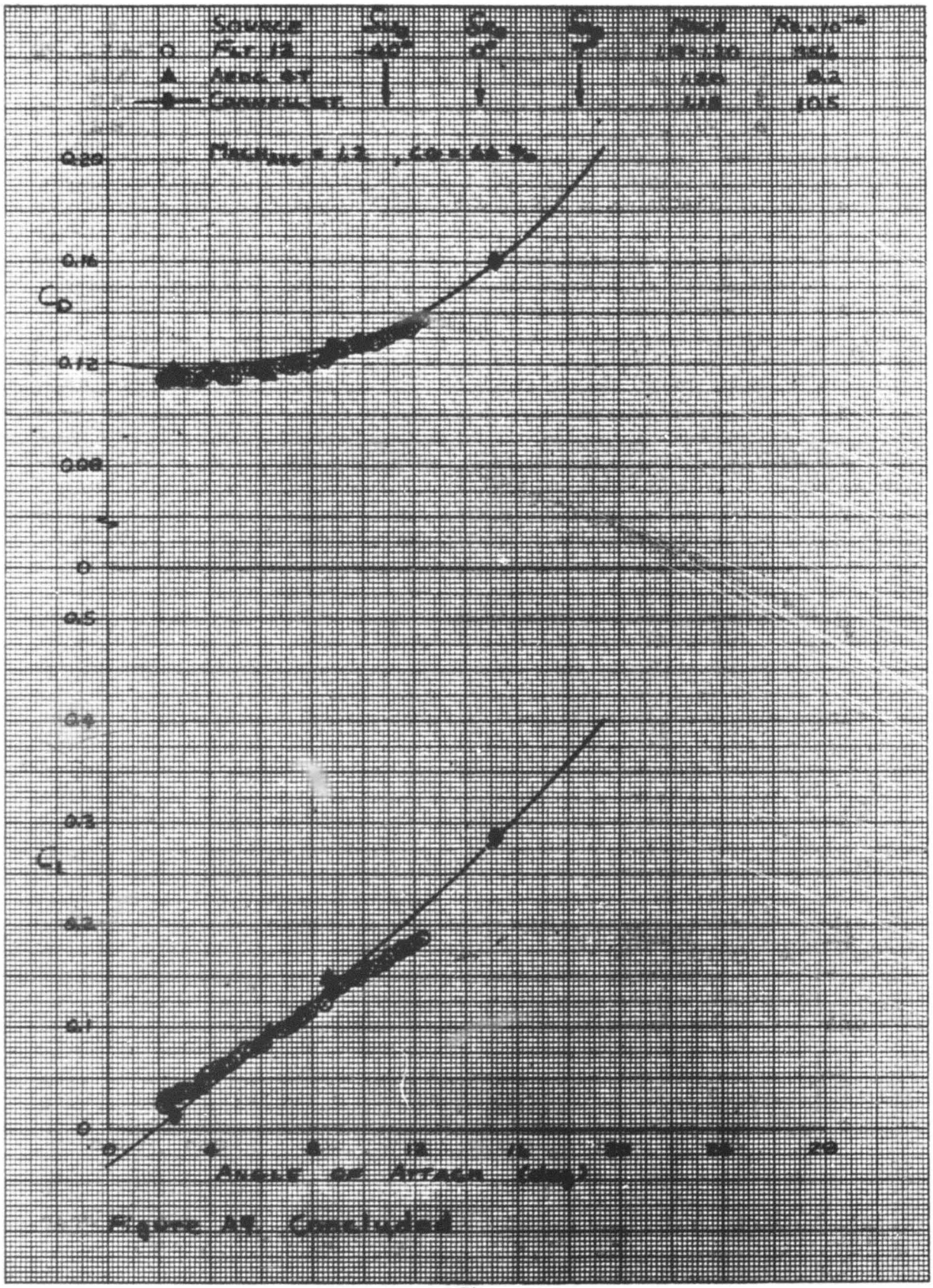

Figure 18. Concluded

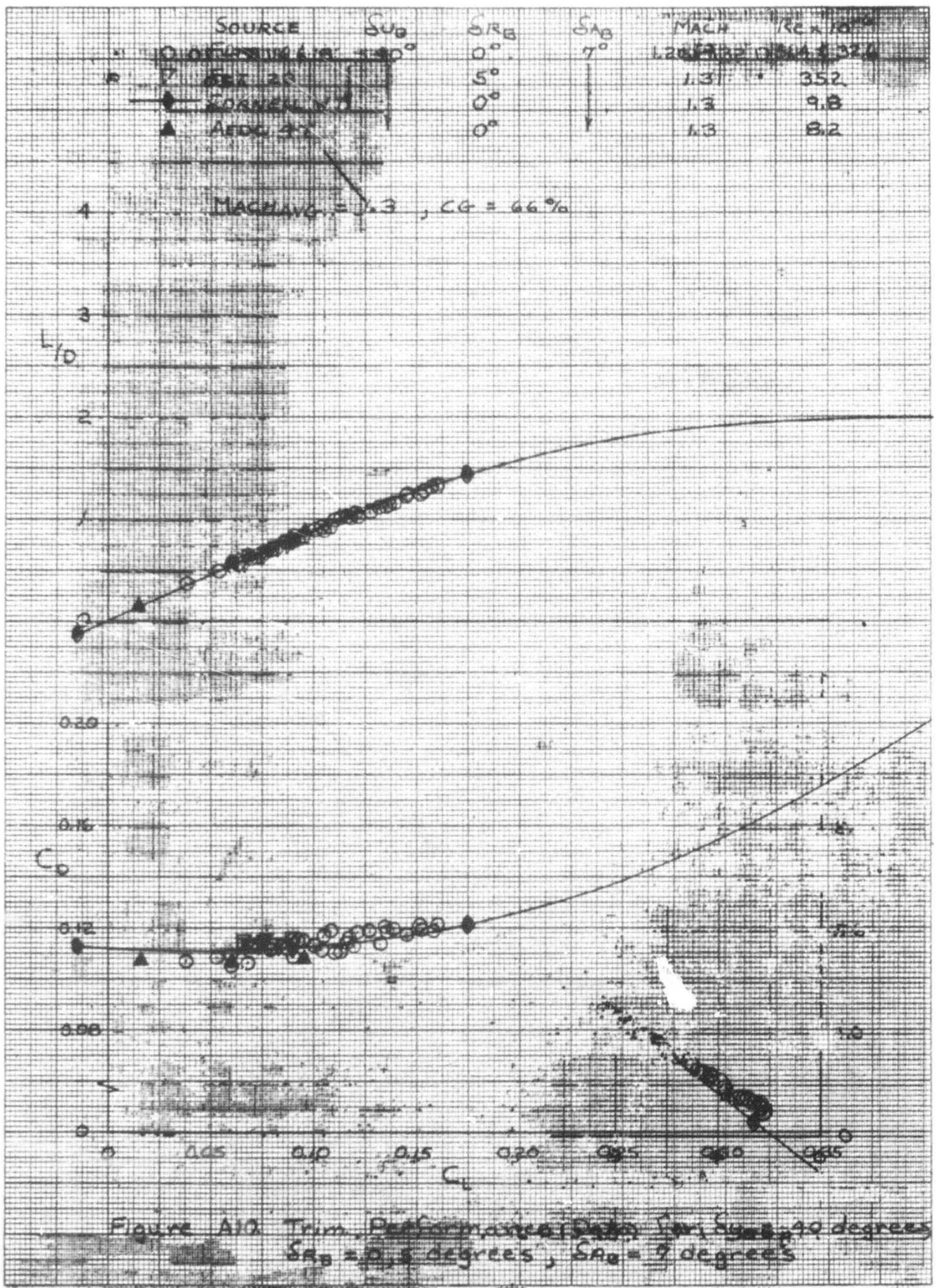

Figure A10 Trim Performance Data for δ_{R_B} = 40 degrees
δ_{A_B} = 0.5 degrees , δ_{A_B} = 7 degrees

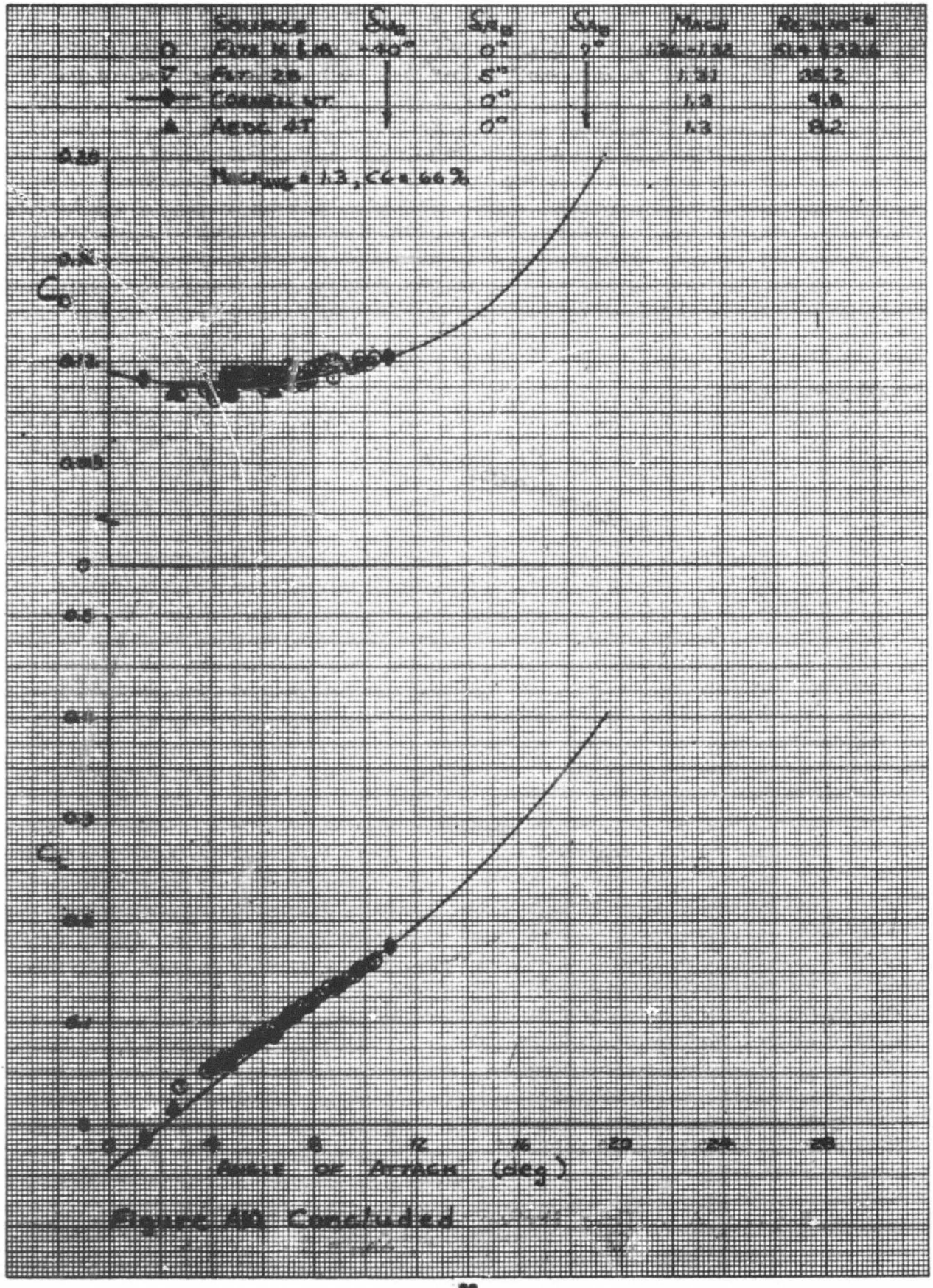

Figure A10 Concluded

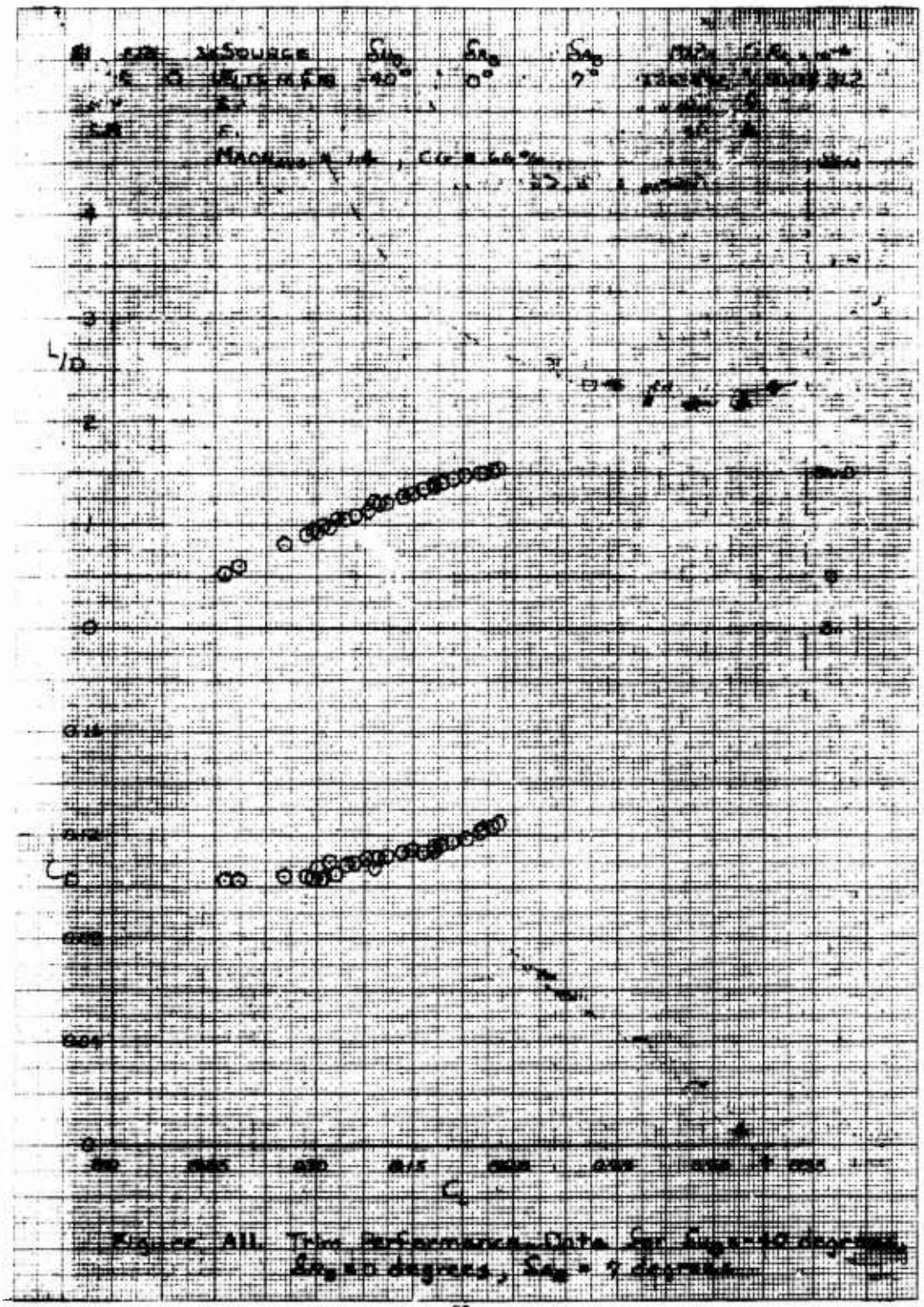

Figure All. Trim Performance Data for δ_{sp} = -40 degrees, δ_{sb} = 0 degrees, δ_{sa} = 7 degrees.

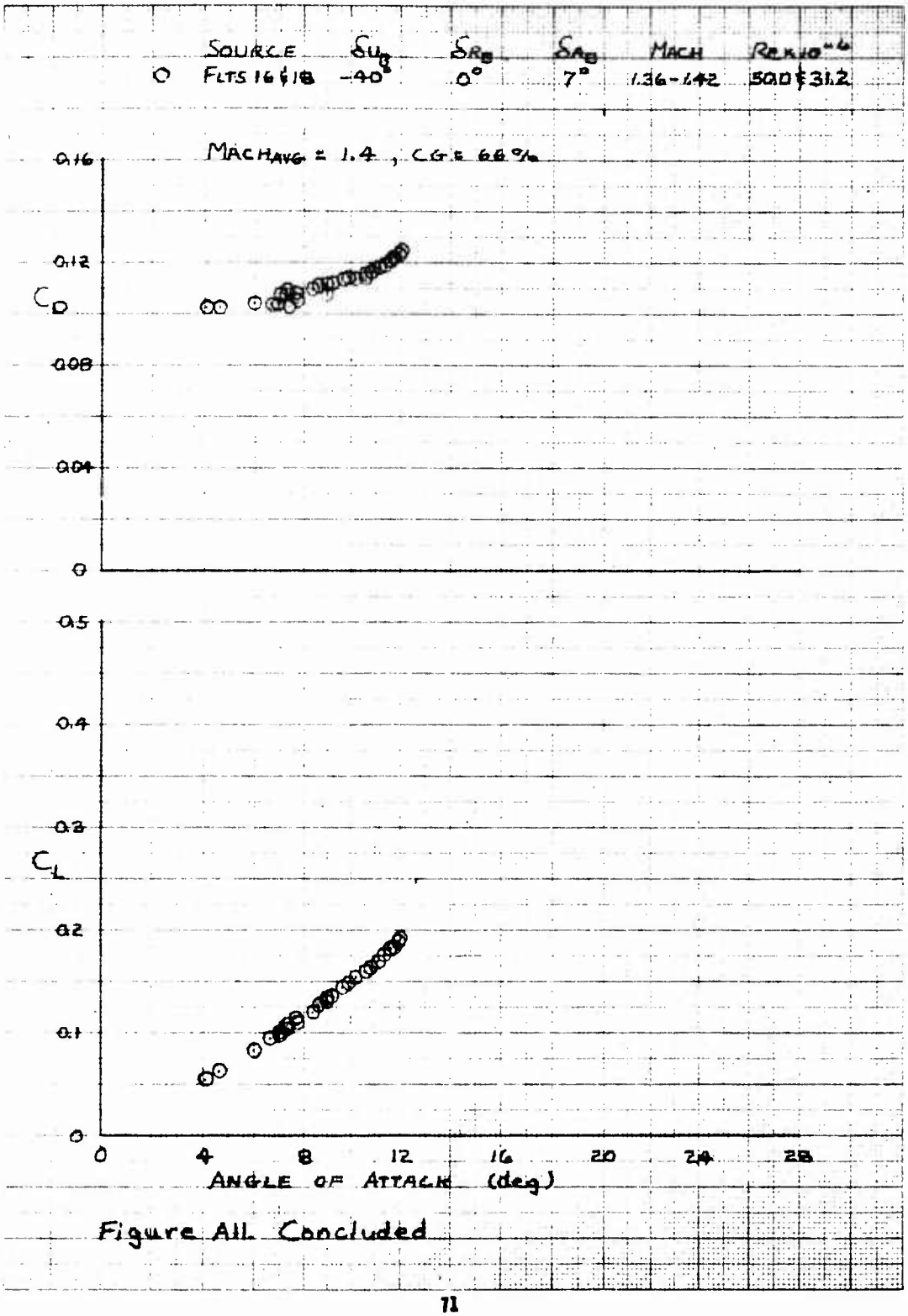

Figure A11. Concluded

	SOURCE	δ_{U_B}	δ_{R_B}	δ_{A_B}	MACH	Re x10^{-6}
O	FLTS 20 & 29	-40°	0°	7°	1.39 - 1.46	27.3 & 28.8

$MACH_{AVG}$ = 1.44 , CG = 66%

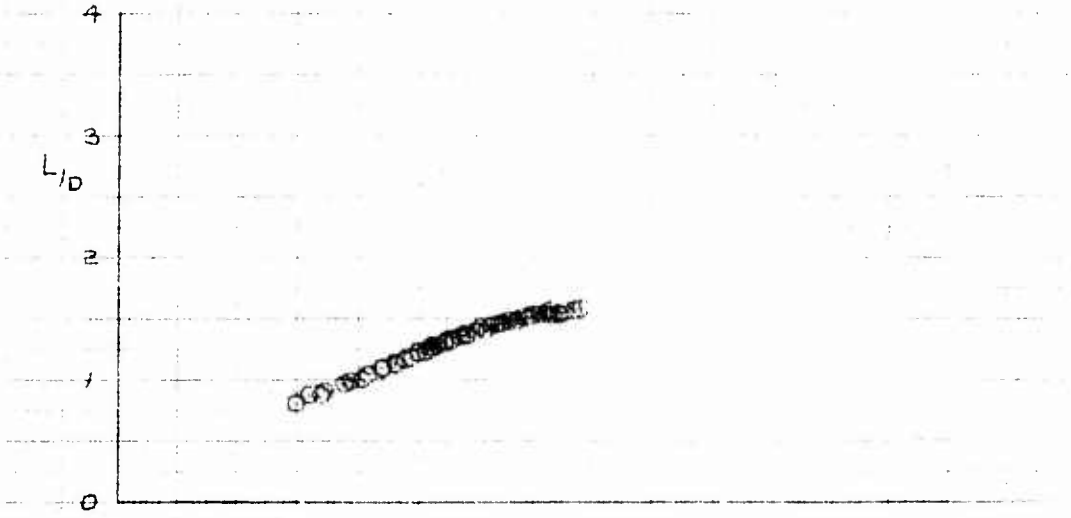

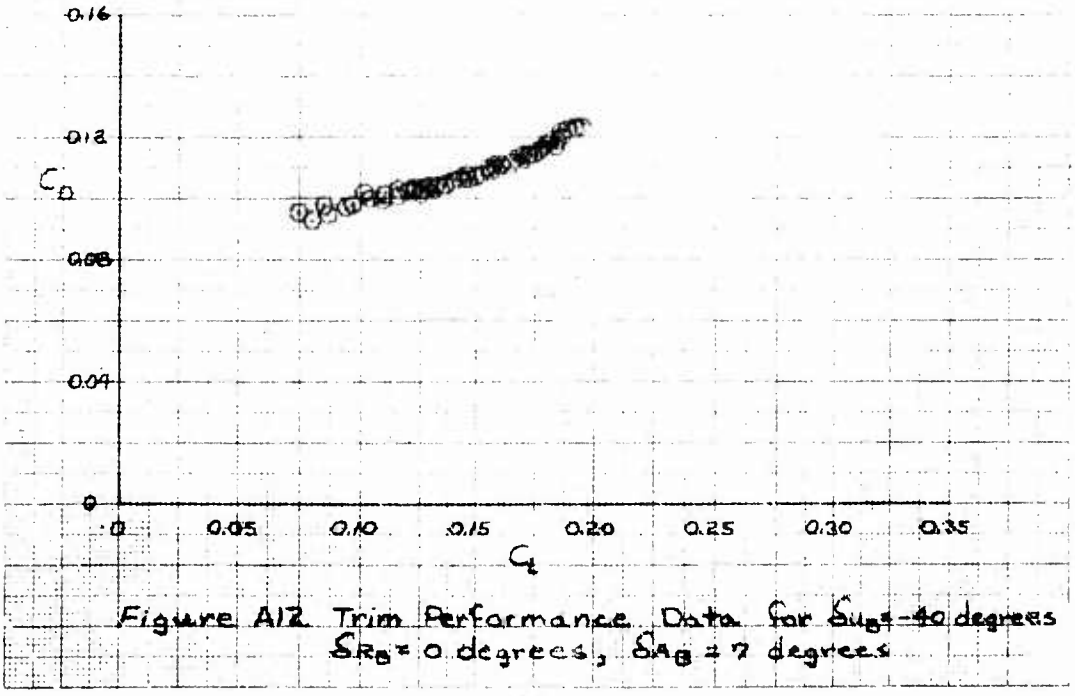

Figure A12. Trim Performance Data for δ_{U_B} = -40 degrees δ_{R_B} = 0 degrees, δ_{A_B} = 7 degrees

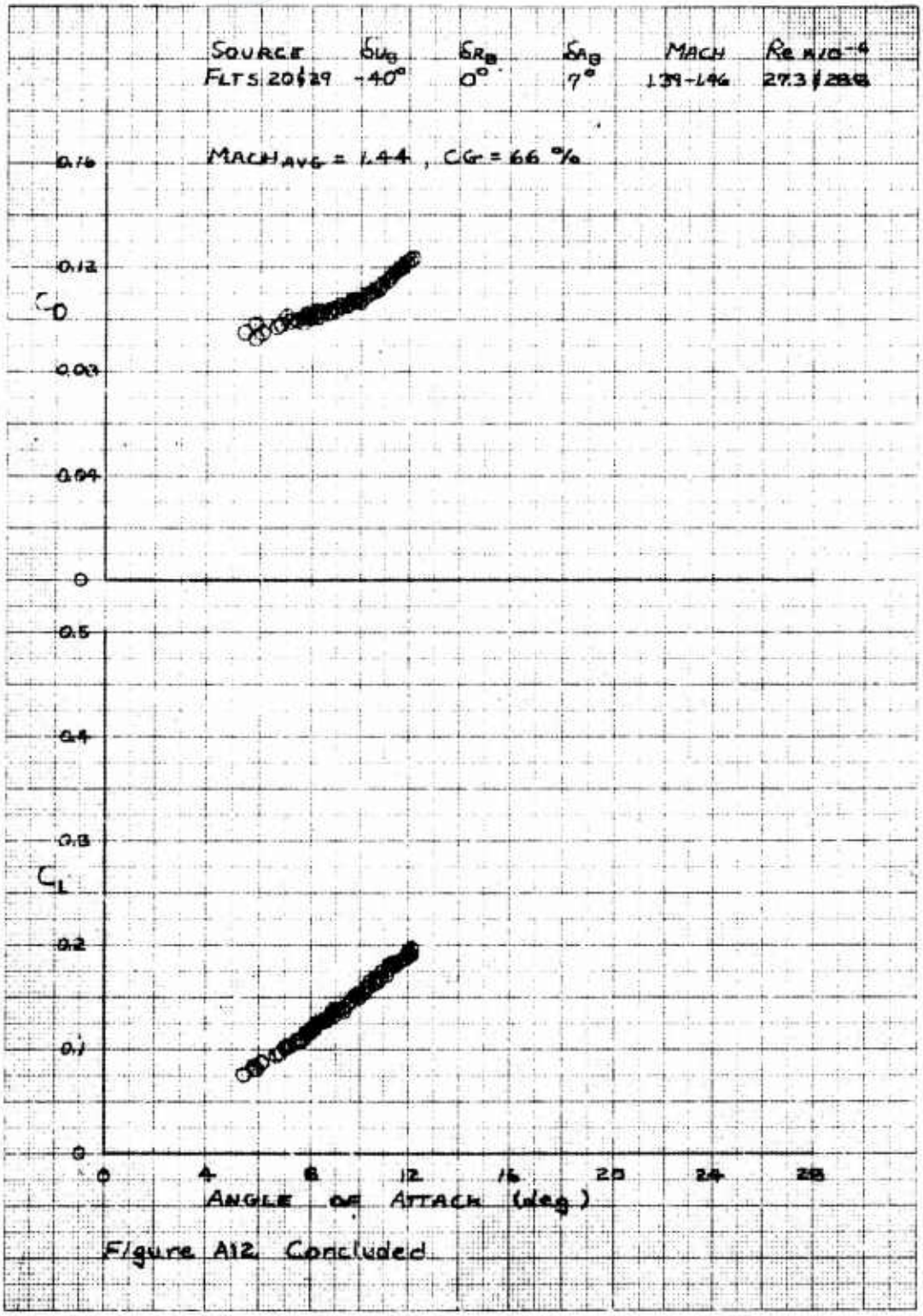

Figure A12. Concluded.

SOURCE	δ_{U_B}	δ_{R_B}	δ_{A_B}	MACH	$R_e \times 10^{-6}$
○ FLTS 18, 19, 23, 24 & 26	-40°	0°	7°	1.47 - 1.53	25.3 - 46.1
✦ AEDC VKF	↓	↓	↓	1.50	8.2

$MACH_{AVG} = 1.5$, $CG = 66\%$

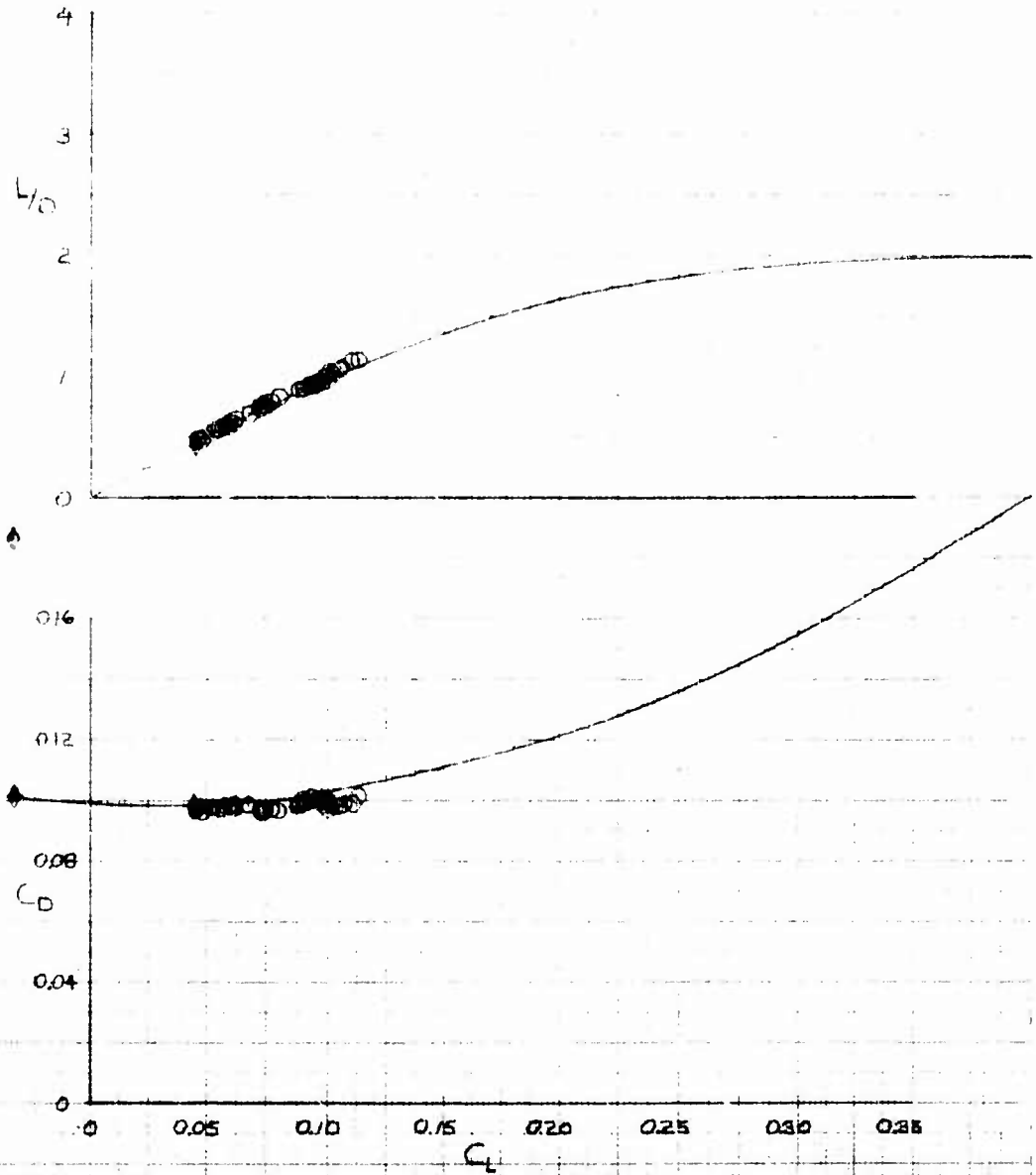

Figure A13. Trim Performance Data for δ_{U_B} = -40 degrees, δ_{R_B} = 0 degrees, δ_{A_B} = 7 degrees

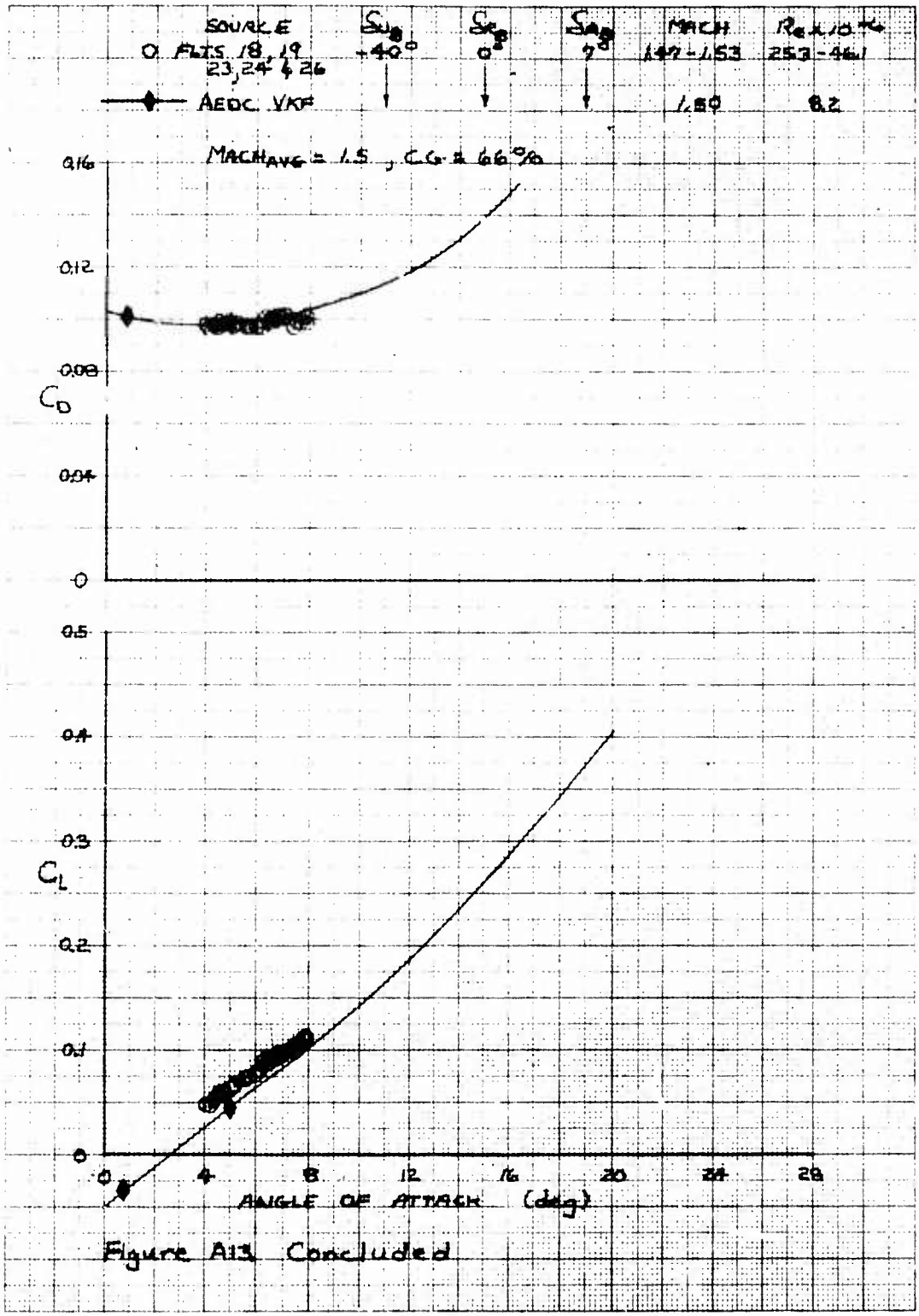

Figure A13 Concluded

SOURCE	δu_B	δR_B	δ_{AB}	MACH	$R_e \times 10^{-6}$
O FLTS 16, 17, 19, 23	-40°	0°	7°	1.58 - 1.62	25.0 - 42.5

$MACH_{AVG} = 1.6$, CG = 66 %

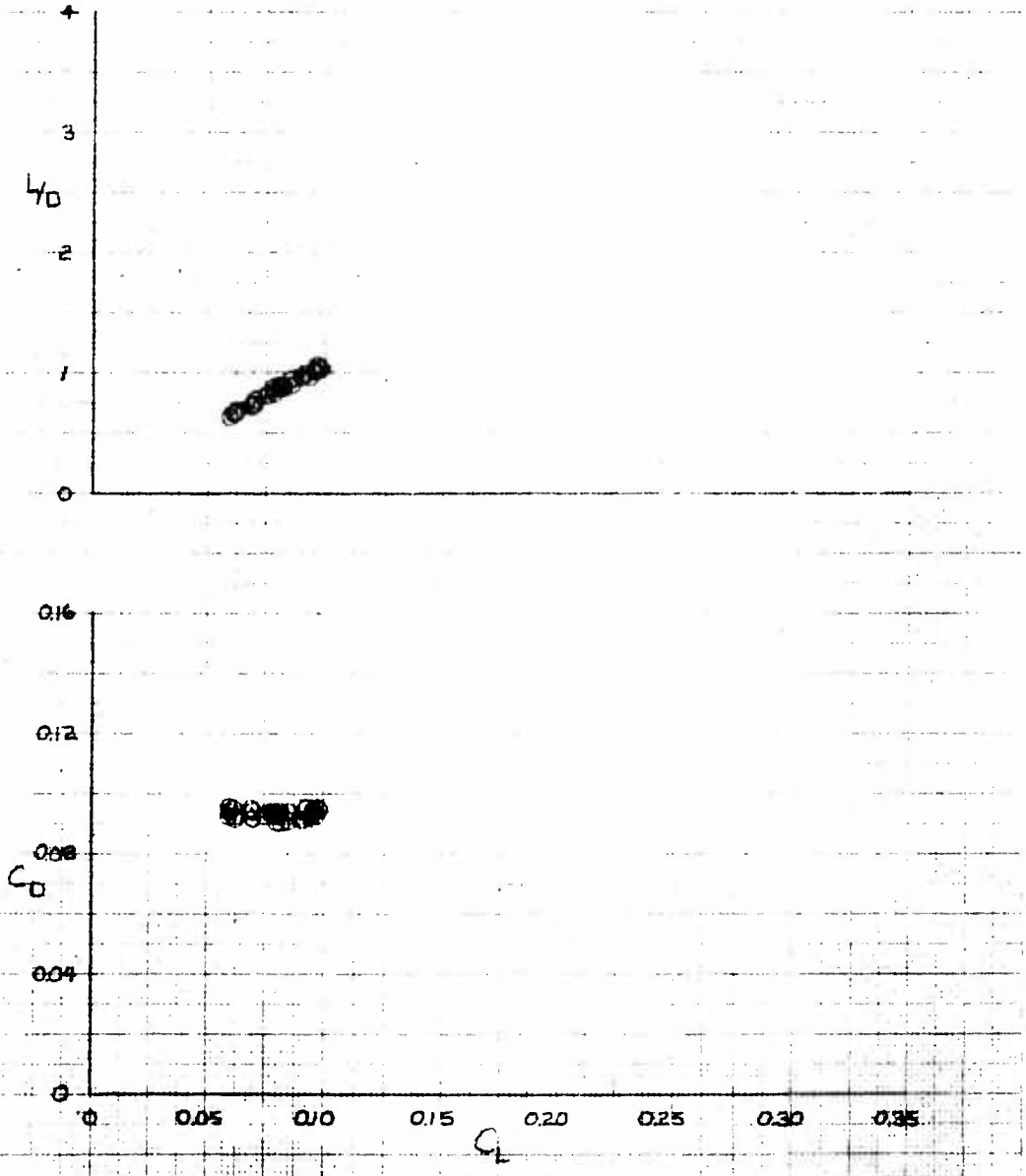

Figure A14. Trim Performance Data for δu_B = -40 degrees, δR_B = 0 degrees, δA_B = 7 degrees

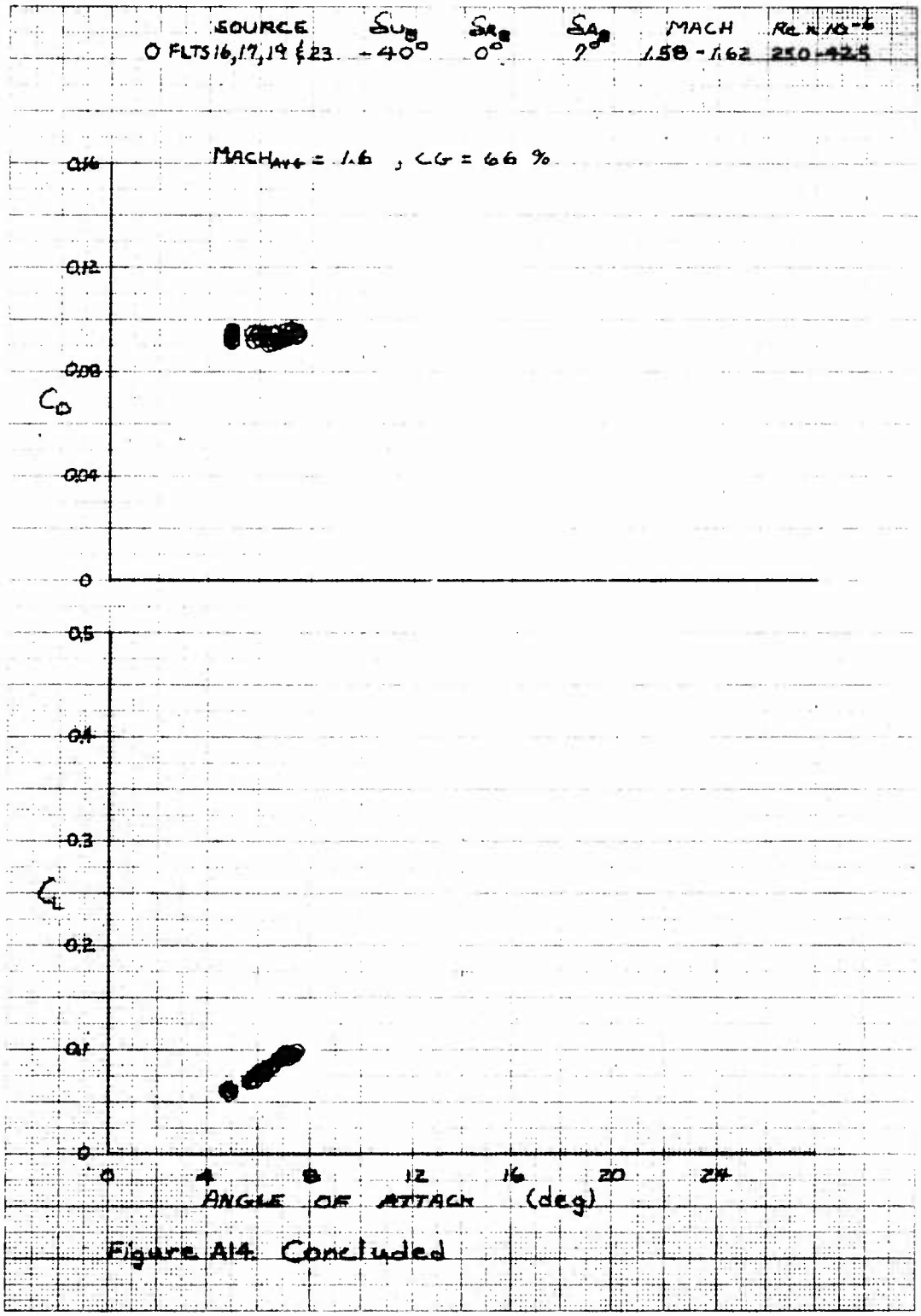

Figure A14. Concluded

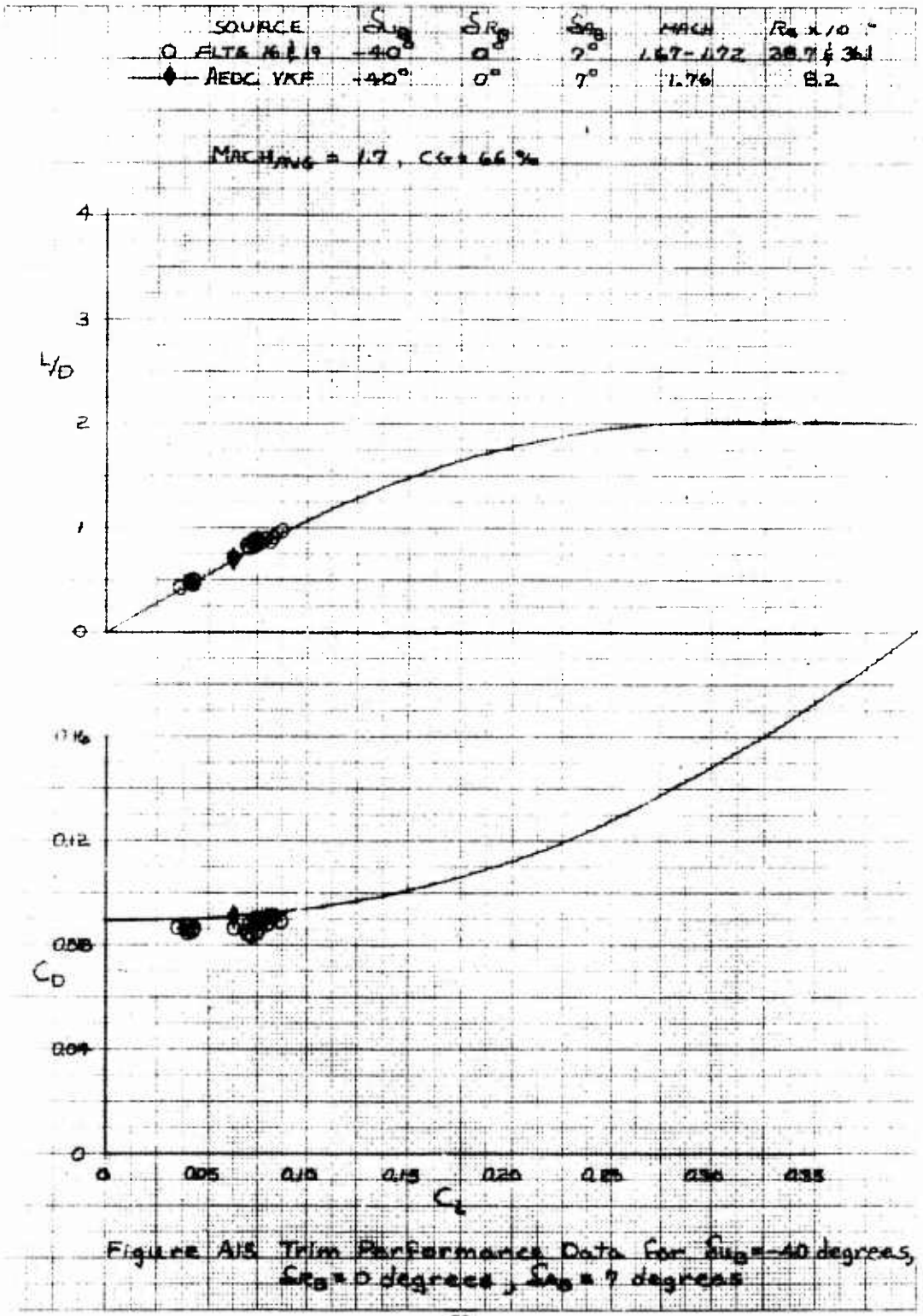

Figure A15 Trim Performance Data for δu_B = -40 degrees, δR_B = 0 degrees, δa_B = 7 degrees

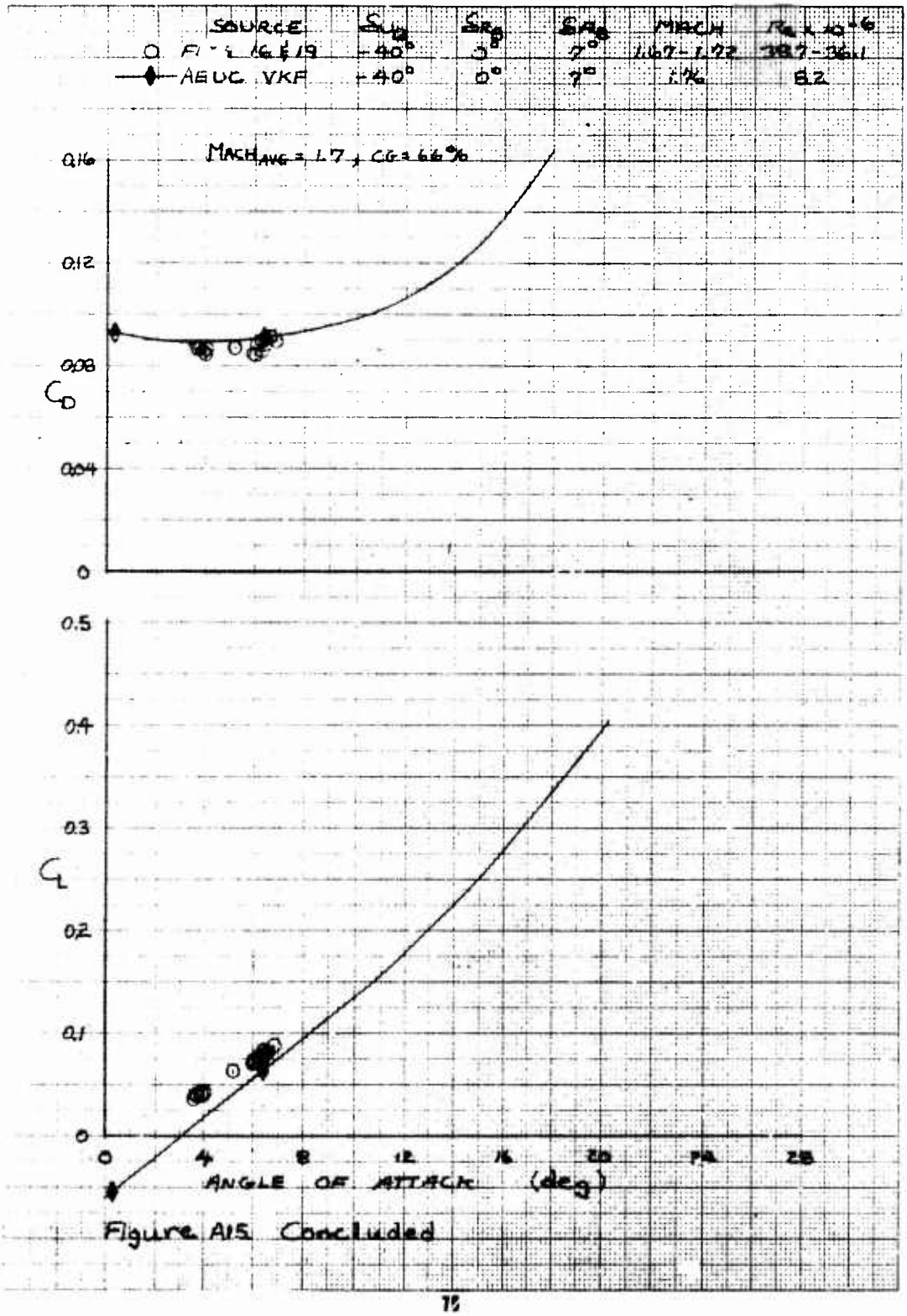

Figure A15 Concluded

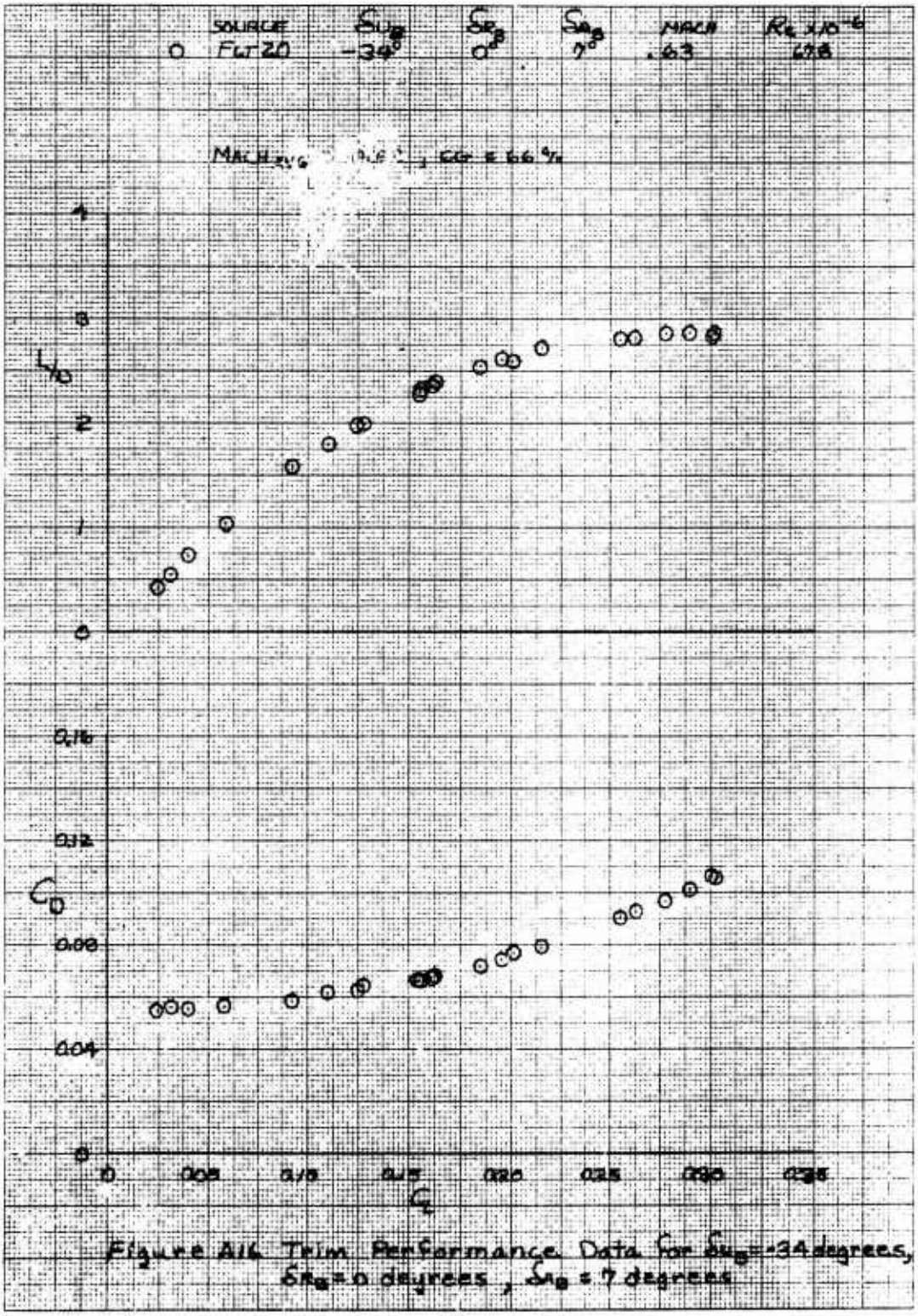

Figure A16 Trim Performance Data for δ_{LE_B} = -34 degrees, δ_{SE_B} = 0 degrees, δ_{H_B} = 7 degrees

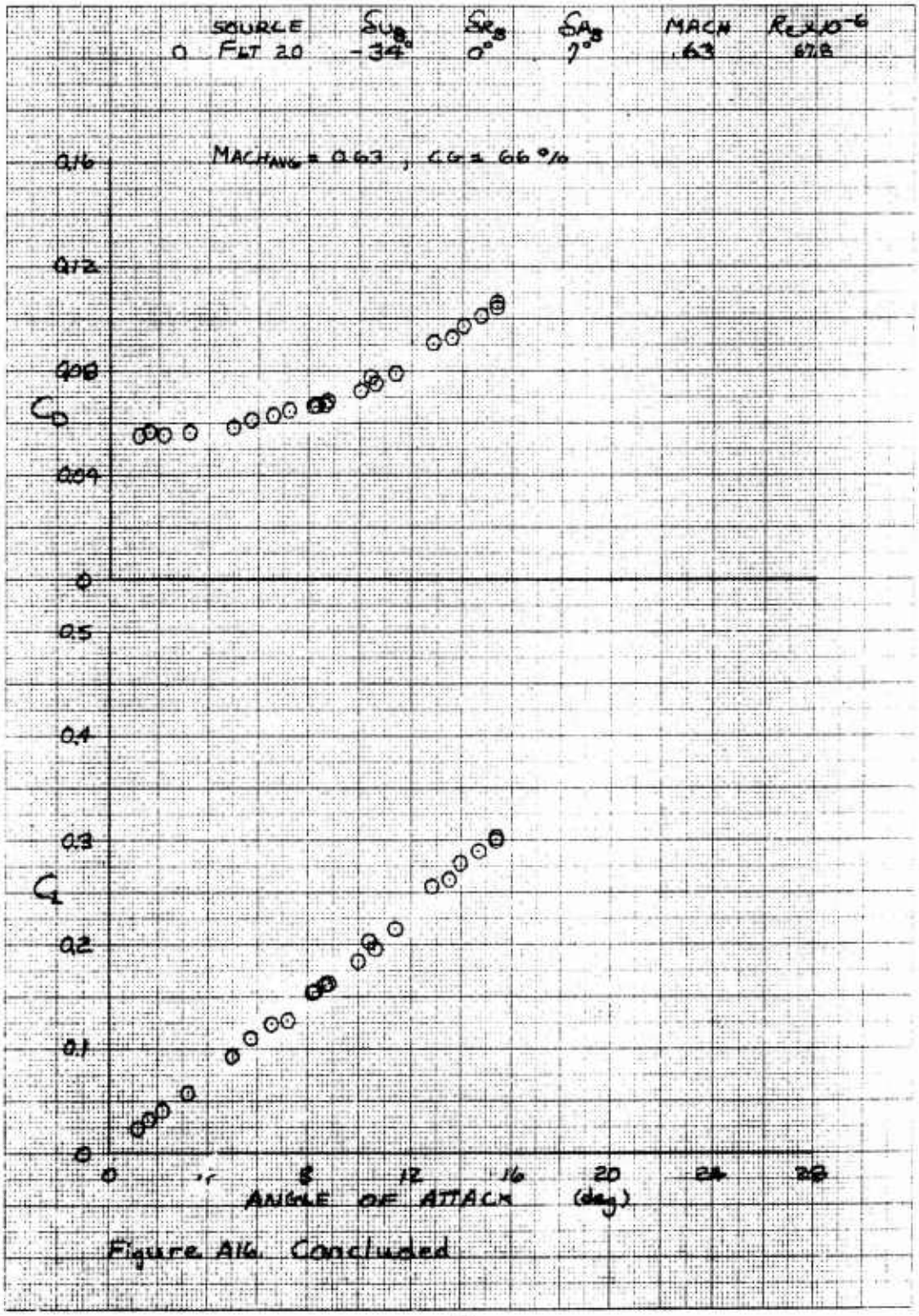

Figure A16. Concluded

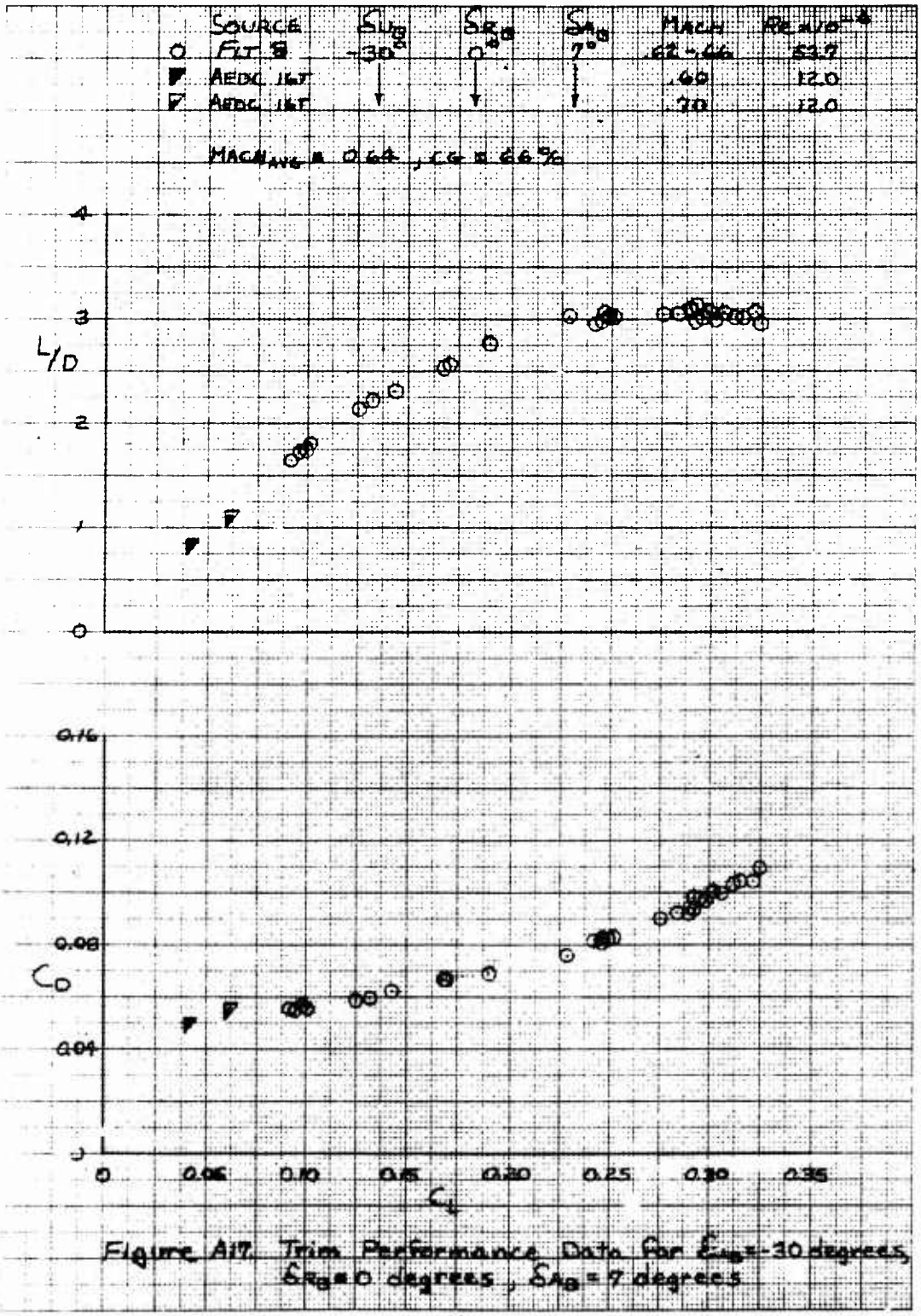

Figure A17. Trim Performance Data for δ_{LE_B} = -30 degrees, δ_{R_B} = 0 degrees, δ_{A_B} = 7 degrees

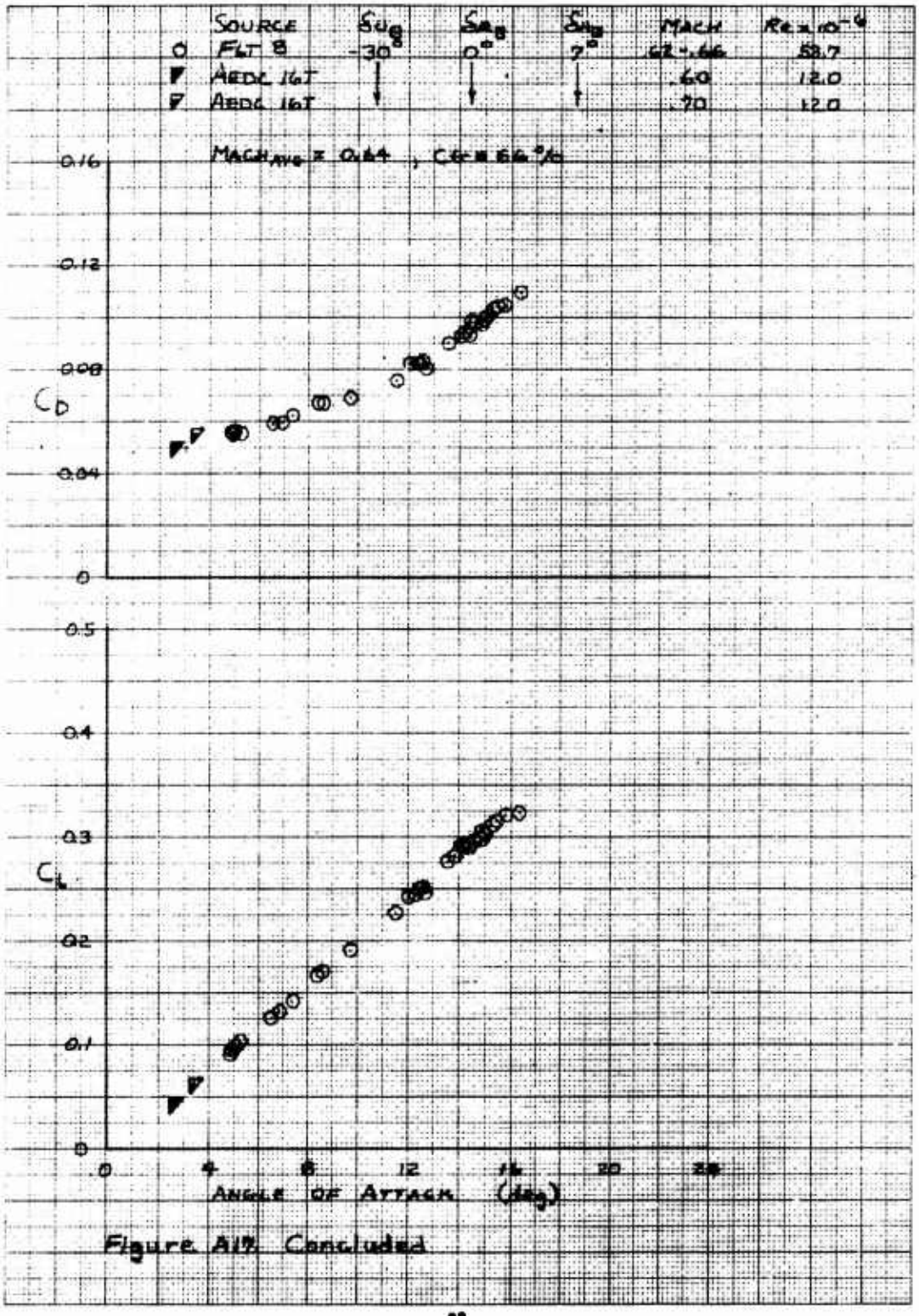

Figure A17. Concluded

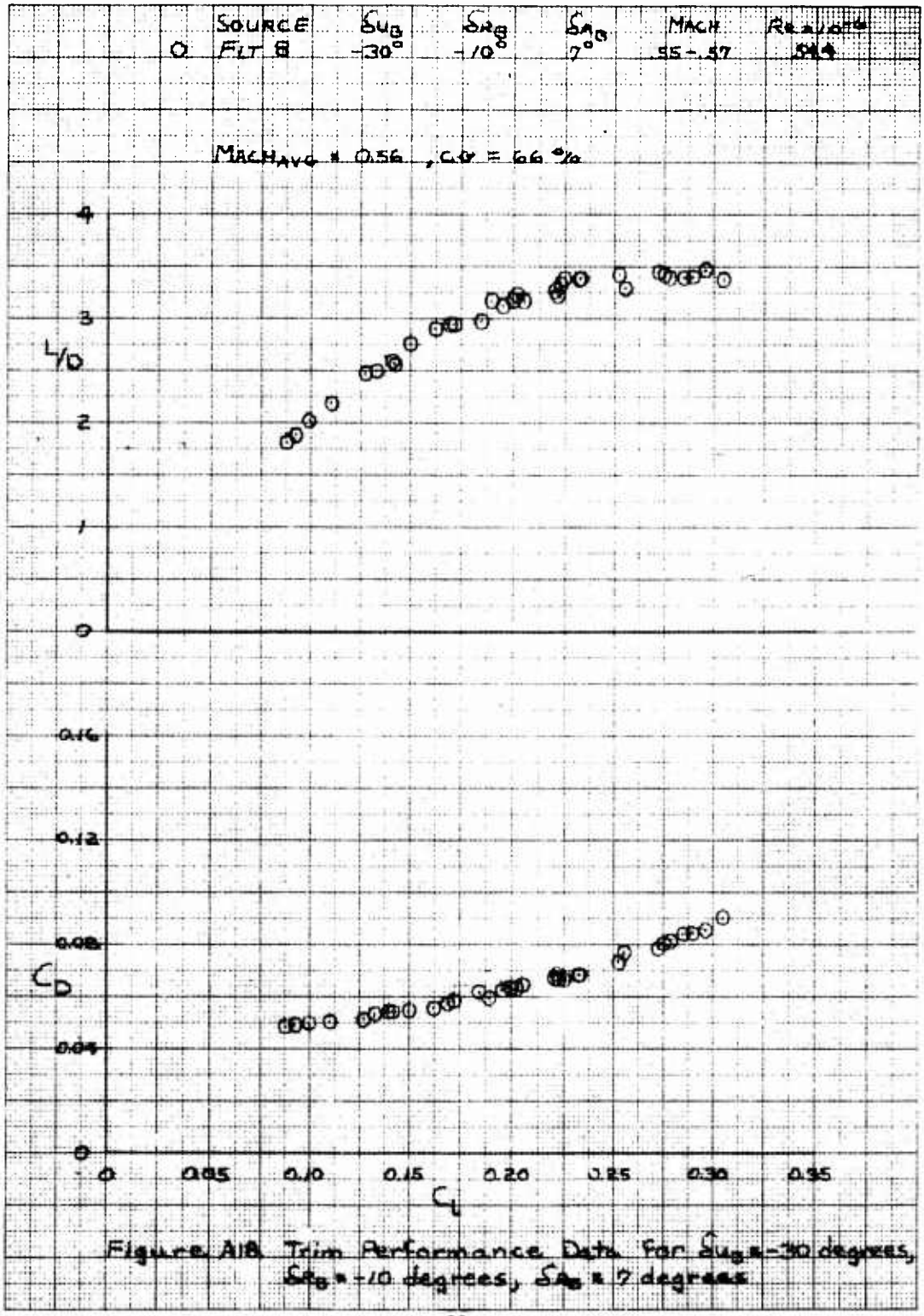

Figure A18. Trim Performance Data for δ_{u_B} = -30 degrees, δ_{R_B} = -10 degrees, δ_{A_B} = 7 degrees

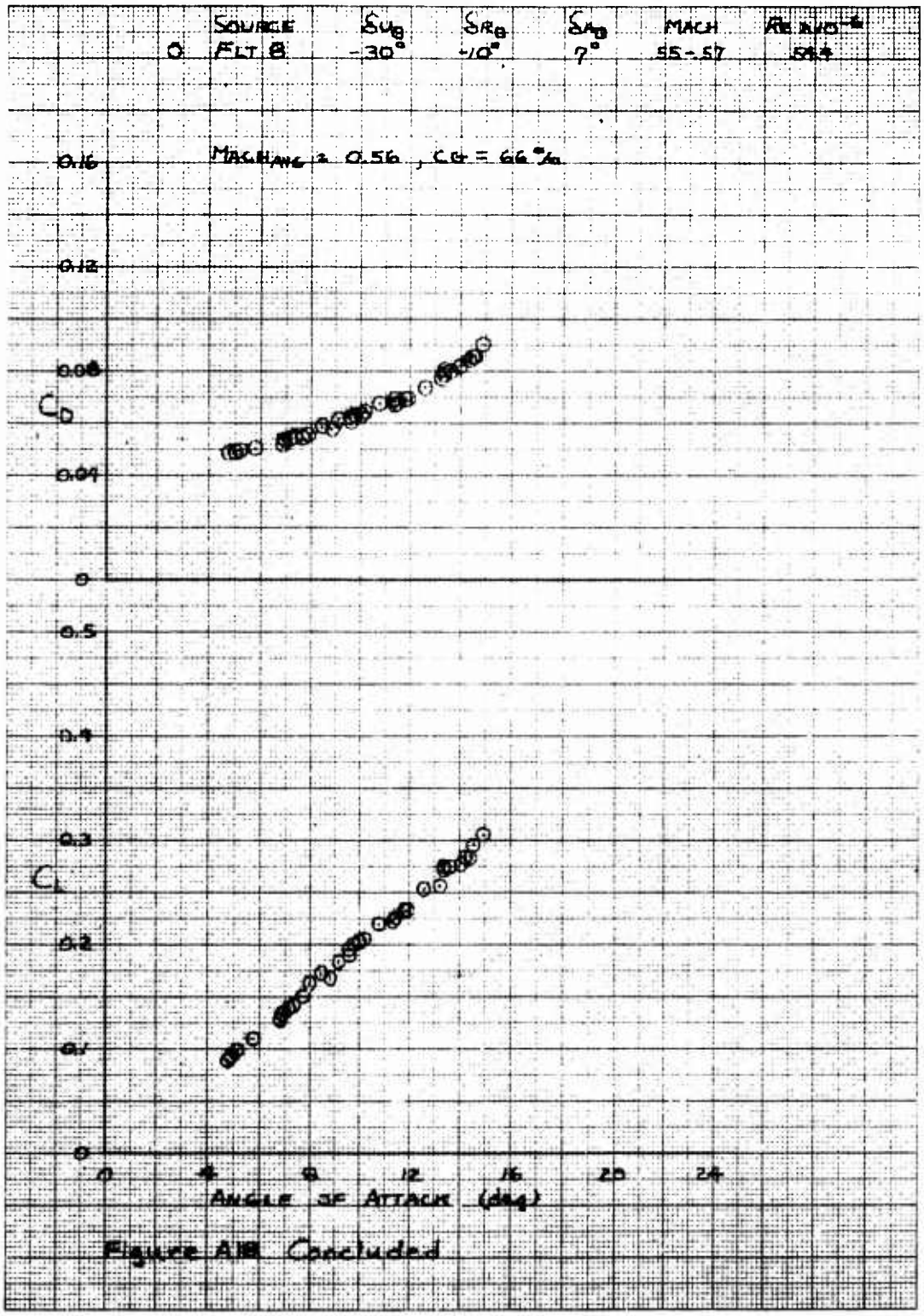

Figure A18 Concluded

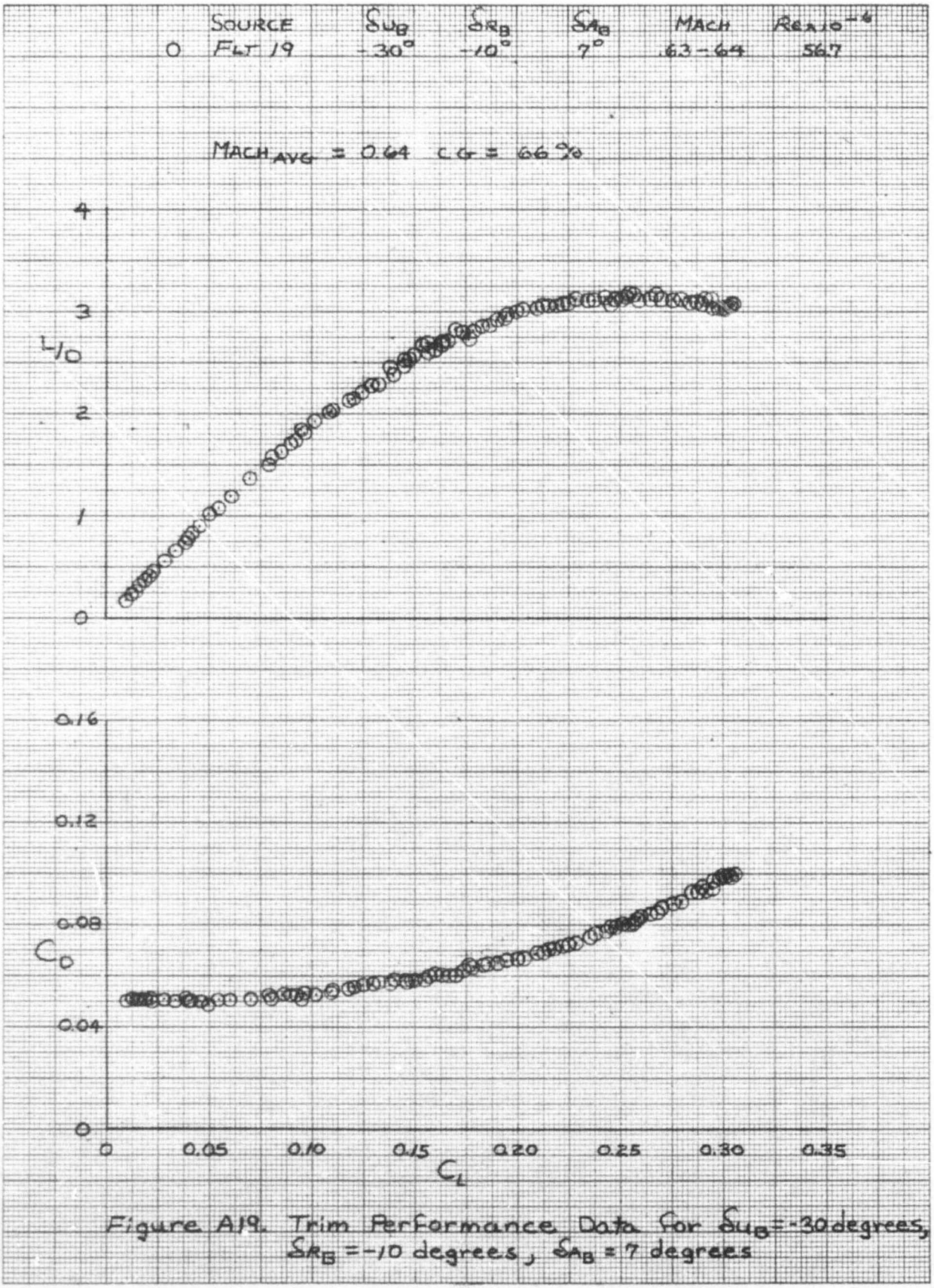

Figure A19. Trim Performance Data for δu_B = -30 degrees, δr_B = -10 degrees, δa_B = 7 degrees

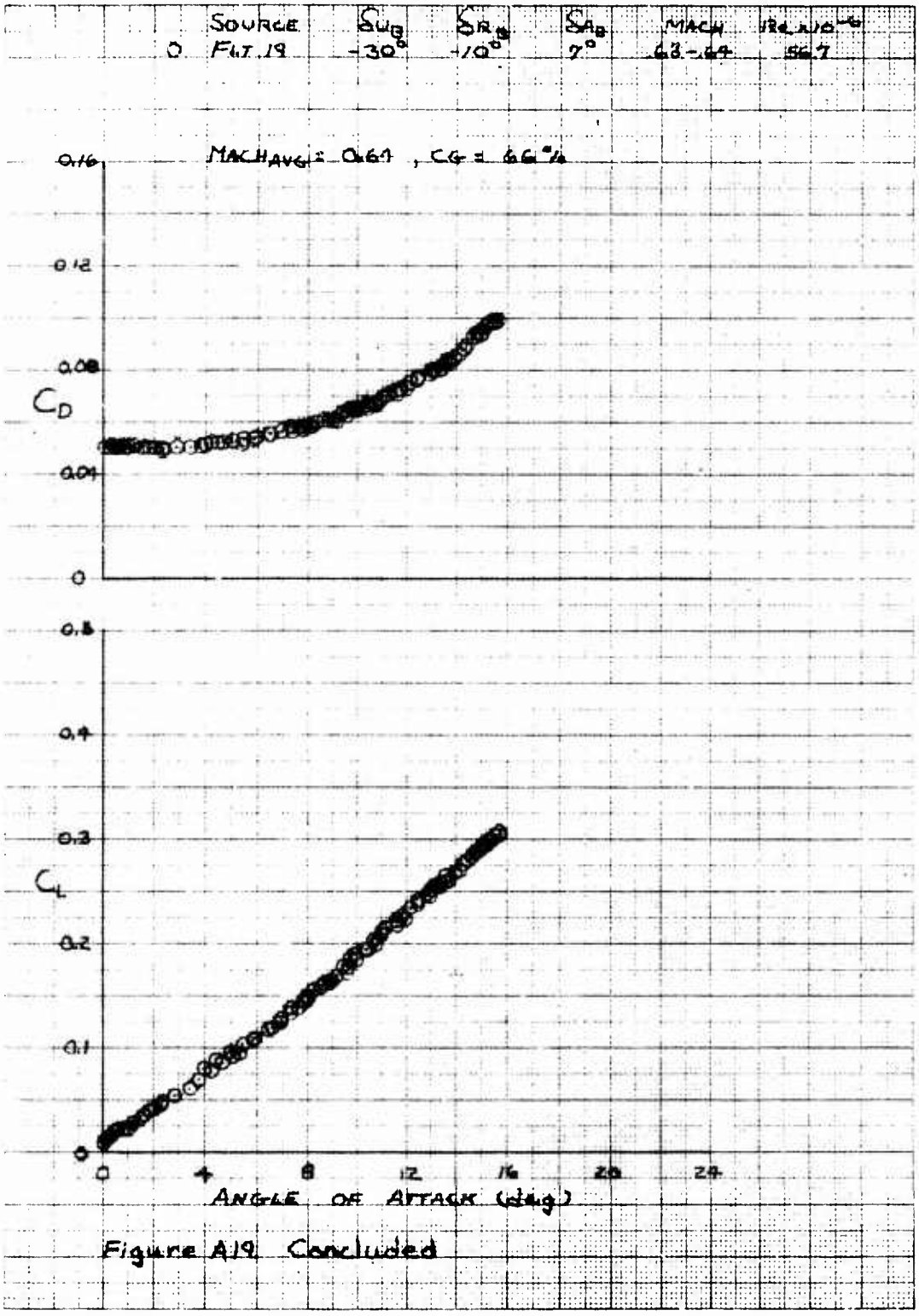

Figure A19 Concluded

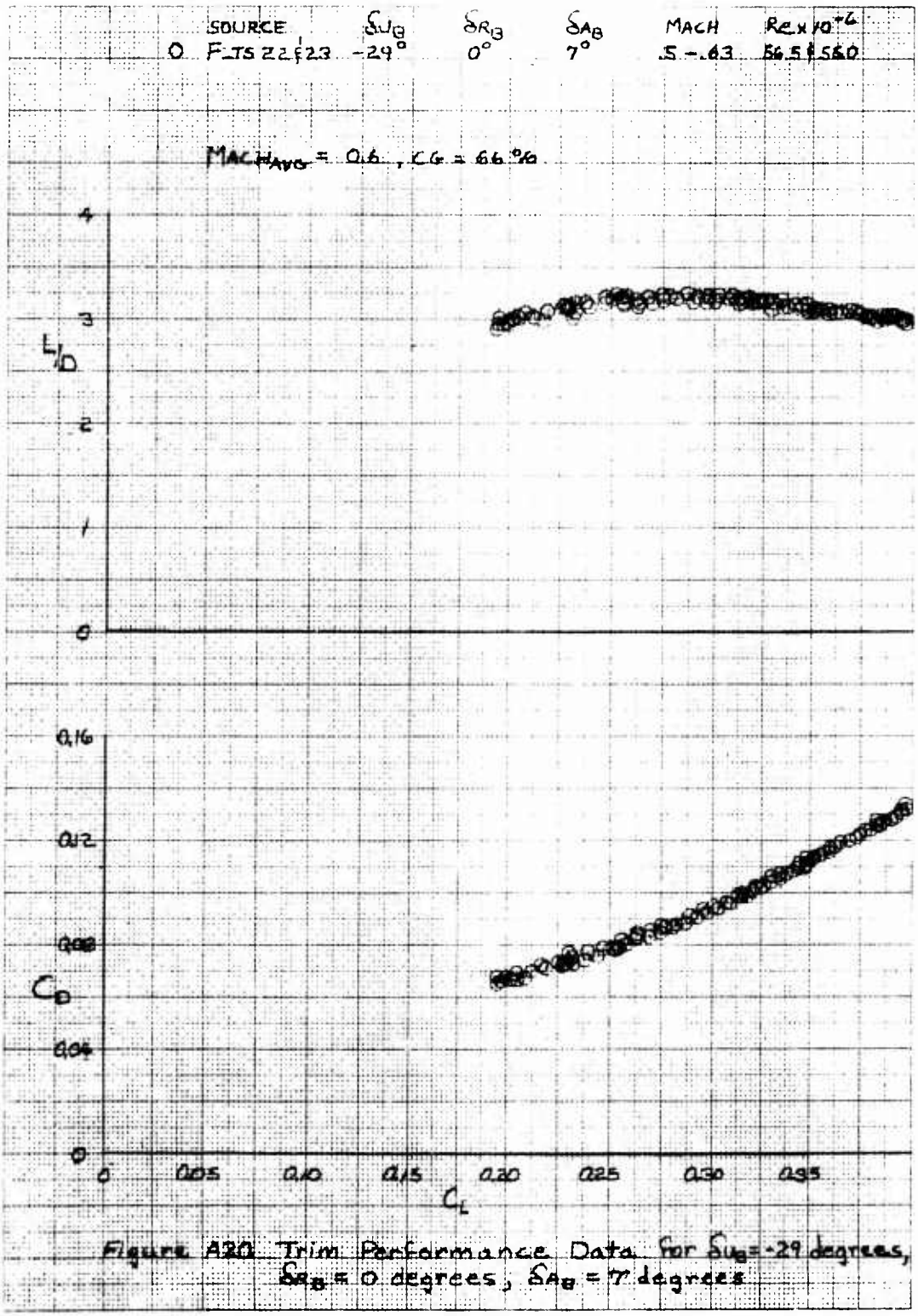

Figure A20. Trim Performance Data for δ_{LE} = -29 degrees, δ_{RB} = 0 degrees, δ_{AB} = 7 degrees.

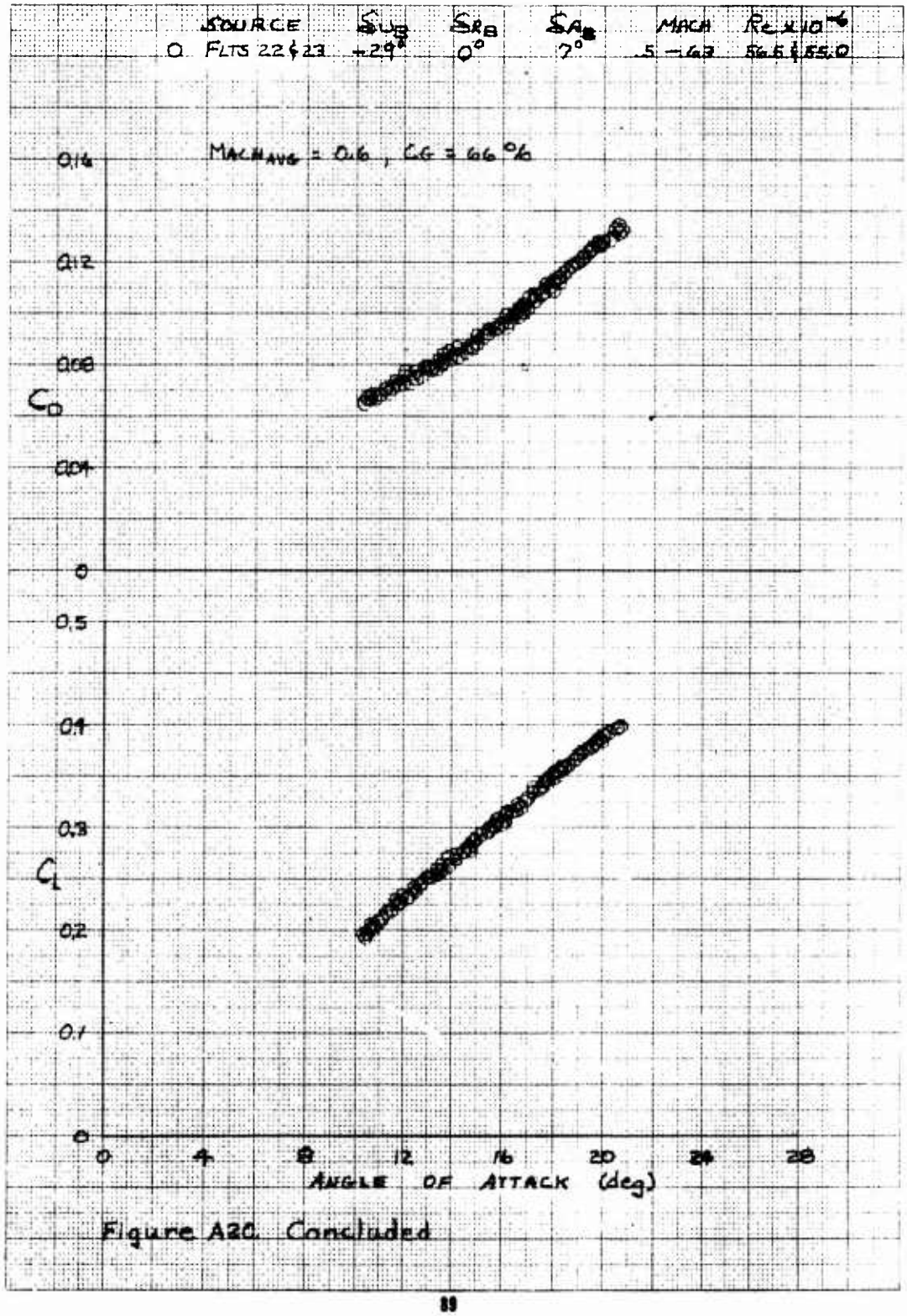

Figure A20. Concluded

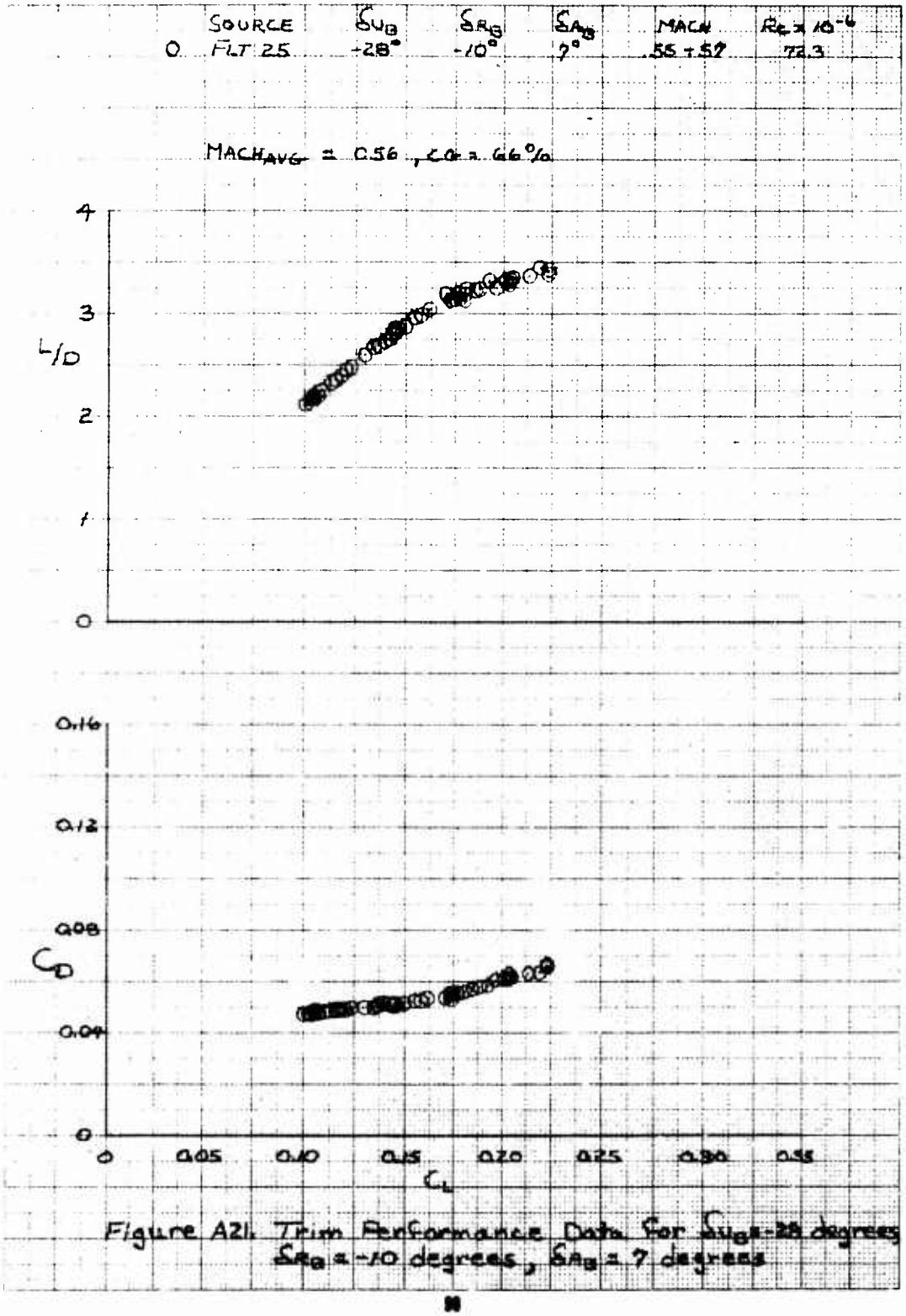

Figure A21. Trim Performance Data for δu_B = 28 degrees, δR_B = -10 degrees, δA_B = 7 degrees

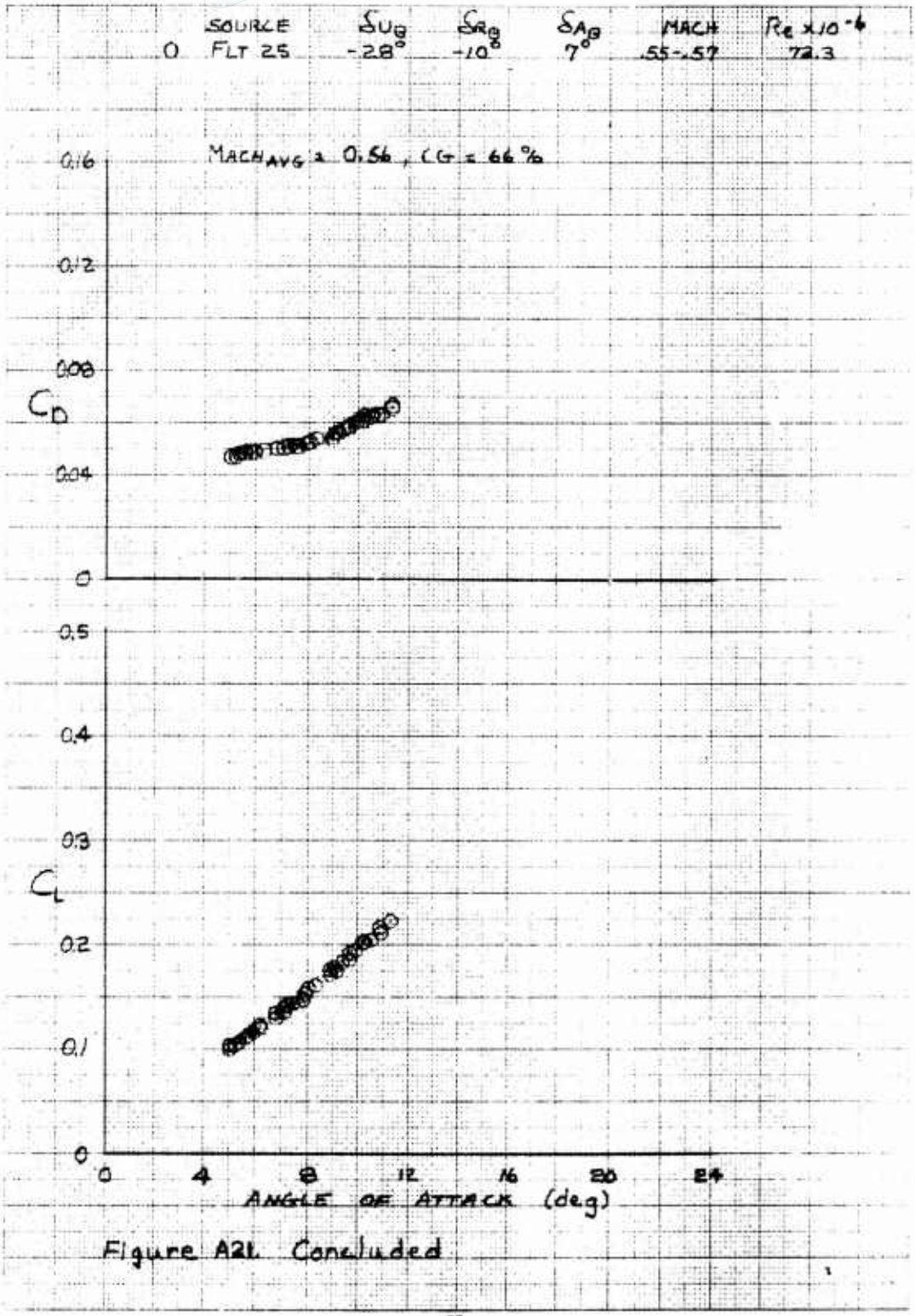

Figure A21. Concluded

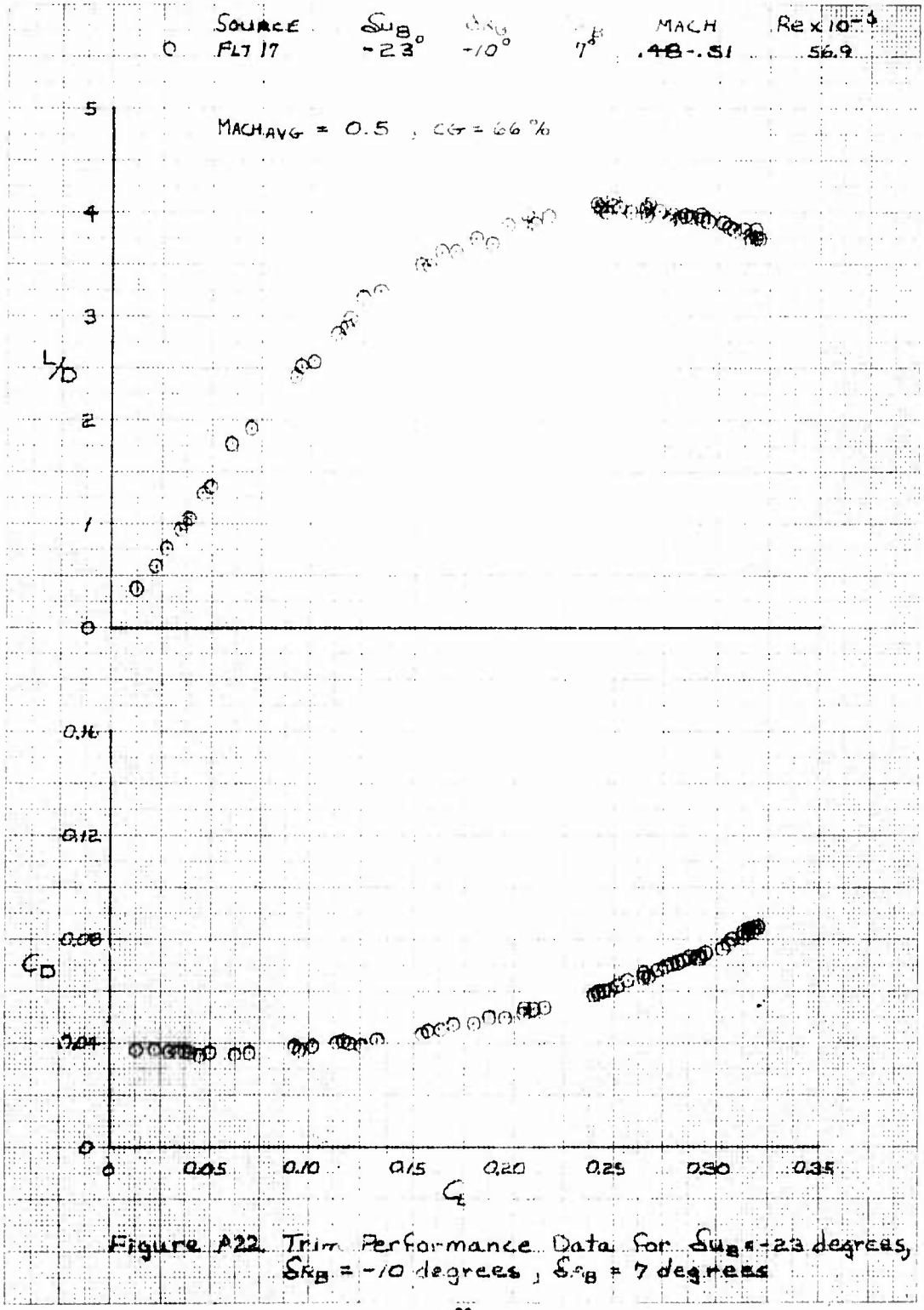

Figure A22. Trim Performance Data for δ_{W_B} = -23 degrees, δ_{K_B} = -10 degrees, α_B = 7 degrees

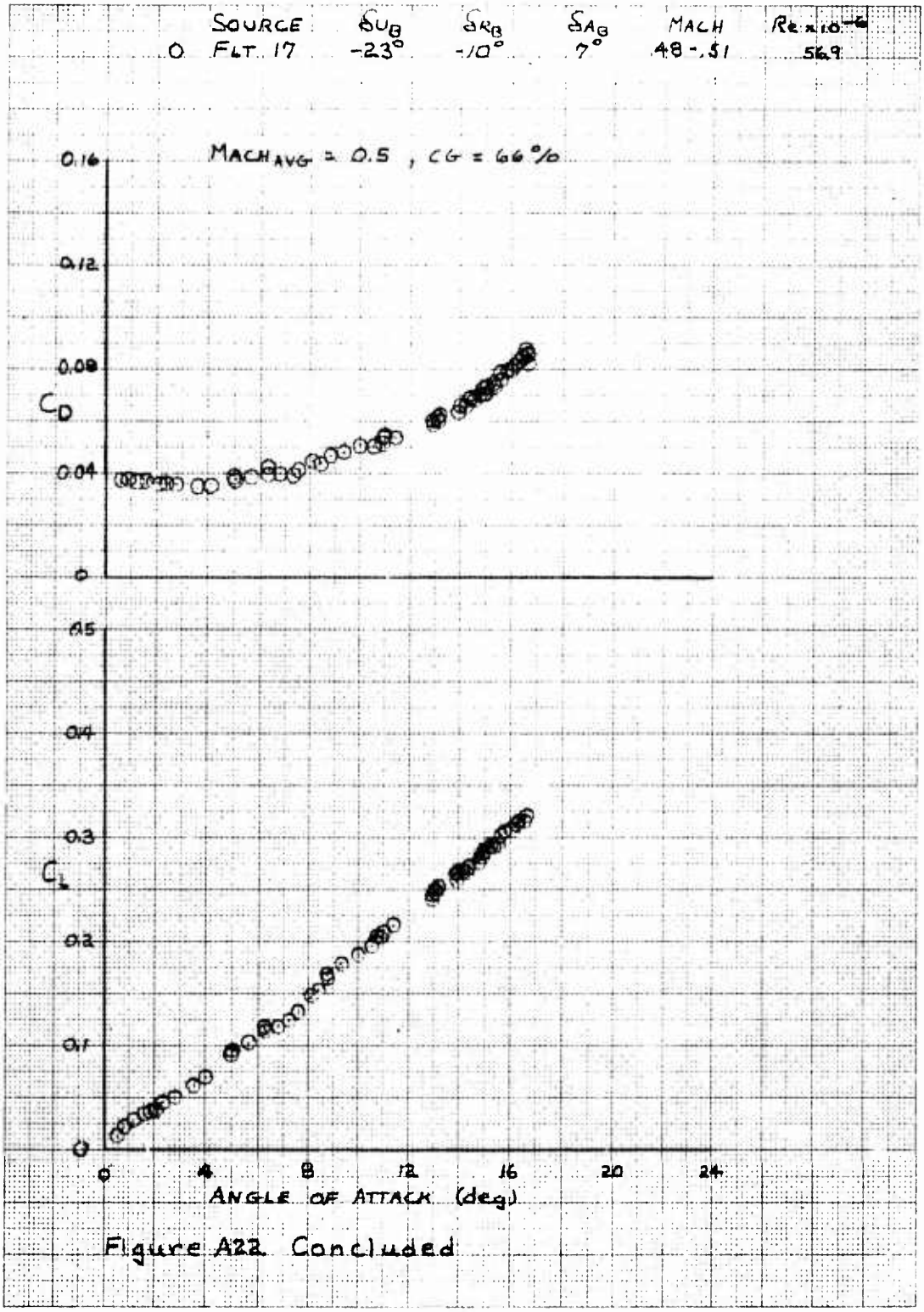

Figure A22. Concluded

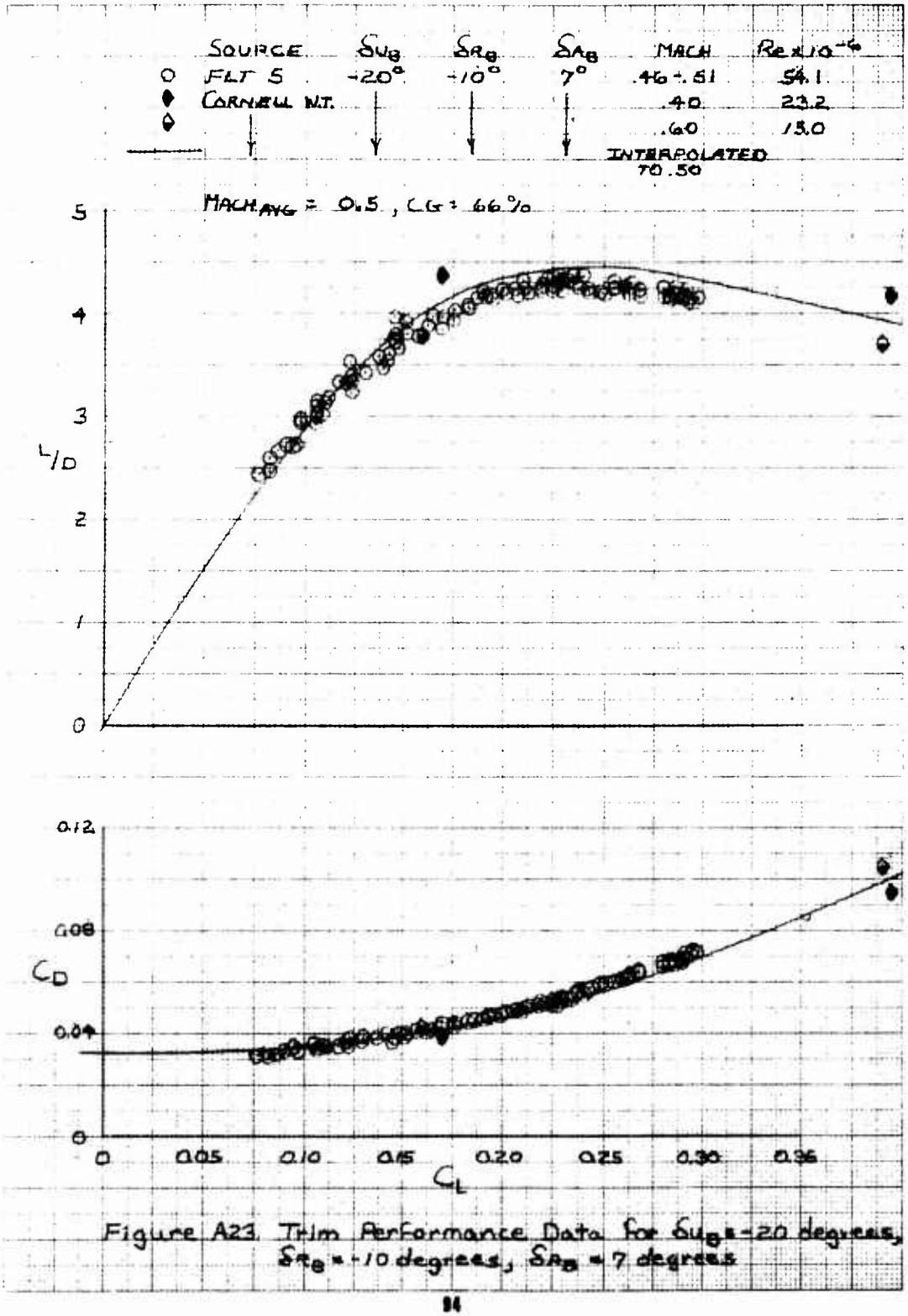

Figure A23. Trim Performance Data for δu_B = -20 degrees, δR_B = +10 degrees, δA_B = 7 degrees

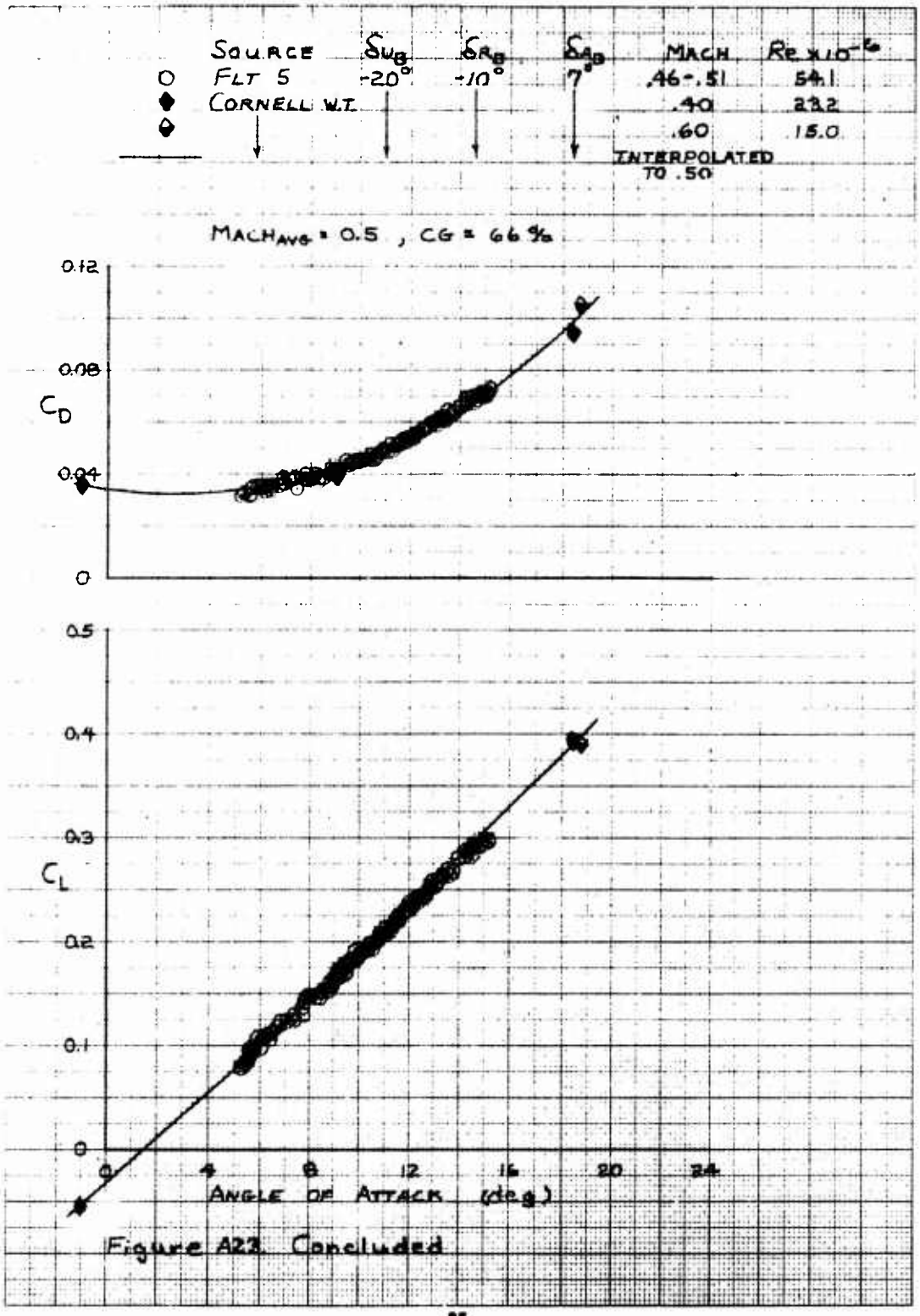

Figure A23. Concluded

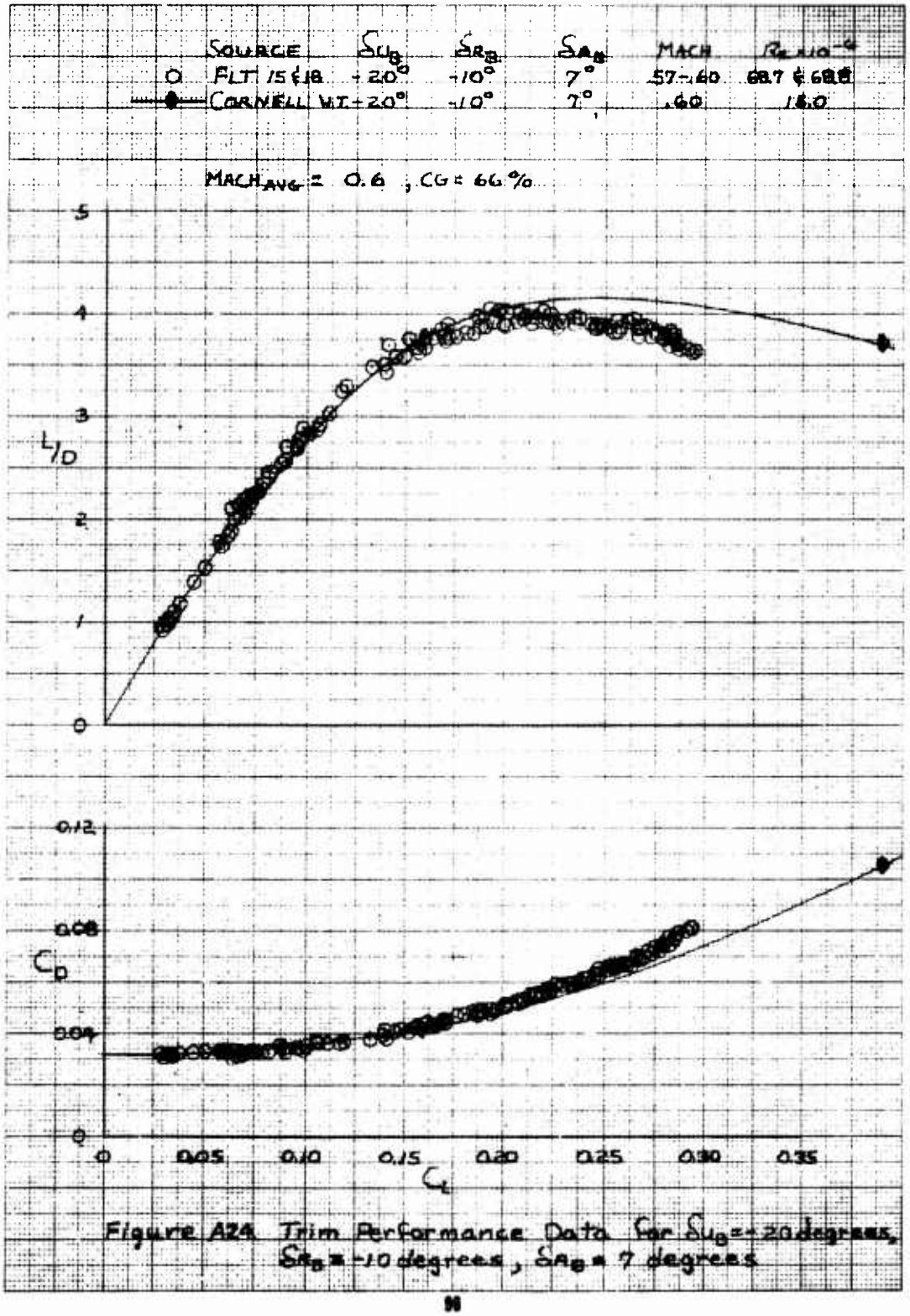

Figure A24 Trim Performance Data for S_{U_B} = +20 degrees, S_{R_B} = -10 degrees, S_{A_B} = 7 degrees

	SOURCE	δ_{u_e}	δ_{e_e}	$\delta_{A_{CG}}$	MACH	$R_e \times 10^{-6}$
O	FLT 15 & 18	+20°	-10°	7°	.57-.60	68.7 & 68.8
—●—	CORNELL W.T.	+20°	-10°	7°	.60	15.0

$MACH_{AVG} = 0.6$, $CG = 66.8\%\bar{c}$

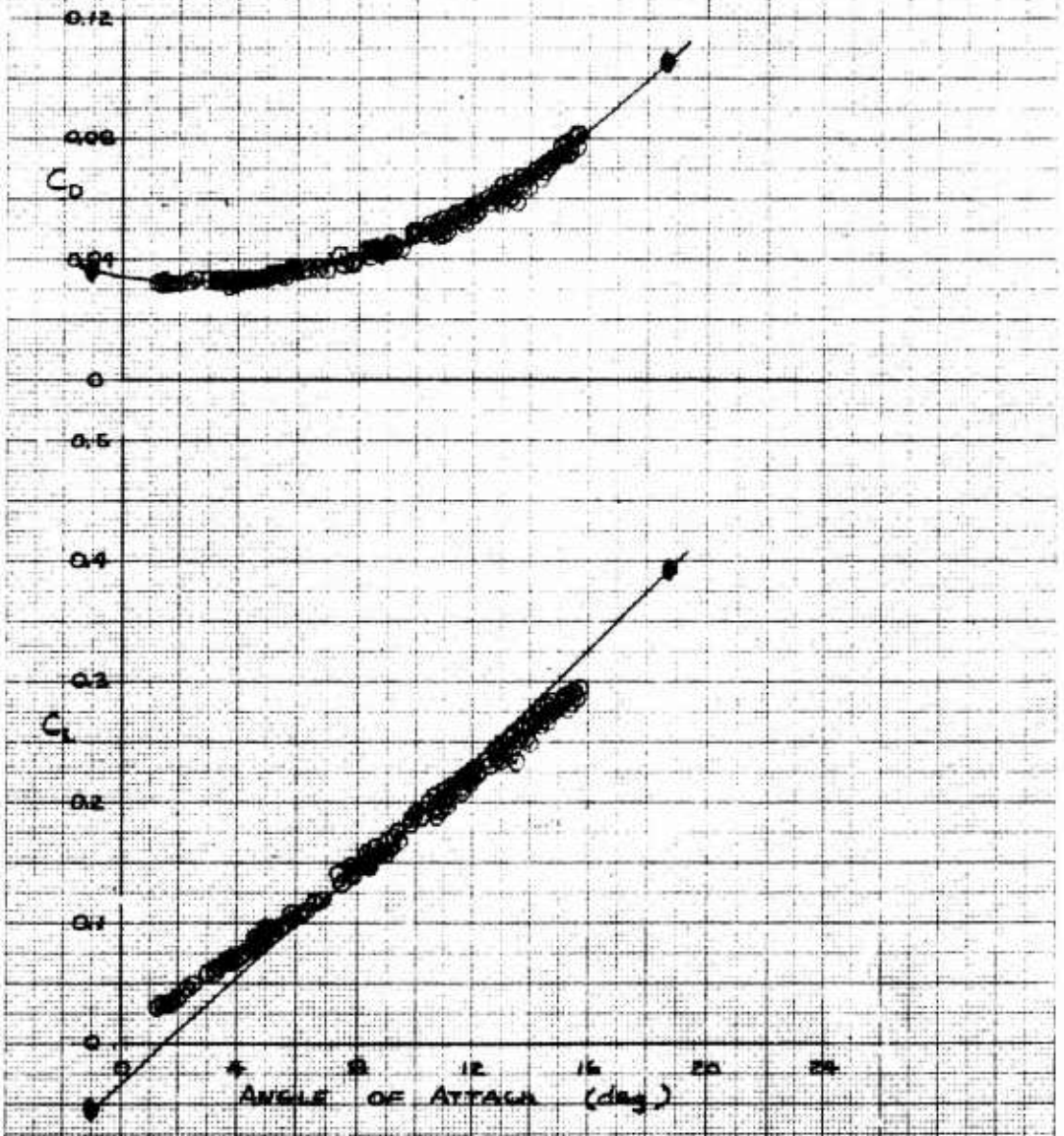

Figure A2A Concluded

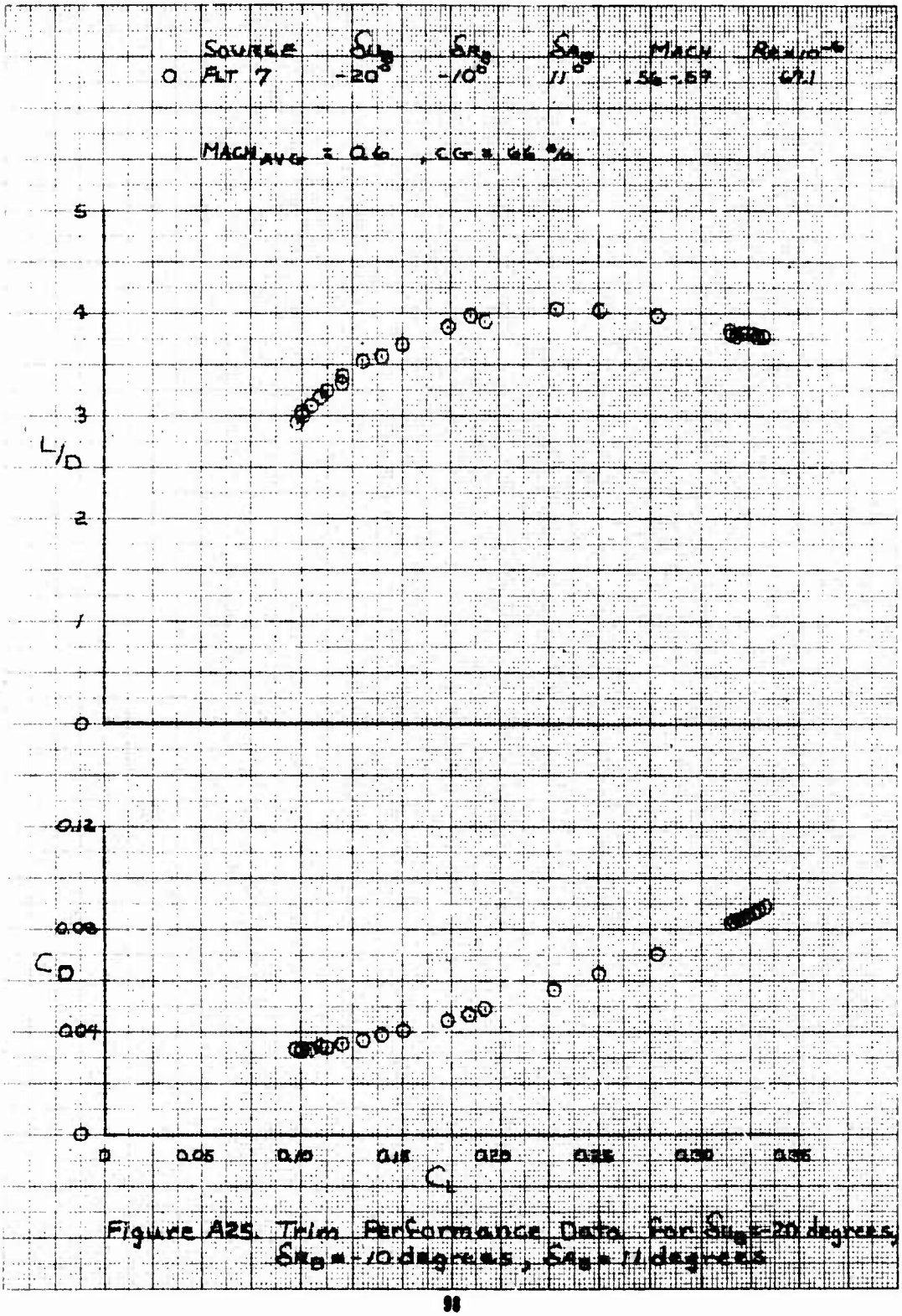

Figure A25. Trim Performance Data for δ_{LE}=-20 degrees, δ_{FB}=-10 degrees, δ_{AB}=11 degrees

	Source	δ_{V_B}	δ_{H_B}	δ_{A_B}	Mach	Re x 10^{-6}
○	Flt 7	-20°	-10°	11°	.56 - .59	6.21

$MACH_{AVG}$ = 0.6 , CG = 66 %

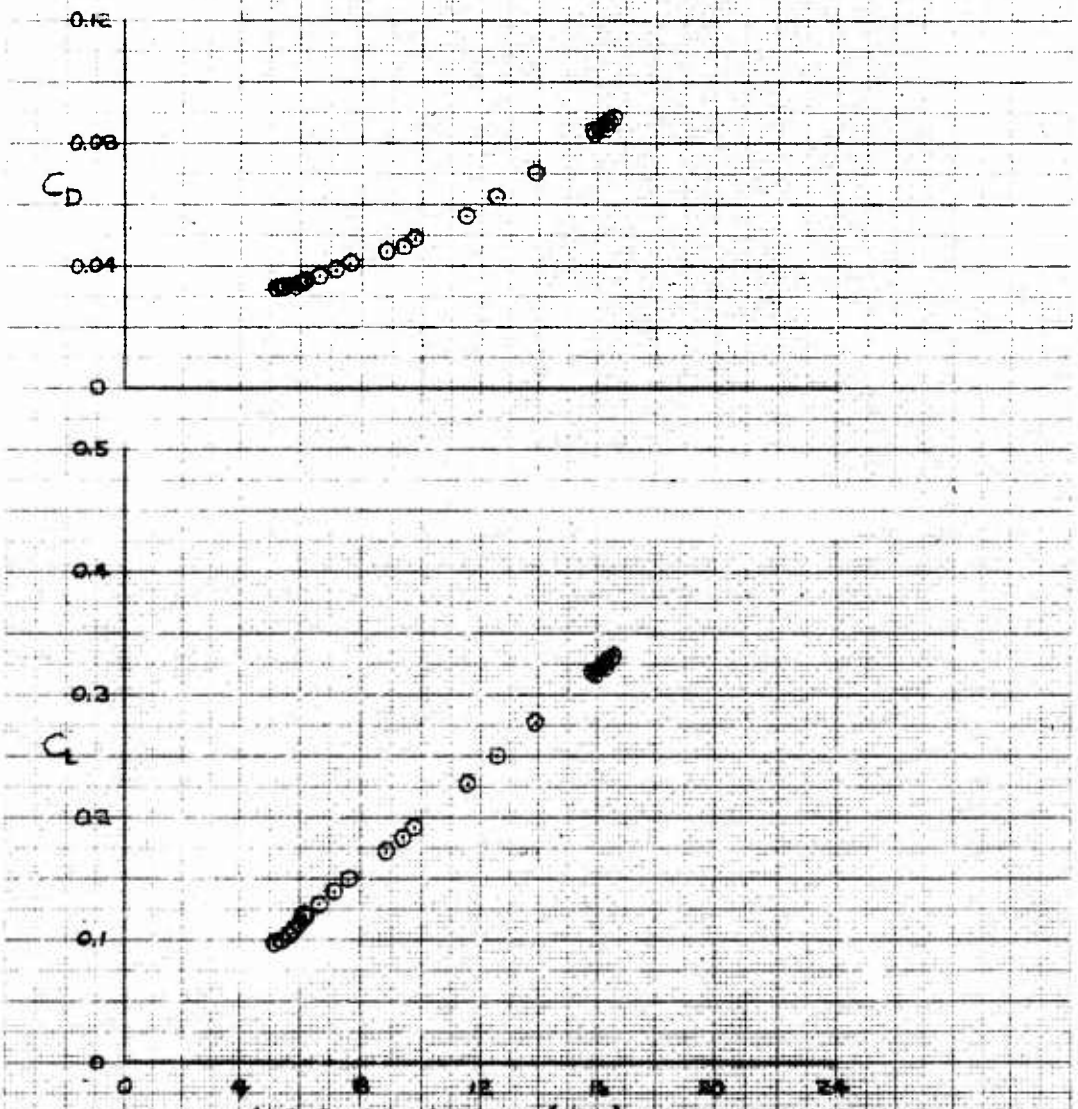

Figure A25. Concluded

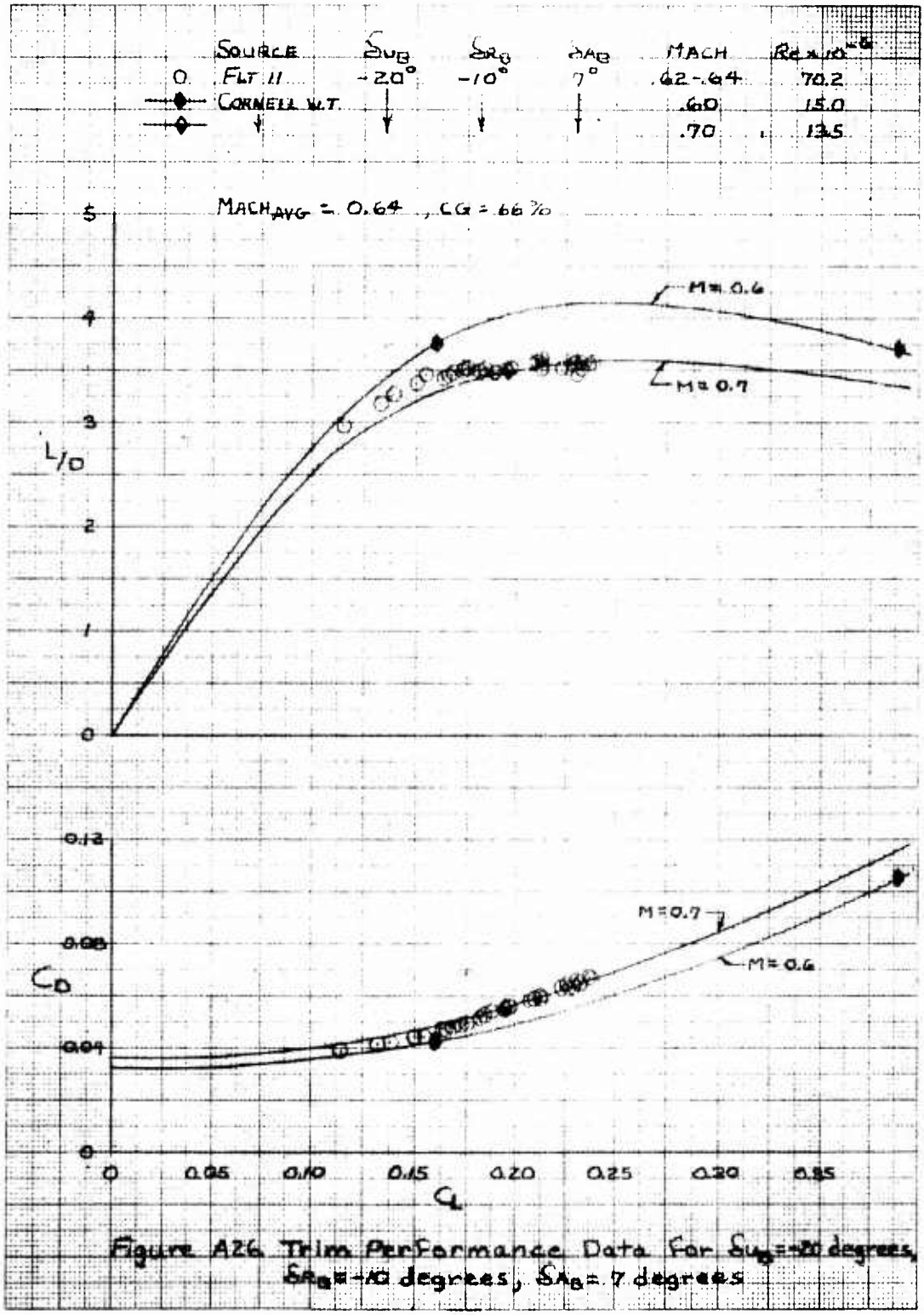

Figure A26 Trim Performance Data for δu_B=-20 degrees, δR_B=-10 degrees, δA_B= 7 degrees

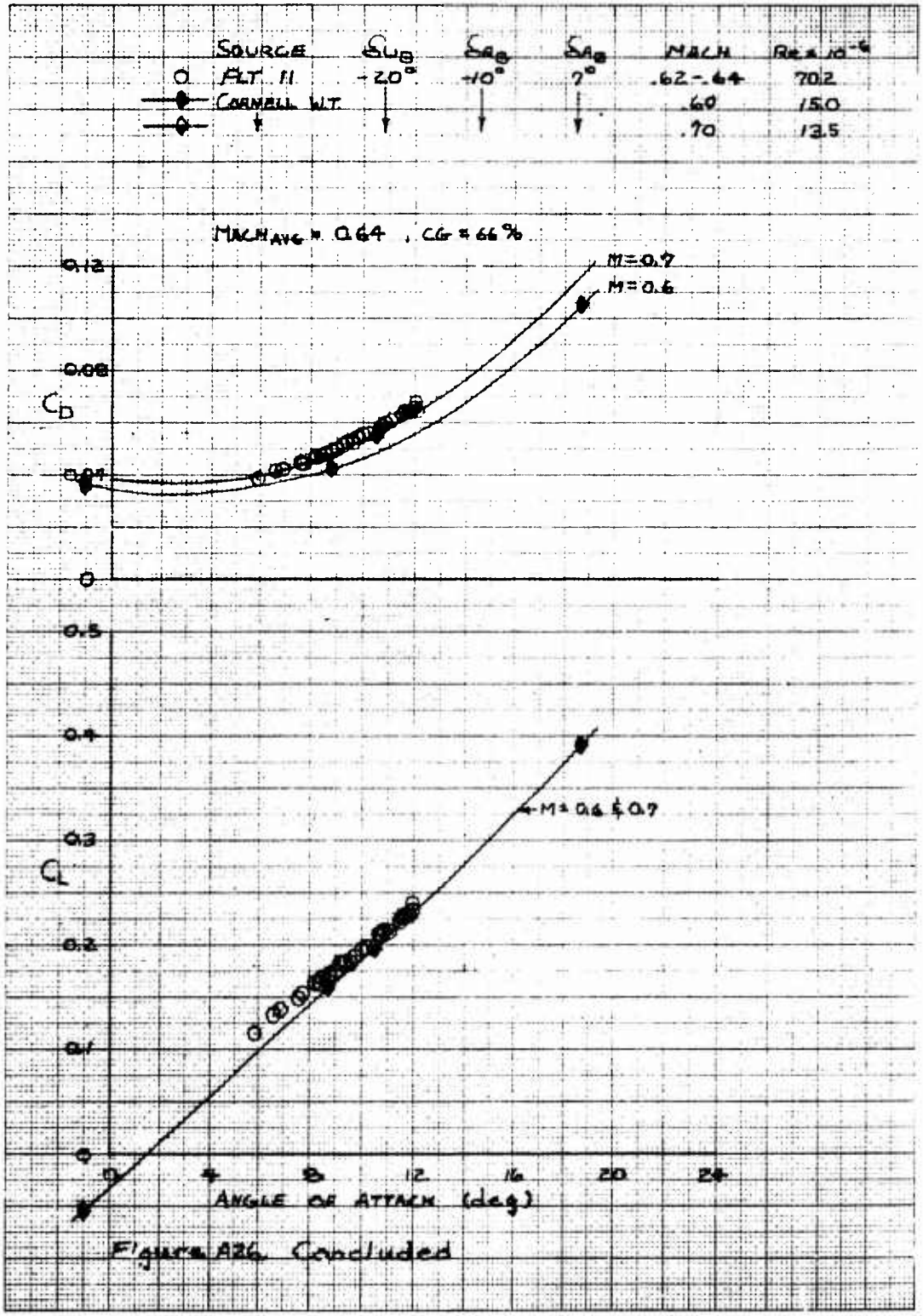

Figure A26 Concluded

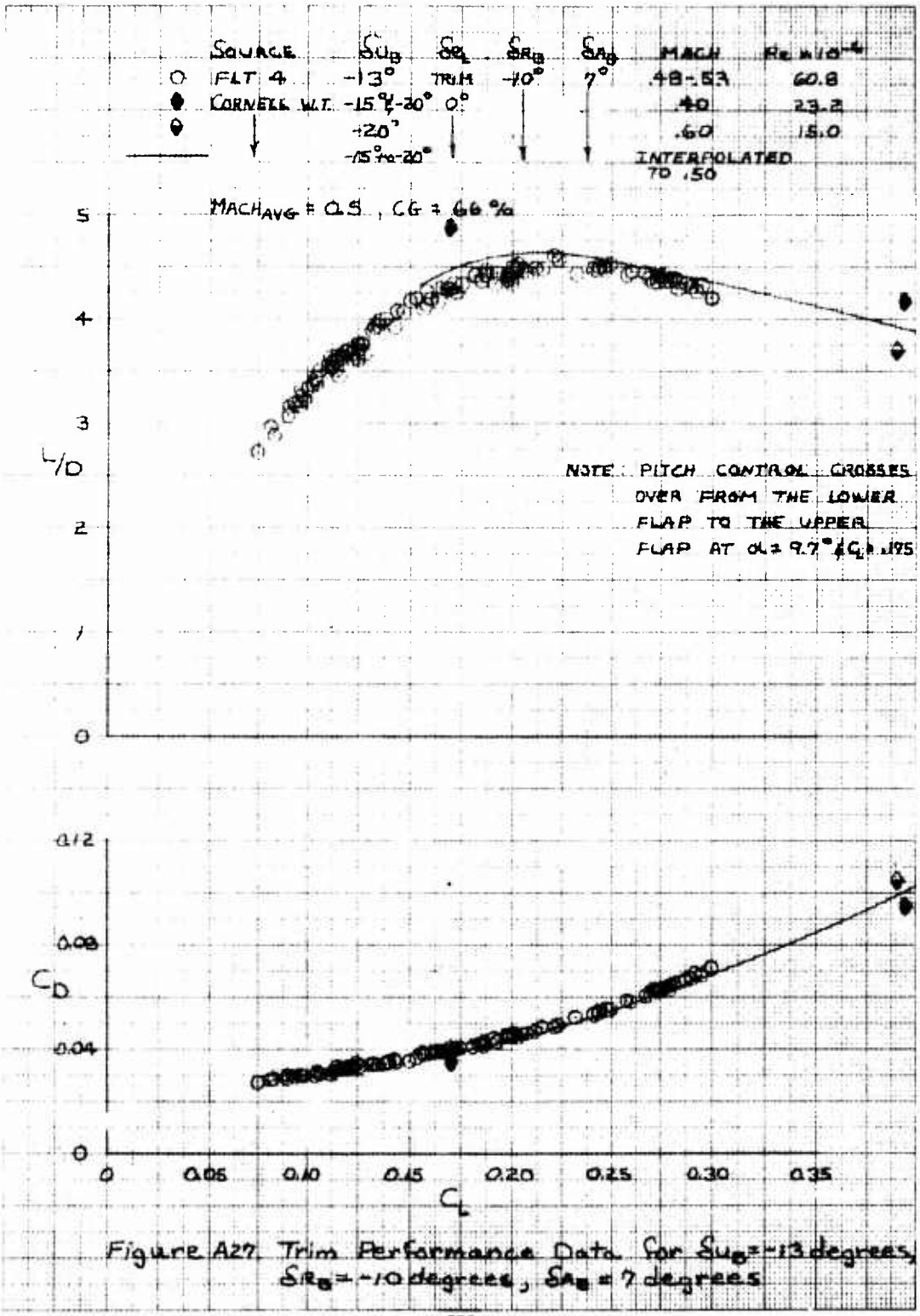

Figure A27. Trim Performance Data for δ_{U_B} = -13 degrees, δ_{R_B} = -10 degrees, δ_{A_B} = 7 degrees

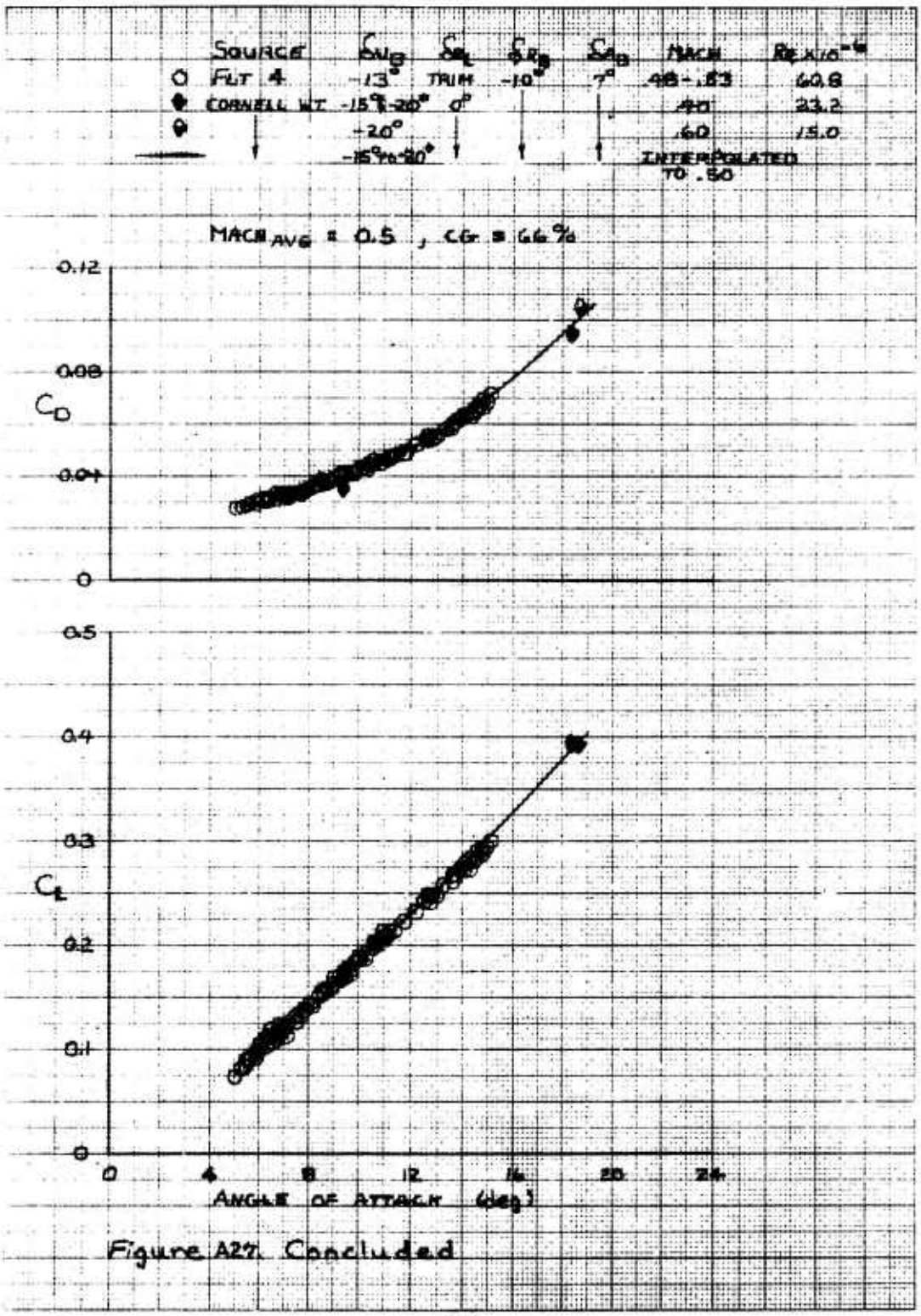

Figure A27. Concluded

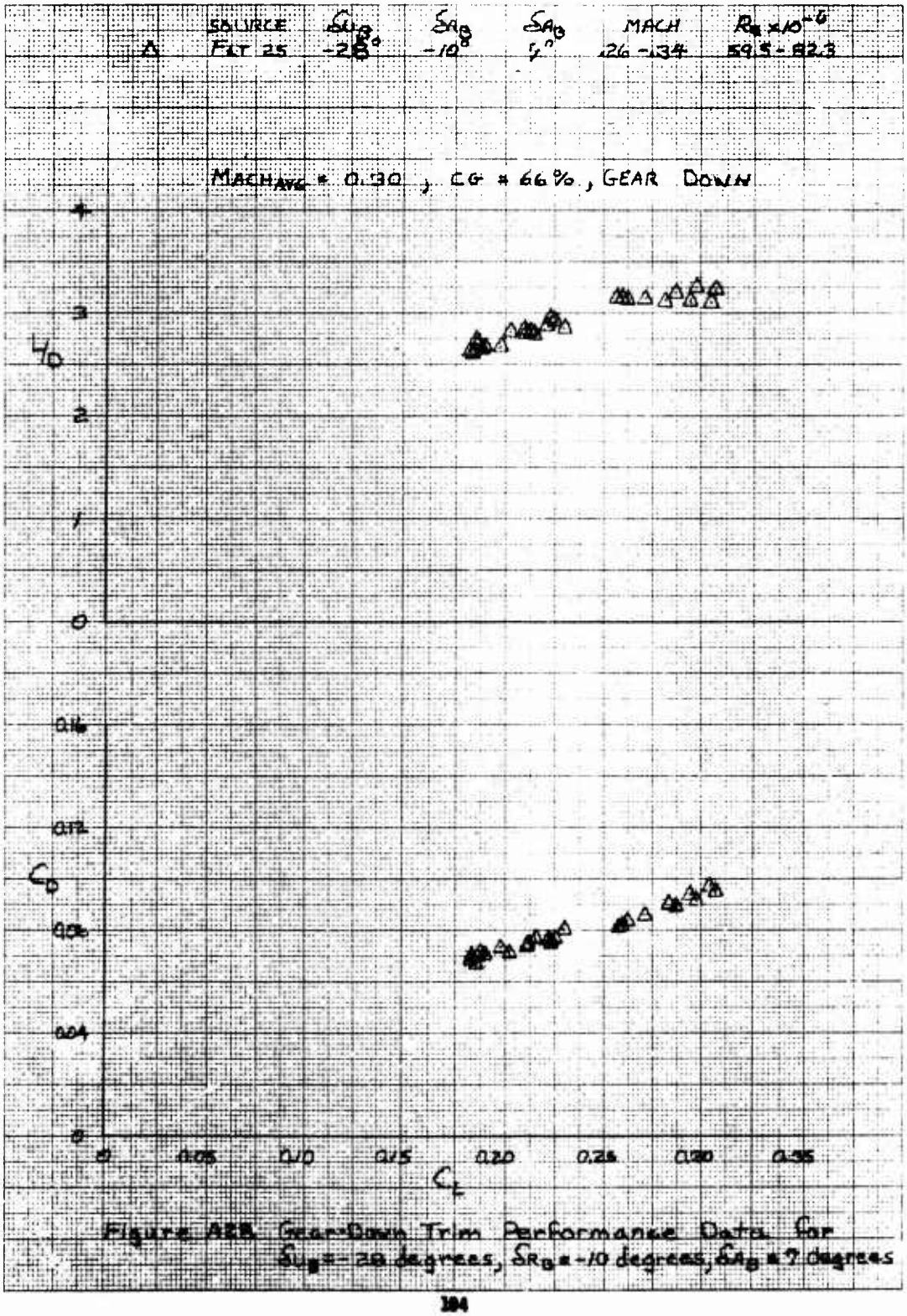

Figure A28. Gear-Down Trim Performance Data for δ_{LE} = -28 degrees, δ_{R_B} = -10 degrees, δ_{A_B} = 7 degrees

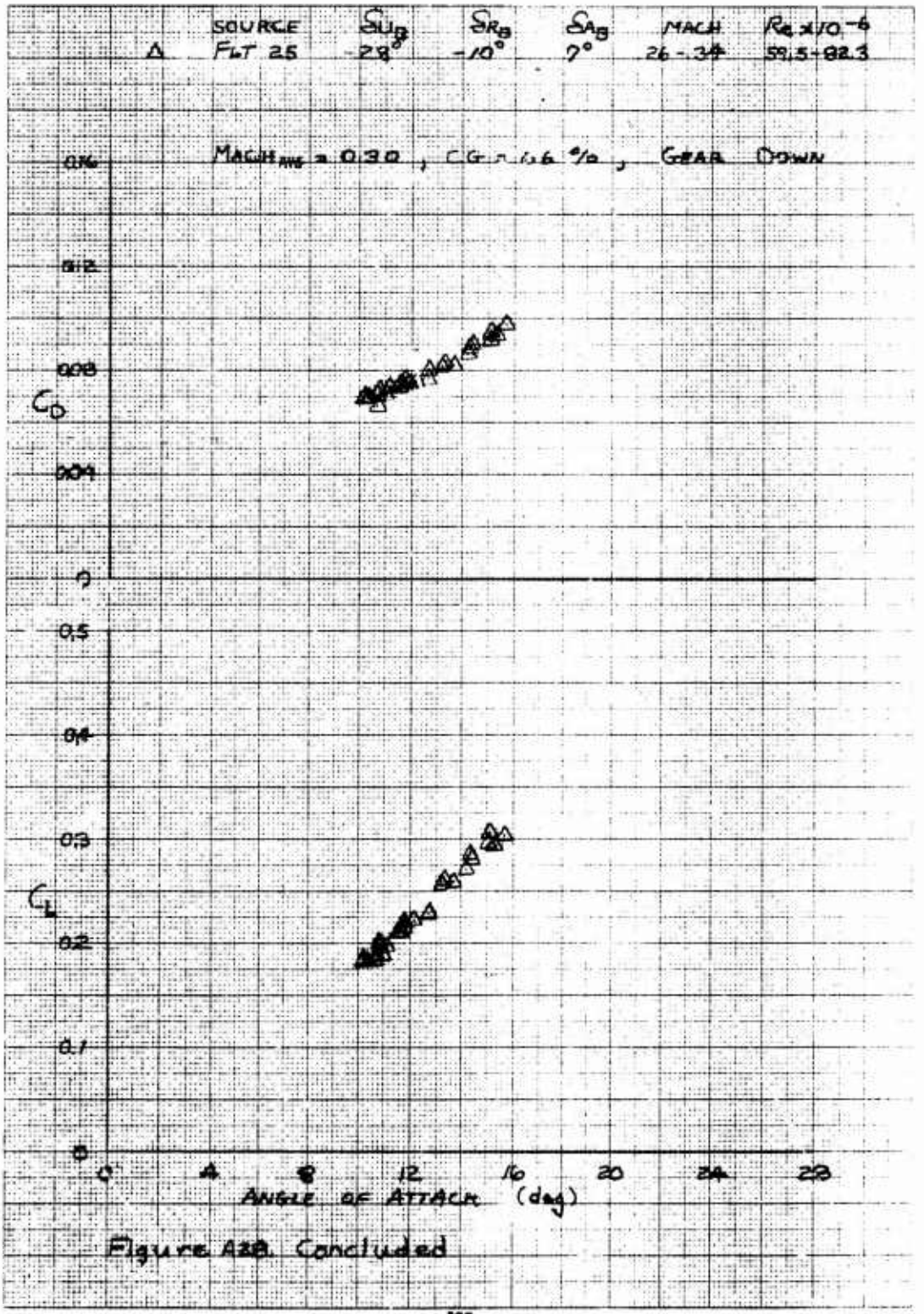

Figure A2B. Concluded

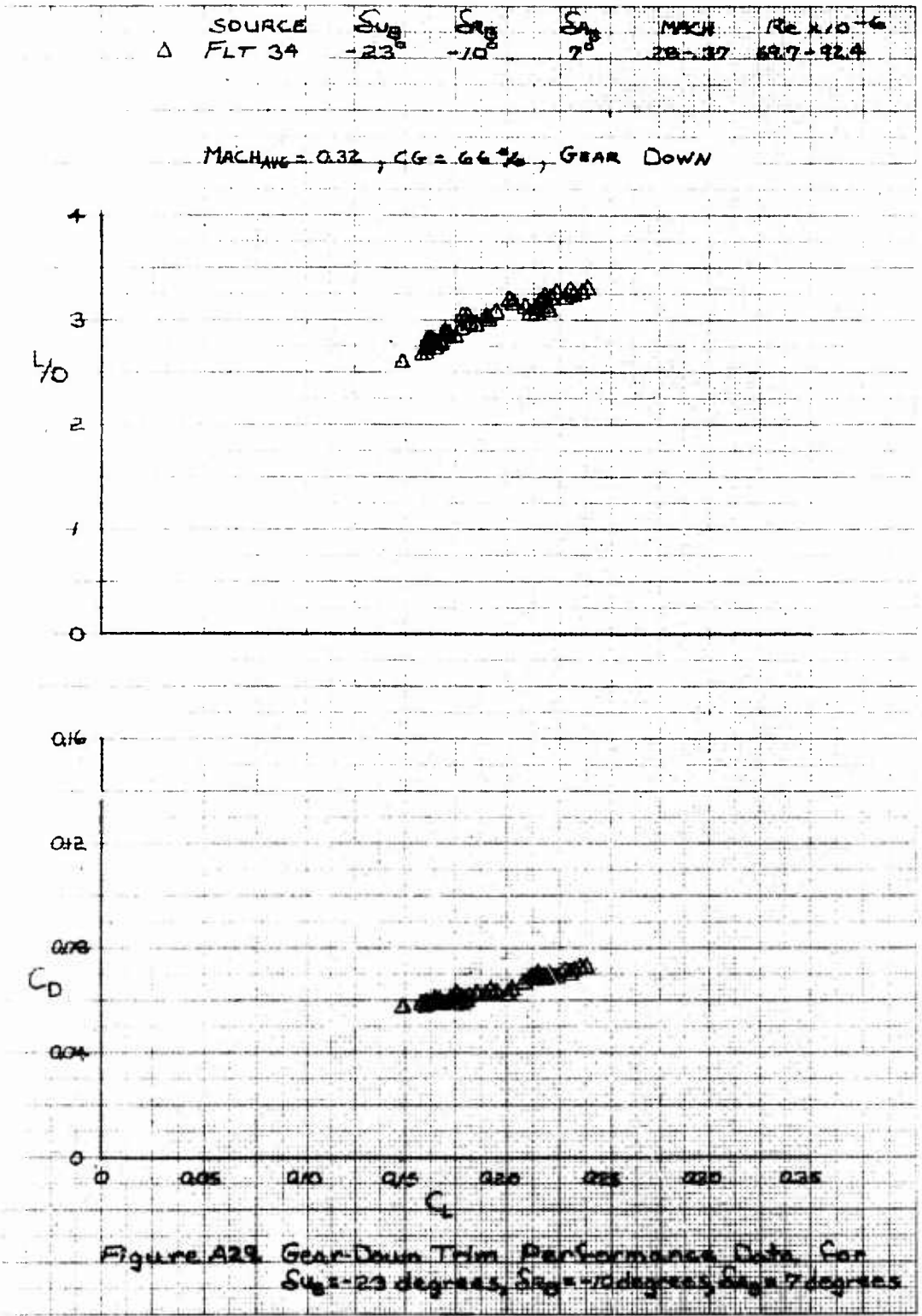

Figure A29. Gear-Down Trim Performance Data, For δ_{U_B} = -23 degrees, δ_{R_B} = -10 degrees, δ_{A_B} = 7 degrees

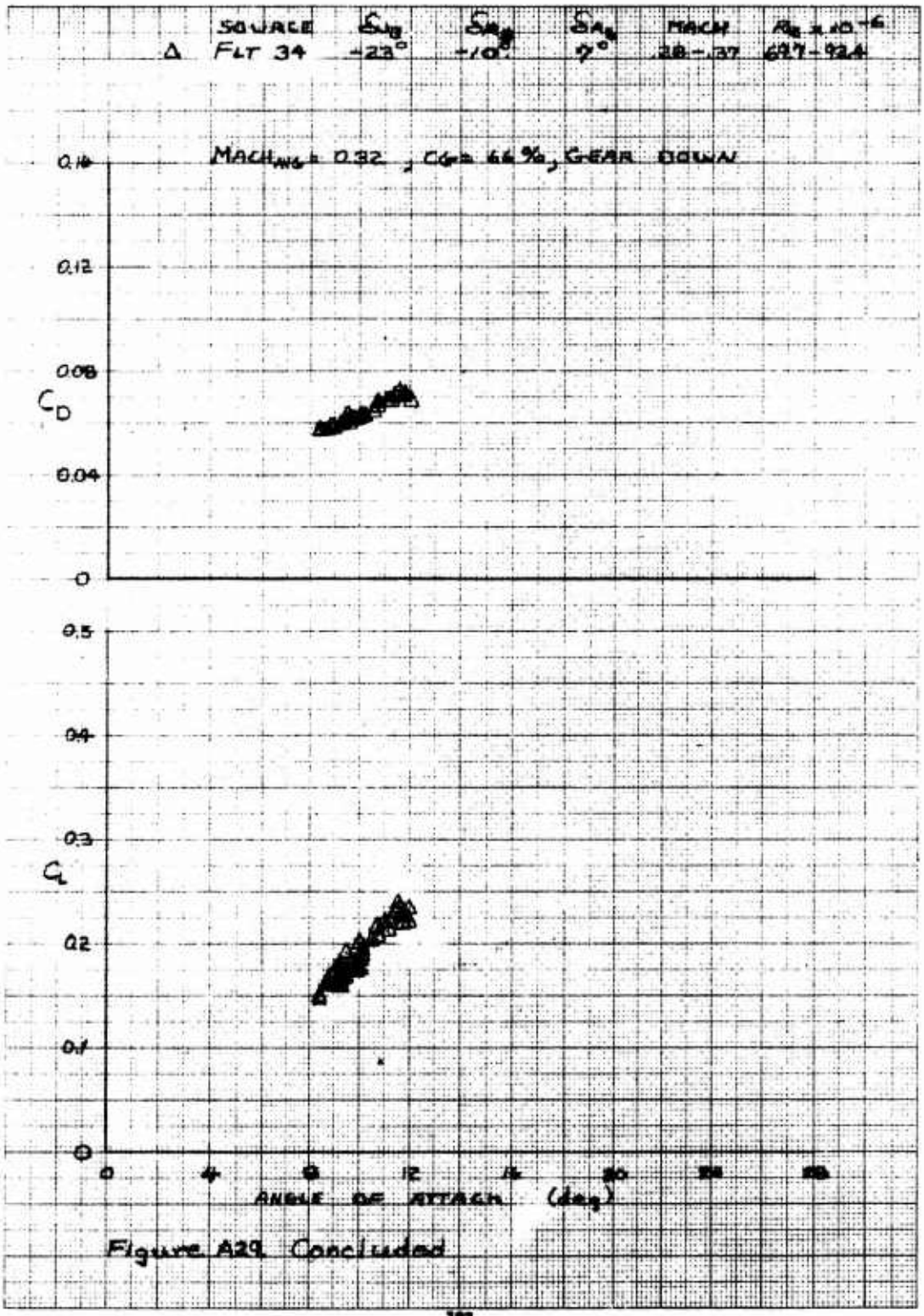

Figure A29 Concluded

	SOURCE	S_{LE_B}	S_{R_B}	α_B	MACH	$R_e \times 10^{-6}$
Δ	Fits 11, 15, 19 & 24	-20°	-10°	7°	.27-.38	64.6-96.8
—■—	AFIT 5 FT W.T.	-20°	-10°	INTERP TO 7°	.17	3.3

$MACH_{AVG}$ = 0.32, CG = 66%, GEAR DOWN

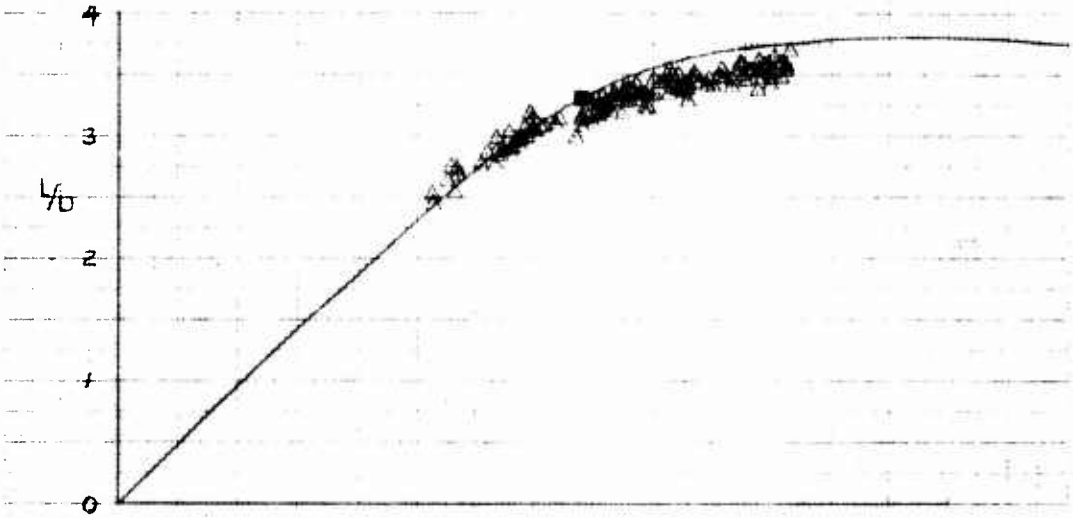

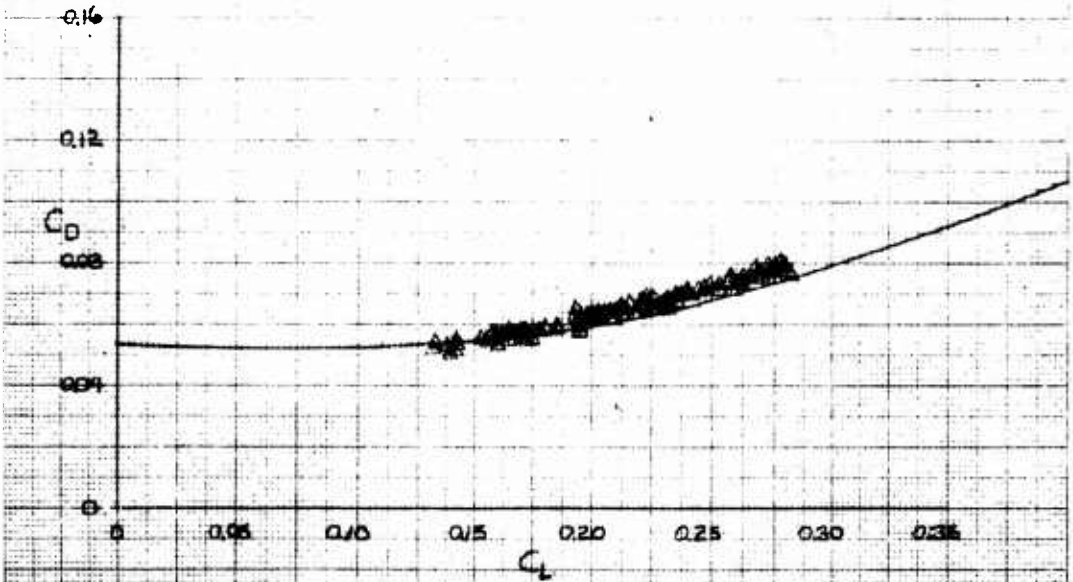

Figure A30 Gear-Down Trim Performance Data for S_{LE_B} = -2.0 degrees, S_{R_B} = -10 degrees, S_{A_B} = 7 degrees

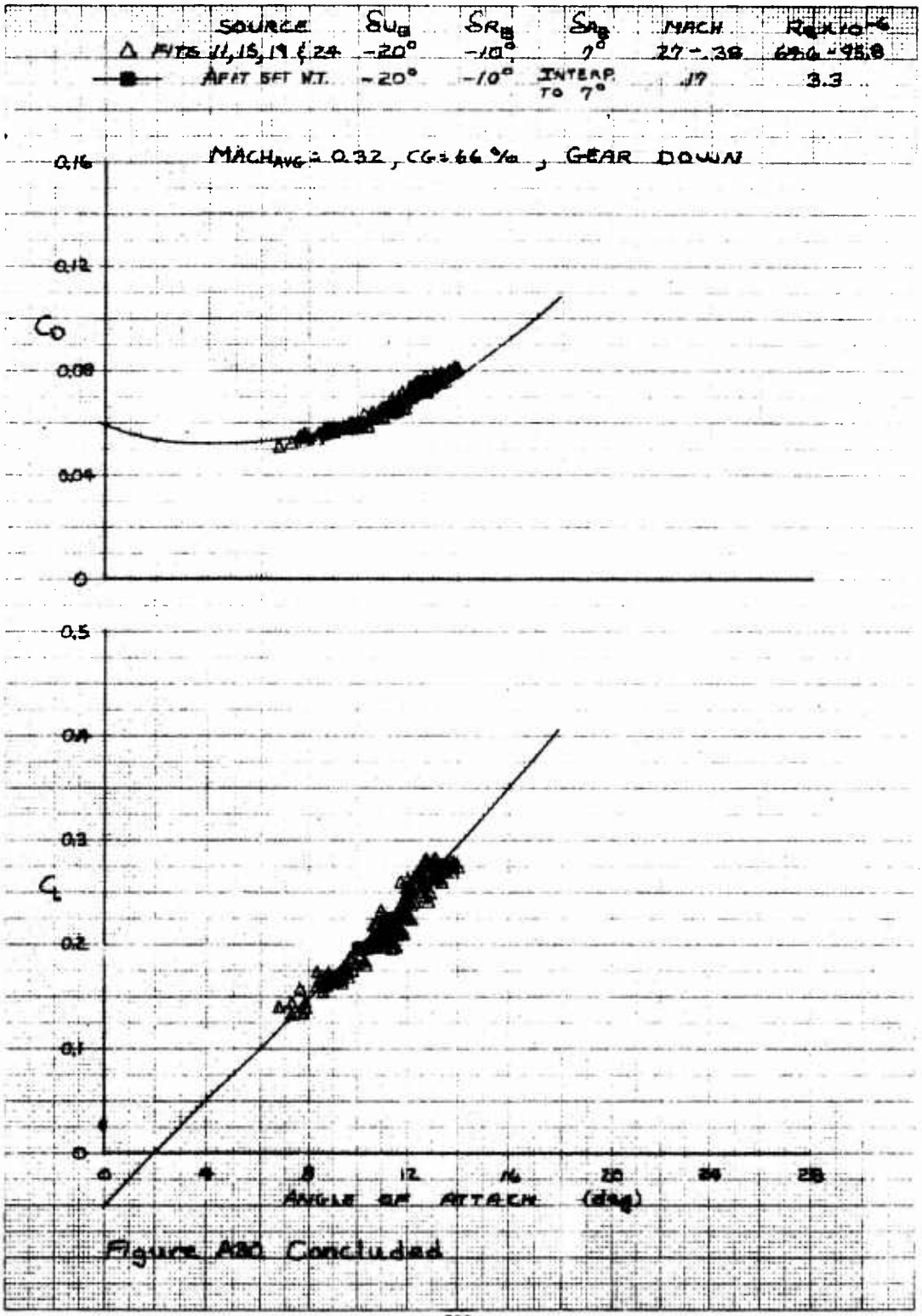

Figure A30 Concluded

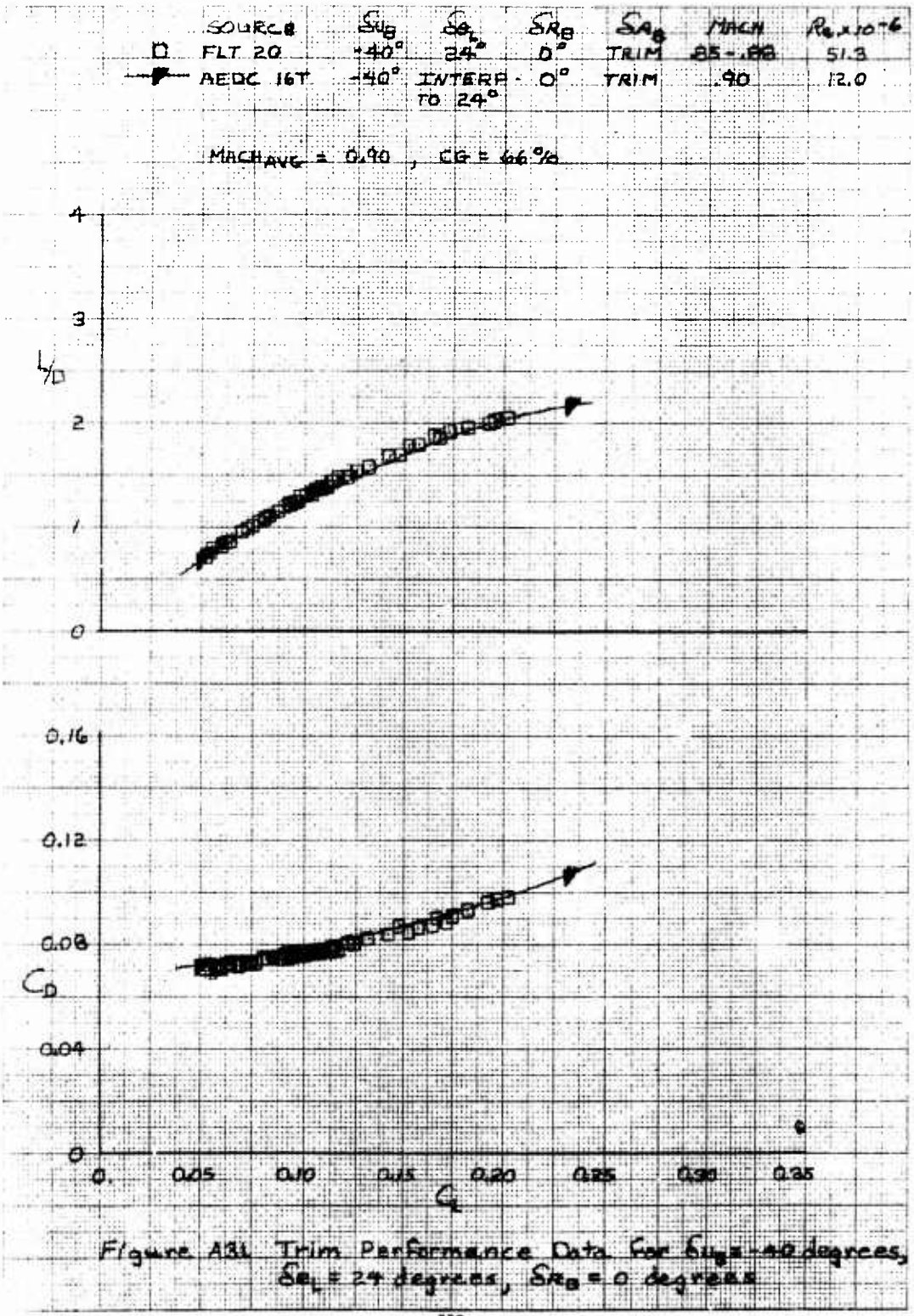

Figure A31. Trim Performance Data for δ_{H_B} = -40 degrees, δ_{e_L} = 24 degrees, δ_{R_B} = 0 degrees

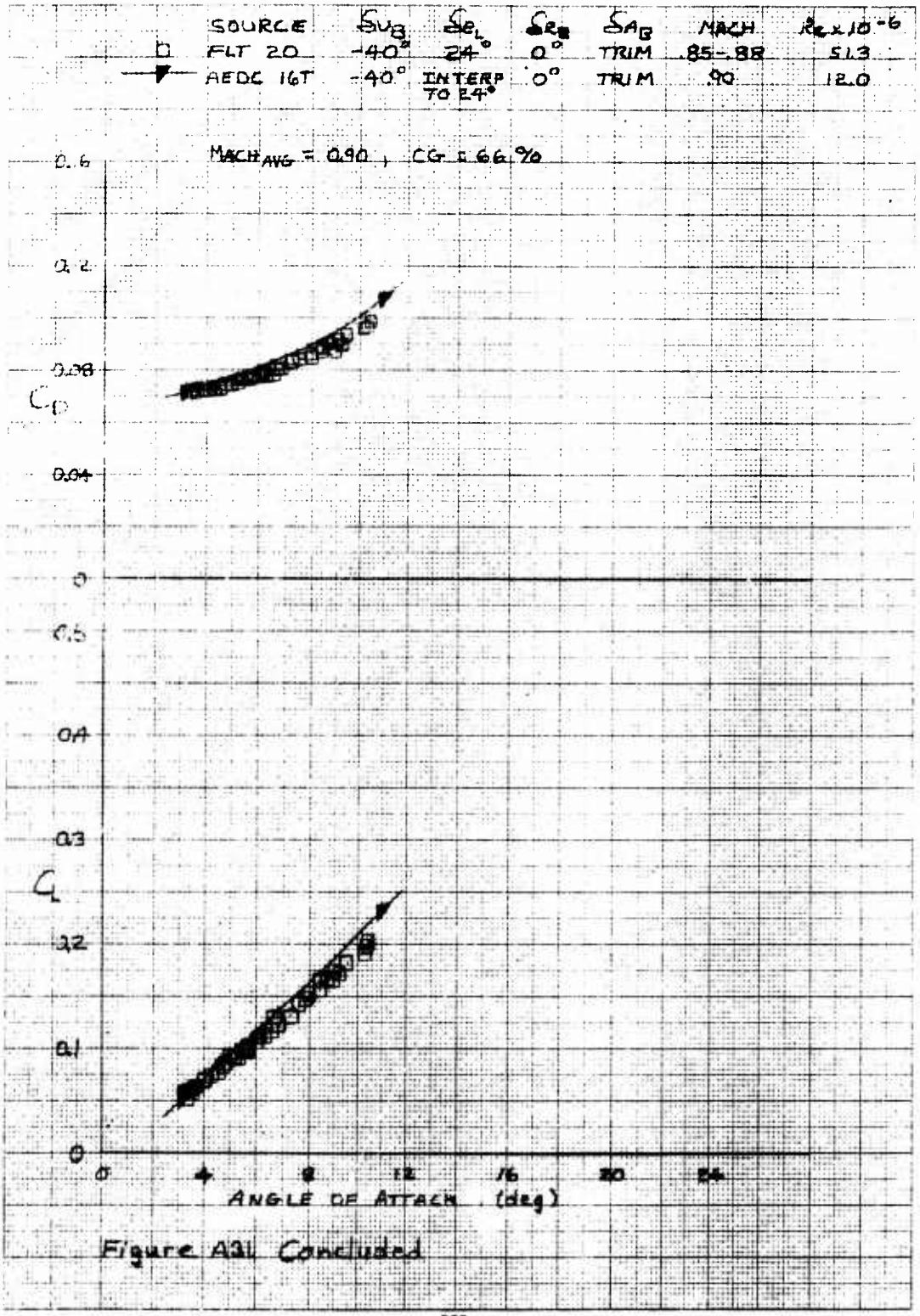

Figure A31 Concluded

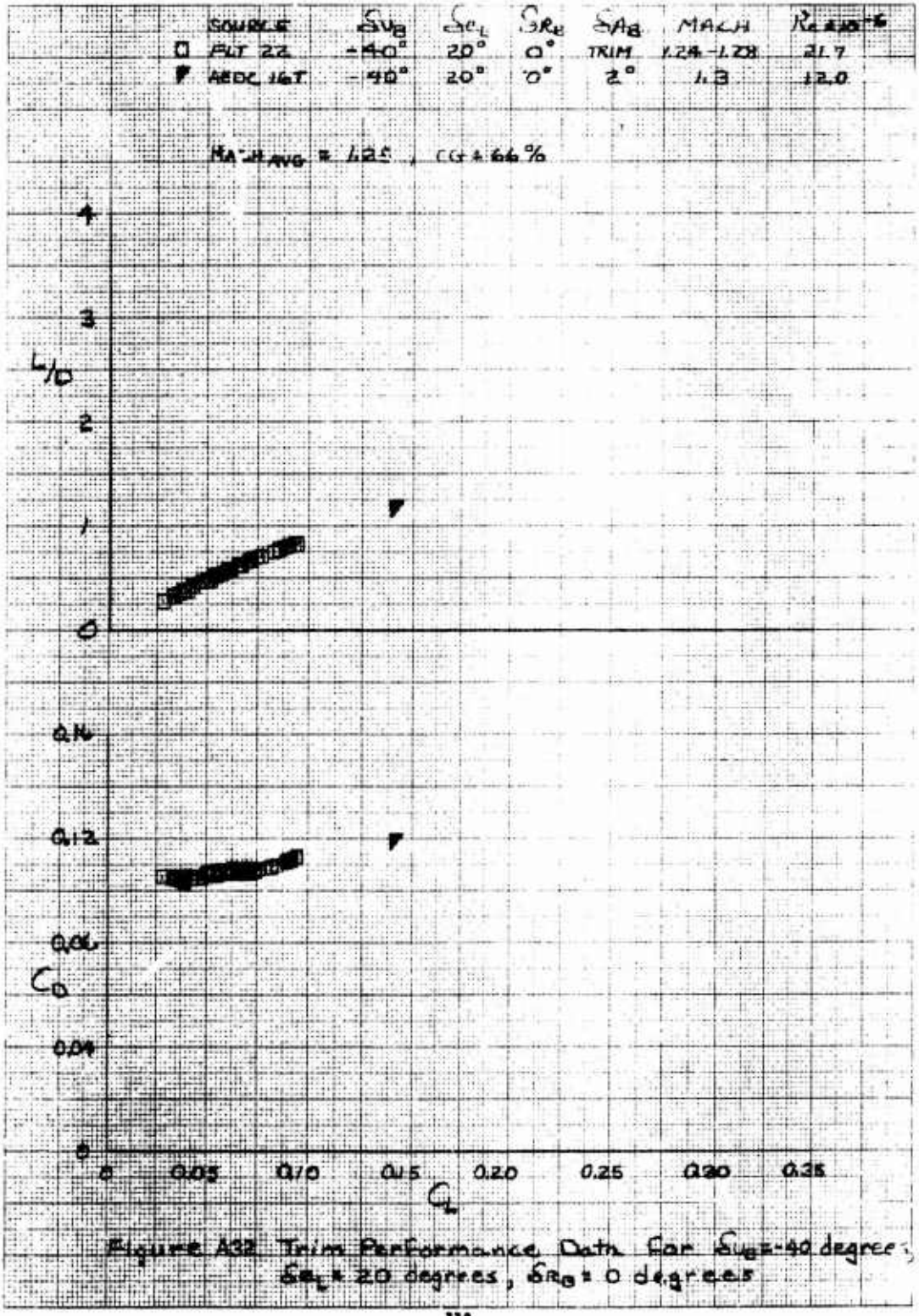

Figure A32 Trim Performance Data for δ_{SB}=-40 degrees, δ_{C_L} = 20 degrees, δ_{R_E} = 0 degrees

	SOURCE	δ_{U_B}	δ_{e_L}	δ_{R_B}	δ_{A_B}	MACH	$R_N \times 10^{-6}$
□	FLT 22	-40°	20°	0°	TRIM	1.24-1.28	21.7
▼	AEDC 16T	-40°	20°	0°	2°	1.3	12.0

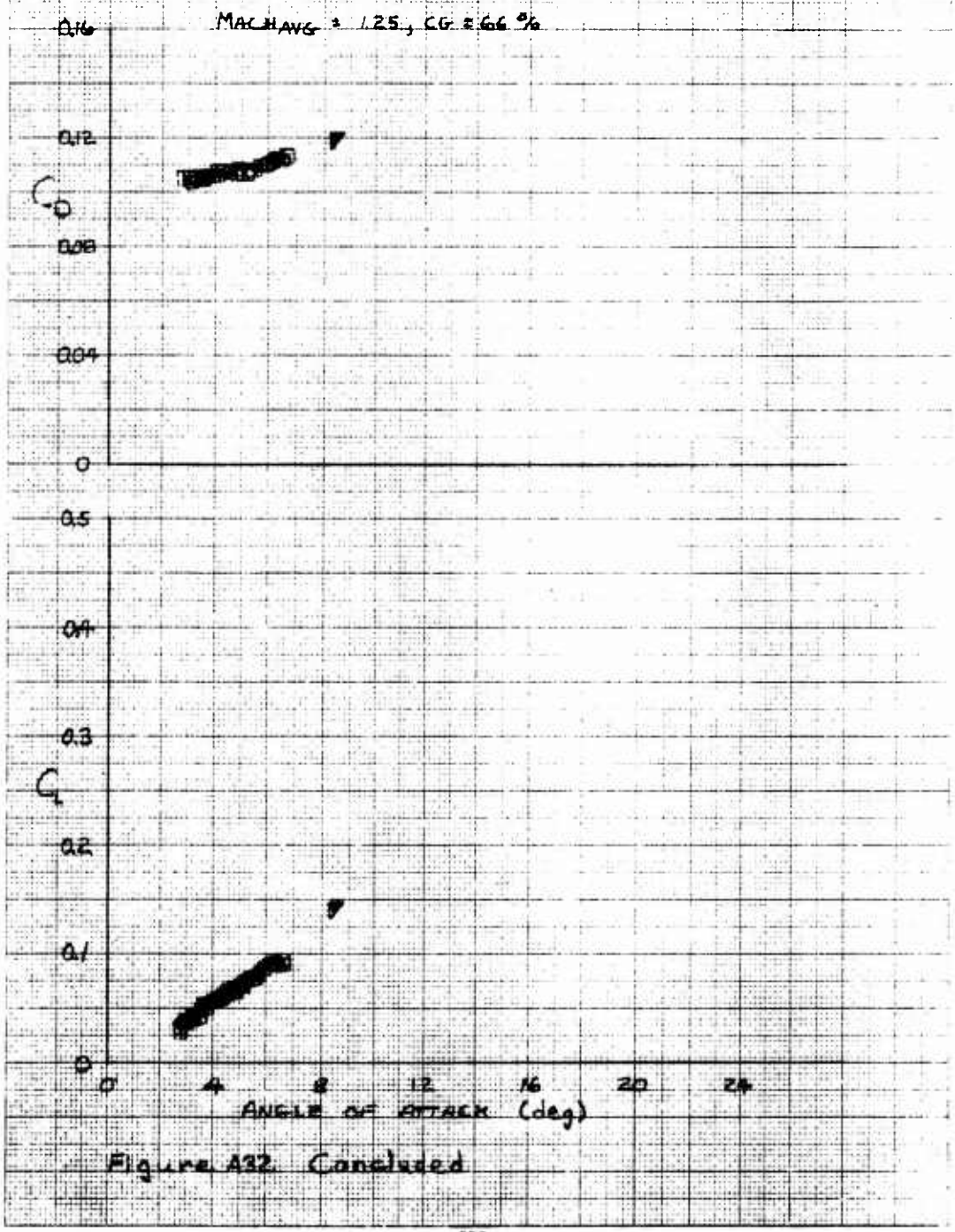

Figure A32. Concluded

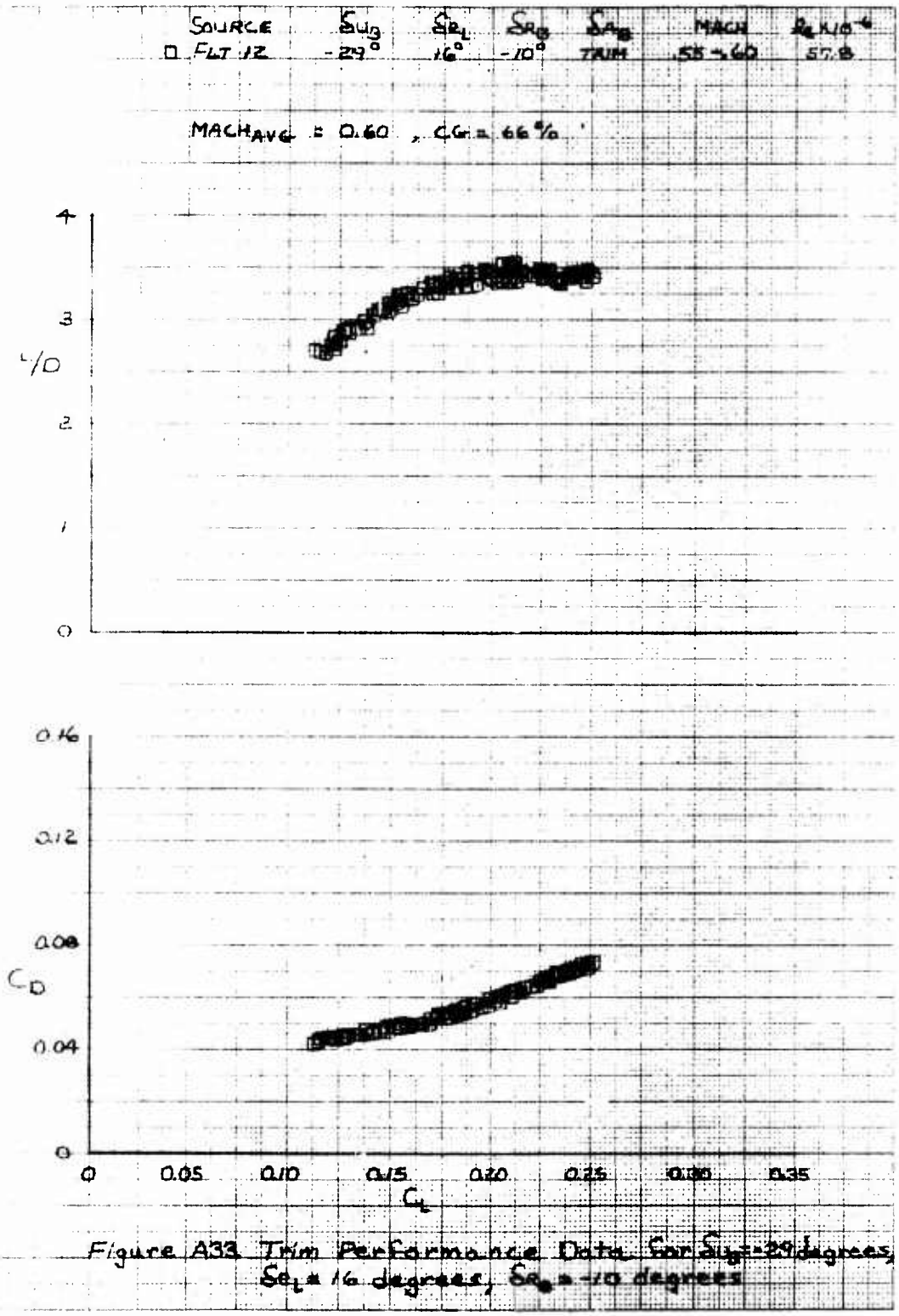

Figure A33 Trim Performance Data for δ_{u_3} = -29 degrees, δ_{e_L} = 16 degrees, δ_{e_B} = -10 degrees

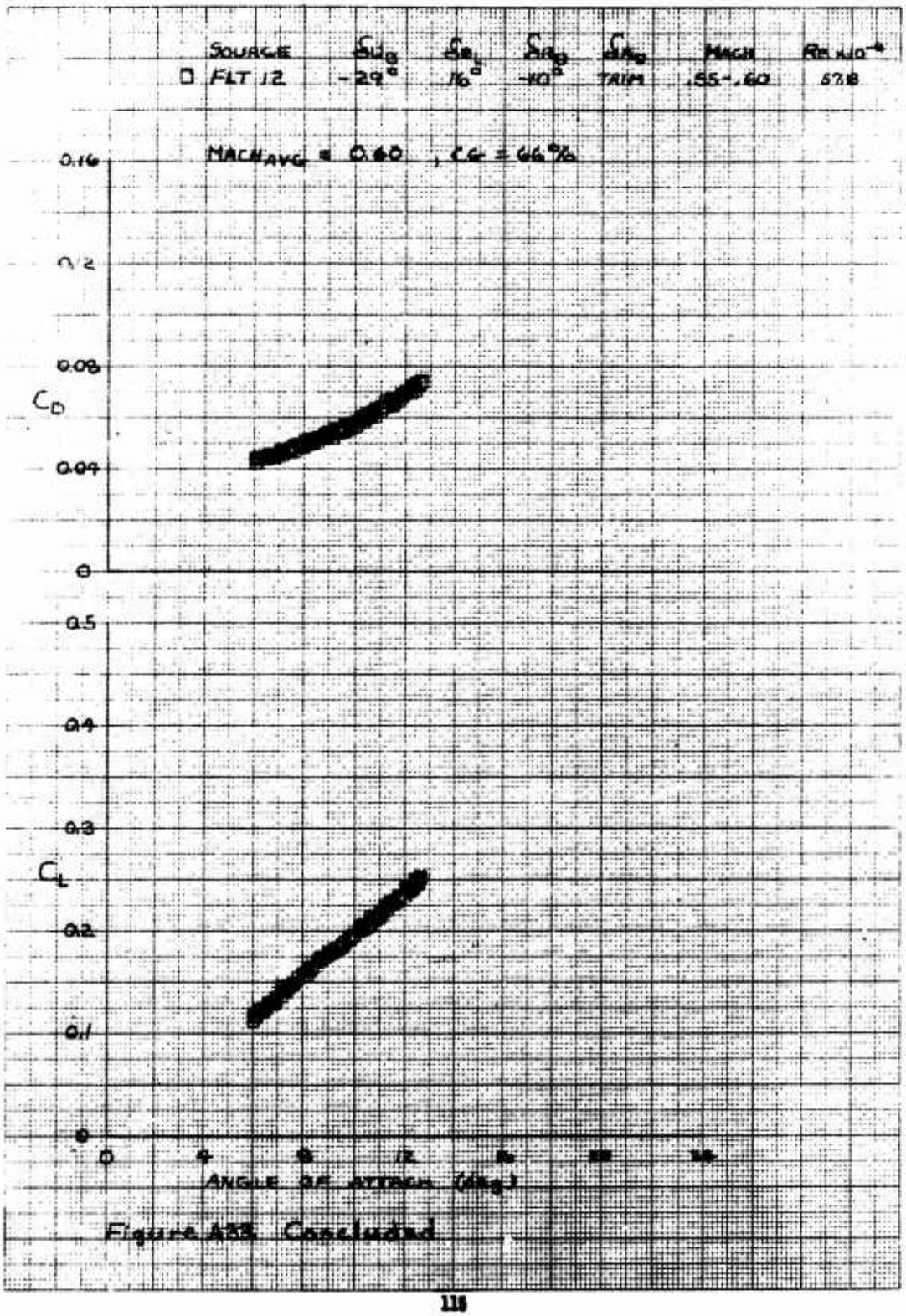

Figure A33. Concluded

APPENDIX B
X-24B POSITION ERROR DETERMINATION

Introduction

The position error measurement on the X-24B aircraft presented problems that are not encountered on most other types of aircraft. The common methods of position error measurement such as the tower fly-by, the groundspeed course and the pacer could not be used with the X-24B because there was little time spent in stabilized flight. The X-24B's only power source was a rocket engine, which made it a boost-glide type aircraft. Thus, the aircraft was either gaining or losing energy very fast. This means that the altitude and/or airspeed was increasing or decreasing rapidly. These changes in altitude and airspeed introduced problems of lag in the static and dynamic pressure and transients in the position error. The techniques used to overcome these difficulties are discussed in detail in reference 3. Only the general techniques and results will be discussed here.

Test Technique

The method of obtaining the position error was basically a comparison between the aircraft-measured static pressure and the actual static pressure at a given altitude. The actual pressure was measured as a function of altitude by a Rawinsonde weather balloon. The balloon was released to coincide with the flight of the X-24B. The static pressures as measured by the weather balloon were correlated to those measured on the X-24B using altitude from a radar track of the aircraft. The difference between the two pressures was normalized in the usual manner and used to calculate a correction to Mach number due to position error. It also corrected all other parameters which used static pressure, such as airspeed, altitude and dynamic pressure. As with the X-24A, C_L effects were neglected so that the position error correction was only a function of instrument corrected Mach number (Mic).

Data Results

Figure B1 shows the position error data accumulated during the X-24B program. These data have been edited and represent about two-thirds of the original data. Data from several flights were deleted when it appeared that zero shifts in the pressure instrumentation were causing the position error data to be biased up or down. The position error curve used for follow-on data correction is also shown in figure B1 and again in figure B2. This curve was developed after the first nine flights of the X-24B (maximum Mach number = 1.1). Although subsequent analysis showed small variations from the original curve, the problem of reprocessing all the follow-on data with a new curve dictated that the small changes be neglected.[16] The major deviation occurred supersonically where flight data indicated a steadily increasing negative increment in Mach number due to the position error. At the maximum Mach number attained during the program this increment was about -0.03. No position error correction was made to the supersonic data in the follow-on data processing computer programs.

[16] These small changes in position error would affect the calculation of dynamic pressure which was used in the computation of C_L and C_D. The maximum error in computing dynamic pressure would be approximately 0.5 percent.

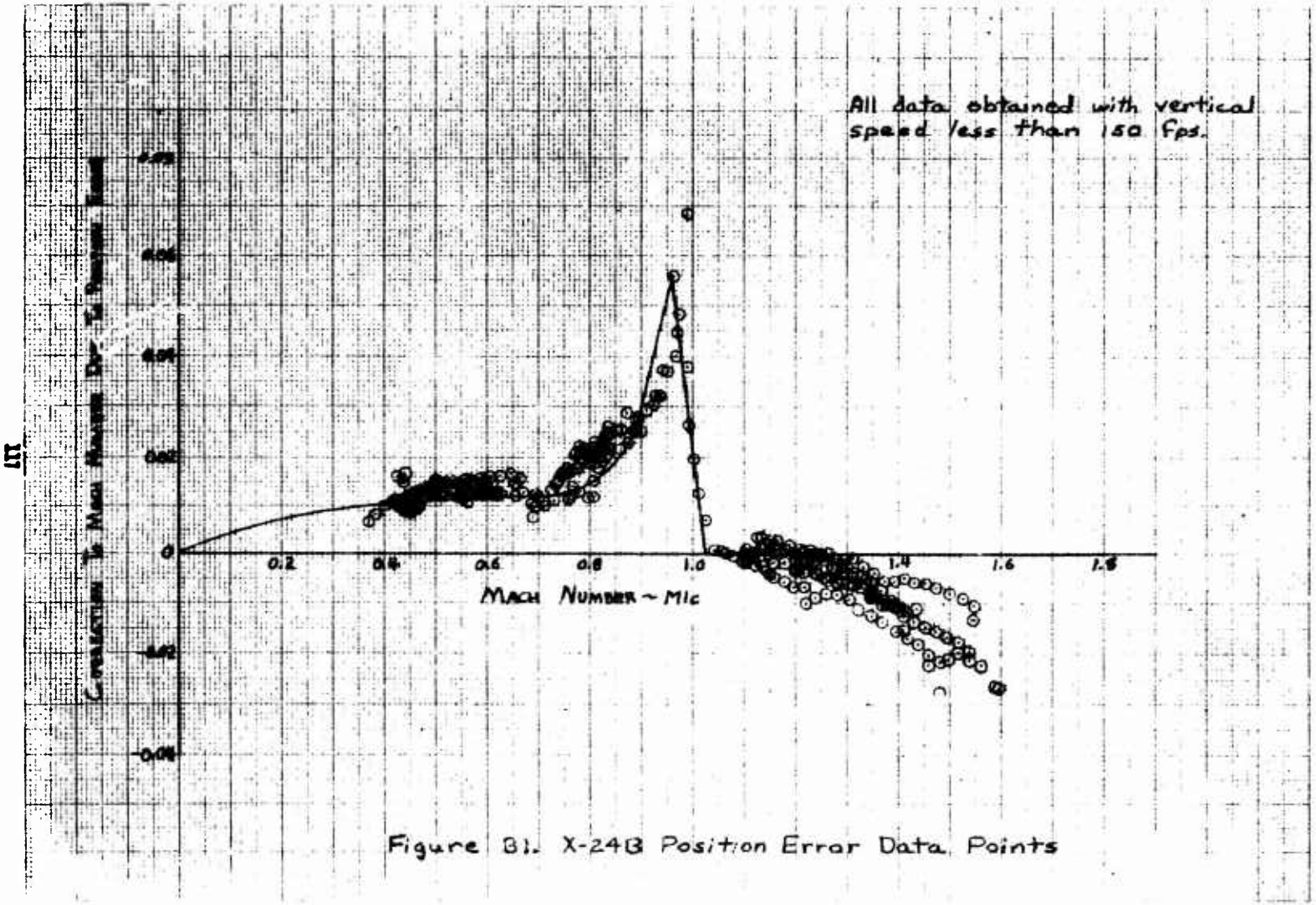

Figure 81. X-24B Position Error Data Points

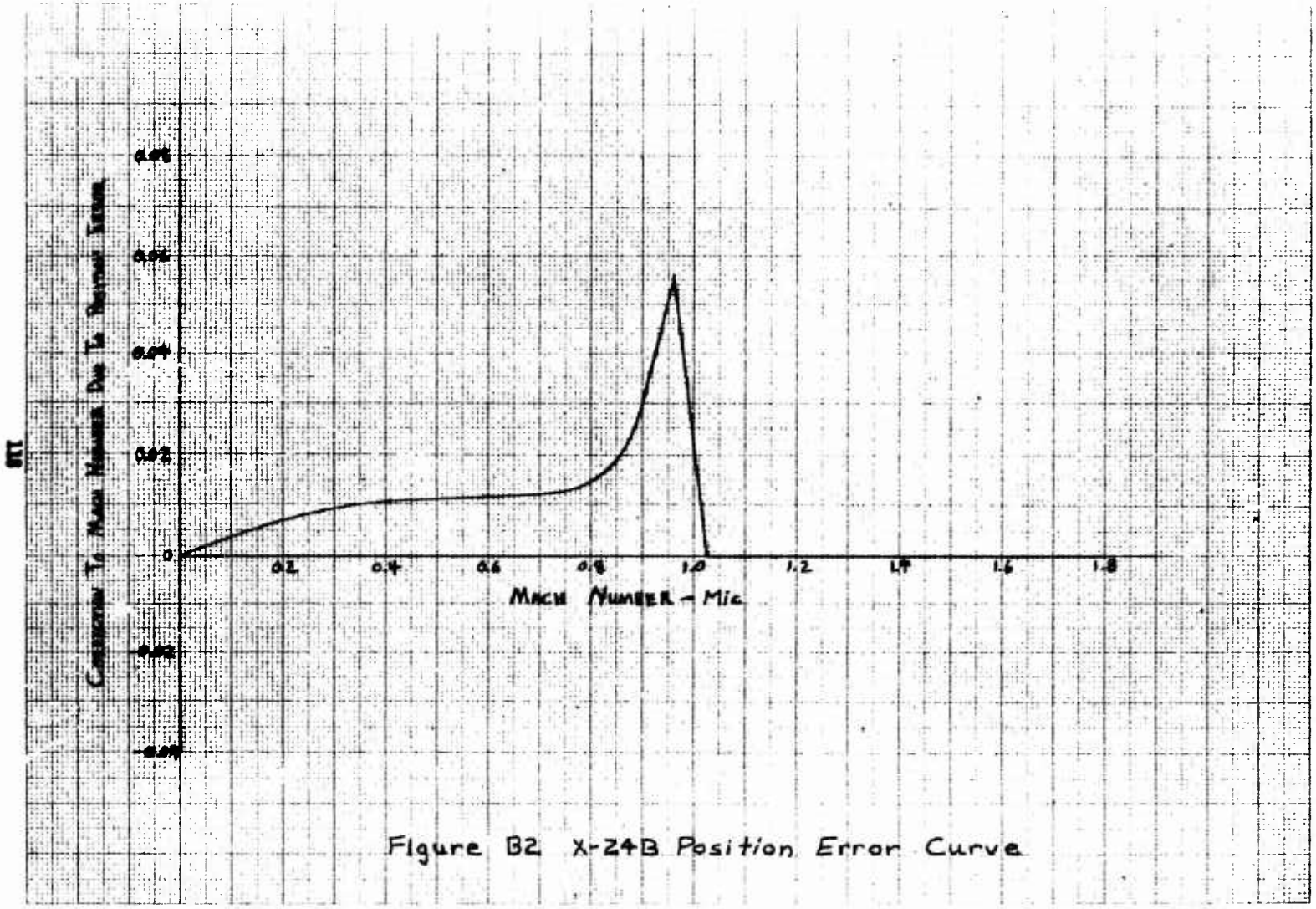

Figure B2 X-24B Position Error Curve

list of abbreviations and symbols

Item	Definition	Units
AEDC	Arnold Engineering Development Center	---
AFFDL	Air Force Flight Dynamics Laboratory	---
AFFTC	Air Force Flight Test Center	---
AFIT	Air Force Institute of Technology	---
b	reference span (19.0 ft)	feet
$\bar{c}$	reference length (37.5 ft)	feet
CDC	Control Data Corporation	---
C_D	total trim drag coefficient	---
C_{D_0}	trim drag coefficient at zero lift	---
cg	center of gravity	percent $\bar{c}$
C_L	trim lift coefficient	---
C_{L_α}	$\delta C_L/\delta\alpha$	per degree
C_m	pitching moment coefficient	---
C_{m_α}	$\delta C_m/\delta\alpha$	per degree
C_N	normal force coefficient	---
C_{N_α}	$\delta C_N/\delta\alpha$	per degree
L/D	trim lift-to-drag ratio	---
L/D_{max}	maximum trim lift-to-drag ratio	---
M	true Mach number	---
Mic	indicated Mach number corrected for instrument error	---
NASA	National Aeronautics and Space Administration	---
$\dot{q}$	pitch acceleration	deg per sec^2
Re	total Reynolds number	---
S	reference planform area (330.5 ft^2)	square feet
VKF	Von Kármán Gas Dynamics Facility	---

Item	Definition	Units
α	true angle of attack	deg
Δ	prefix meaning increment	---
δA_B	aileron bias position	deg
δe_L	lower flap position	deg
δR_B	rudder bias position	deg
δU_B	upper flap bias position	deg
δw	wedge angle ($\delta w = \delta e_L - \delta U_B$)	deg